Molecular modification of starch during thermomechanical treatment

René van den Einde

Promotor:

Prof. dr. ir. R.M. Boom
Hoogleraar Levensmiddelenproceskunde, Wageningen Universiteit

Co-promotor:

Dr. ir. A.J. van der Goot
Universitair docent, sectie Proceskunde, Wageningen Universiteit

Promotiecommissie:

Prof. dr. R.J. Hamer
Wageningen Universiteit

Prof. dr. P. D. Iedema
Universiteit van Amsterdam

Prof. dr. ir. E. van der Linden
Wageningen Universiteit

Dr. J.J.G. van Soest
Agrotechnology & Food Innovations, Wageningen

René van den Einde

Molecular modification of starch during thermomechanical treatment

Proefschrift
Ter verkrijging van de graad van doctor
op gezag van de rector magnificus
van Wageningen Universiteit,
Prof. Dr. Ir. L. Speelman,
in het openbaar te verdedigen
op dinsdag 27 januari 2004
des namiddags te vier uur in de Aula.

Einde, R.M. van den 2004. Molecular modification of starch during thermomechanical treatment. Thesis Wageningen University – with summary in Dutch.

ISBN: 90-5808-964-9

Contents

Chapter 1

General introduction

1. Starch: origin and production

Starch is the form of carbohydrate reserve in nearly all green plants and it is the major carbohydrate component in food (Van den Berg, 1981). In many food products, such as for example pasta, snack foods (crisps) and cereals, starch is an important component and changes in starch properties, for example by heating and shearing, largely contribute to the final product structure and properties. On industrial scale, starch is isolated from seeds of cereal grains (corn, wheat, rice), tubers (potato), roots (tapioca, sweet potato) and the pith of the tapioca palm (Swinkels, 1985). Worldwide, approximately 48.5 million tons of starch are produced each year (European Union, 2002). Corn starches, which were used in the work described in this thesis, are the most important starches on world scale (figure 1). Half the world’s corn is grown in the USA; China, the second largest corn producer in the world, grows about 10% (Eco-foam.com, 2003). Nowadays also new starch sources have been explored, such as yam (Alves *et al.*, 1999; Sebio and Chang, 2000) and pea (Barron *et al.*, 2000, 2001; Della Valle *et al.*, 1994).

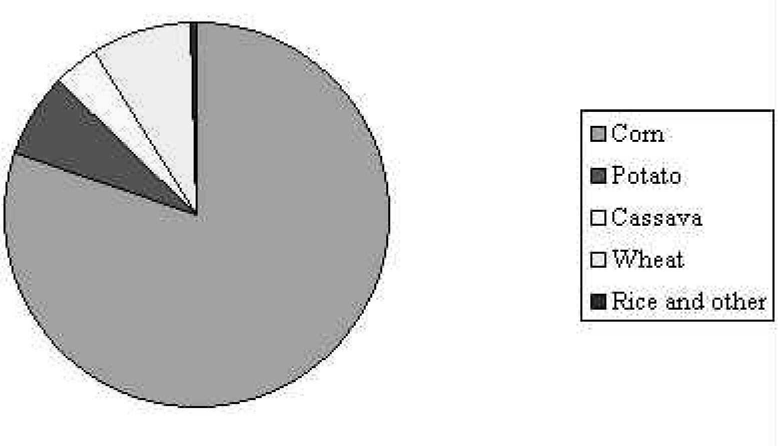

Figure 1: Starch distribution world wide by raw material (Starch.dk, 1999).

2. Starch structure

Starch is a mixture of two types of polymers each consisting of D-glucose-units linked by α-glycosidic bonds: amylose and amylopectin. Amylose is defined as a linear molecule of α-1,4 linked D-glucopyranosyl units, but it is known that some amylose molecules can be slightly branched (Buléon *et al.*, 1998). The degree of polymerization (*DP*) varies from a few hundred up to about 10000, resulting in molecular weights ranging from 10^4 to 10^6. Amylopectin is α-1,4 linked with about one α-1,6 link per 20 monomer units (Swinkels, 1985). The α-1,6-links form the so-called branching points (figure 2). In this way, a branched structure is formed. The degree of polymerisation is about 10^6 or more, resulting in molecular weights of about 10^8. Starches of different origins contain different amylose-amylopectin ratios. On average, corn and waxy corn starch contain 72 and >99% (on dry matter) amylopectin respectively (Swinkels, 1985; Fritz *et al.*, 1994).

Various proposals on the structure of amylopectin have been made (figure 3). The model based on the cluster structure (figure 3c) as proposed by Robin *et al.* (1974) has found wide acceptance. The average length of a chain in such a structure was shown to be 18.3 glucose units for waxy corn starch (Gérard *et al.*, 2000).

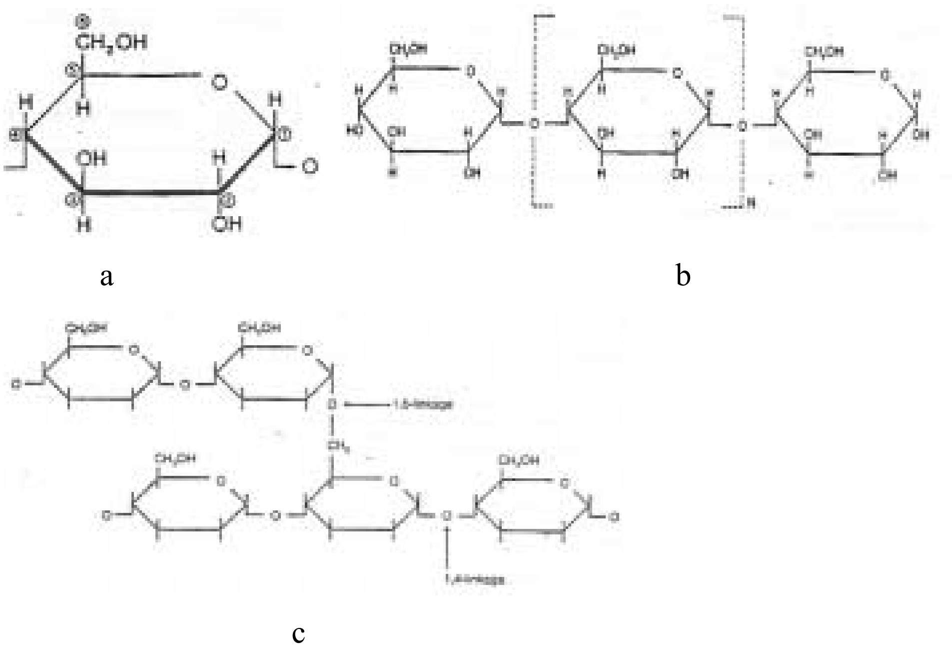

Figure 2: Structure of starch components (Swinkels, 1985); a = structure of one α-D-glucopyranosyl unit; b = linear-chain structure of amylose molecules; c = structure of amylopectin branching points.

Starch is present in almost all green plants in semi-crystalline granules, with sizes ranging from 5 to 100 µm (Barron *et al.*, 2001). Amylose and branching regions of amylopectin form the amorphous regions in the starch granules. Ordered linear segments of amylopectin form the crystalline regions. Native corn and waxy corn starch have the A-type crystal structure, which consists of a double helix. A schematic model for the crystalline regions is shown in figure 4. Due to these crystalline regions, starch granules show a cross under a polarization microscope.

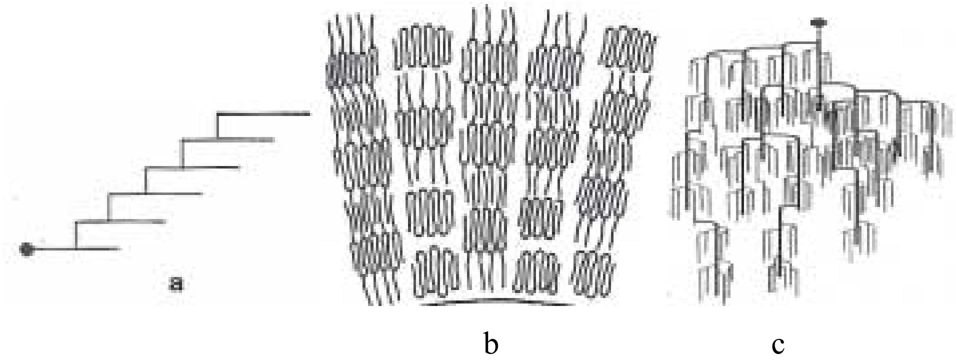

Figure 3: Proposals for the fine structure of amylopectin and native starch (Van den Berg, 1981); a = laminated structure, one of the earliest models; b = folded molecules; c = a star type structure for waxy maize amylopectin.

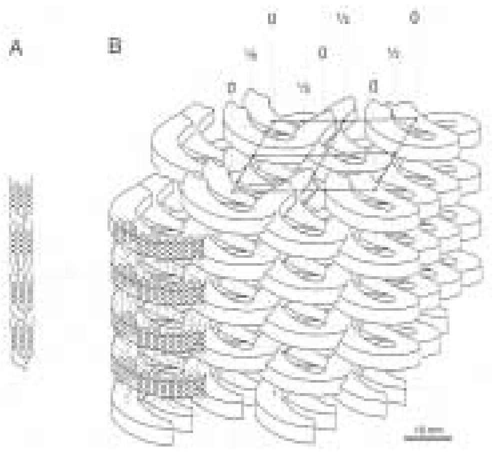

Figure 4: Schematic model for the arrangement of amylopectin in potato starch (Oostergetel and Van Bruggen, 1993).

3. Thermomechanical processing of starch-water mixtures

3.1 Effects of thermomechanical treatment on low moistened starch

During the production of starch-based products, heating and mechanical (shear) forces are often applied simultaneously. A well-known example is the extrusion cooking process (see the next section). If starch is extruded with water, the water content is relatively low, between 12 and 47% (Camire, 1998; Govindasamy *et al.*, 1996; Gomez and Aguilera, 1984). This means that the traditional gelatinization phenomena that are occurring in a surplus of water do not take place during extrusion. If low moistened starch is heated with shear, the starch granules are partially transformed, both by heat (loss of crystalline structure) and shear (granular fragmentation) (Barron *et al.*, 2001). The combined effect of temperature and shear finally leads to formation of a macroscopically homogeneous phase, often characterized as a starch melt, although melting is often incomplete. Shear contributes towards starch melting (Zheng and Wang, 1994), but temperature is a crucial factor for obtaining a homogeneous molten phase (Barron *et al.*, 2001). The melting temperature is dependent on starch source and moisture content. The melting temperature of waxy corn starch at 30% moisture content (used in chapters 2 and 3 of this thesis) is 125°C (Barron *et al.*, 2001). A schematic representation of starch restructuring under shear and temperature is shown in chapter 7.

Upon subsequent cooling, the starch may re-crystallize. Waxy corn starch shows almost no re-crystallization (Tegge, 1984), whereas corn starch (used in chapters 4 and 5) can re-crystallize. It seems to be more difficult for the branched amylopectin to realign after the conversion of the original structure during heating or heating-shearing (Fritz *et al.*, 1994). The crystallite types arising are different from the native corn starch. Often, the term retrogradation is used to describe the changes upon cooling after cooking of starch. Tegge (1984) states that retrogradation is basically a crystallization process, based on the formation of hydrogen bonds between the hydroxyl groups of starch molecules that are located next to each other. Due to the reduced ability to incorporate water, water is separated. From a product point of view, retrogradation (and hence re-crystallization) is often disadvantageous. For example, retrogradation influences the staling of baked goods (Mua and Jackson, 1997).

The high viscosity of the melt that arises during heating-shearing as described above results in large shear and elongation stresses, which may break down the starch, especially the large amylopectin molecules. Amylopectin can not align itself effectively in the streamlines of the flow, resulting in reduced molecular size (Davidson *et al.*, 1984). This thesis is dealing with molecular breakdown of starch under these circumstances, as further explained in section 4 of this chapter.

3.2 An example of thermomechanical processing: extrusion

A well-known example of a thermomechanical process is extrusion cooking. Extrusion has been utilized to produce various food products for more than 60 years (Akdogan, 1999). The process is also used for the production of plastic products.

The main layout of an extruder is shown in figure 5. Ingredients in a powdery or granular form are added at the feed point. Some extruders require mixing with water to the desired moisture level before extrusion; in other types the water is added in the extruder near the feed point. From this point, the material is transported towards the end by a rotating screw. During this transport, the material is subjected to heat (by friction or by a heated barrel) and shear. At the end of the extruder, the material is pushed through a die to the desired shape. If water is present, part of it flashes off due to a pressure drop. The flash-off results into expansion of the extrudate as the steam stretches the still molten material (Camire, 1998). Single screw extruders contain one rotating screw; twin screw extruders contain two screws, which can be co- or counter-rotating. Different types of screw elements can be used (figure 6). *Transport elements* cause only low shear rates in the starch melt due to the relatively large distance between the element and the barrel. Only at the tip, high shear rates occur, which are, however, applied to a small fraction of the material only. *Single lead elements* are used to build up pressure due to their smaller pitch compared to transport elements. The distance between the element and barrel is also in this case relatively large resulting in low shear rates; high shear rates occur at the tip only. *Reverse screw elements* have a reverse flight pushing the material backwards. They are often used to obtain an intensive exchange of solids and melt between the screws and within screw channels providing optimal mixing (Van Zuilichem *et al.*, 1999). The average shear rate is generally higher than in the transport and single lead elements (Yacu, 1985). *Paddles* are used to knead mixtures of starch or flour and water to a homogeneous melt. These high shear elements are highly important for obtaining the right product properties as they influence mixing, residence time and various physicochemical changes (Choudhury and Gautham, 1998). Paddles can be placed on the screw shaft in a positive or negative conveying direction. Various angles between the pairs of paddles can be used (see for example figure 6).

Extruders have often been used to study molecular breakdown of starch. Complicating factors in the use of the extruder for studying the effect of various (process) parameters on starch modification are the inhomogeneous distributions of temperature and shear and elongation rates and the coupled effects of the process parameters that can be adjusted. For example, if the screw speed is increased, the treatment time decreases, whereas stresses increase and locally temperatures may increase.

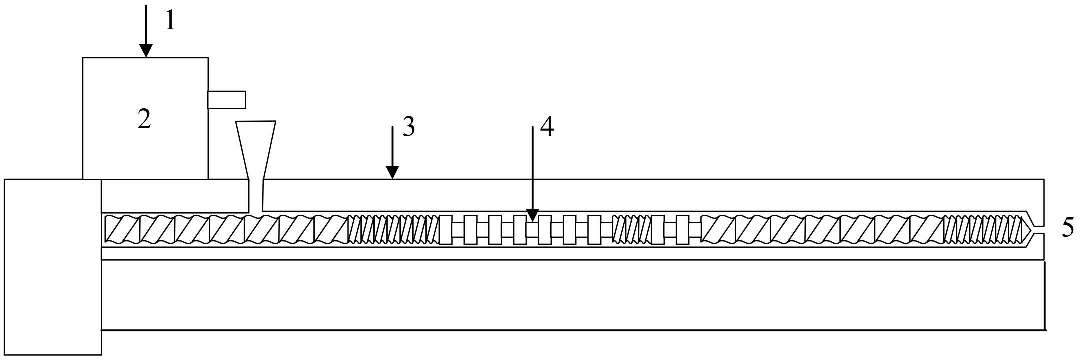

Figure 5: Schematic drawing of an APV MPF 50 twin screw extruder: 1 = feed point; 2 = hopper; 3 = heating / cooling system; 4 = screw; 5 = die.

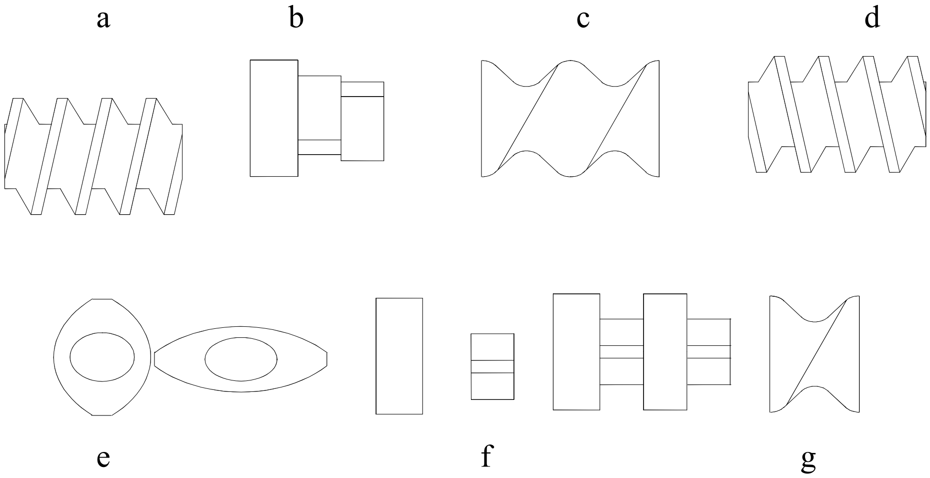

Figure 6: Different types of extruder screw elements: (a) single lead element, (b) side view paddles +60°, (c) transport element, (d) reverse screw element, (e) pair of paddles, (f) various side views paddles +90°, (g) transport element.

4. Outline of this thesis

Although molecular breakdown of starch during thermomechanical treatment, for example extrusion, has been observed in many studies (see, for example, Willett *et al.*, 1997, Baud *et al.*, 1999, Orford *et al.*, 1993; more references are given in chapter 7) and its importance for certain product properties such as cold paste viscosity, water solubility and expansion behavior has been acknowledged widely (Bruemmer *et al.*, 2002, Harper, 1986), the exact processing conditions under which the breakdown occurs are still largely unknown. Understanding the molecular breakdown and the influences of process parameters on it would reveal insights on efficient new process design in this respect. Therefore, we decided to study the effects of process parameters in a well-defined shear field. Due to the high viscosity of the molten low moistened starch and its tendency to induce slip, it is difficult to carry out such investigations on conventional rheological equipment. For this reason, a new device able to apply a well-defined thermomechanical treatment to low moistened starch was developed, allowing high shear rates and stresses, comparable to those occurring during extrusion. The aims of the investigations described in this thesis were:

1. to gain insight into and to model the effect of the different process parameters involved in thermomechanical treatment (time, temperature, shear or elongation stress, energy input, moisture content) on the degree of macromolecular degradation of starch;
2. to apply these results to existing processes (extrusion) in order to be able to describe the molecular weight reduction during these processes and to asses the scope for development of processes regarding controlled selective starch breakdown.

The effects of different process parameters on the degree of macromolecular degradation are the subject of chapters 2, 3 and 4. Chapters 5 and 6 discuss the application to extrusion processes. The two aims are integrated in chapter 7.

Chapter 2 of this thesis describes an experimental study using the newly developed device to investigate the effect of shear and thermal treatment on a mixture of waxy corn starch and water. At the temperature range investigated, thermal effects were negligible; all degradation was induced mechanically. The central question in this chapter is whether mechanically induced starch breakdown is time-dependent or independent within the time scales generally used during thermomechanical treatment. In **chapter 3**, a molecular scale model describing the molecular breakdown by shear forces of low moisture amylopectin melts is derived that couples the engineering scale experiments of chapter 2 to molecular scale processes. In

chapter 4, experiments are extended in such a way that thermal breakdown becomes important. Thus, the combined effects of shear and thermal treatment are investigated.

In **chapter 5**, the molecular weight reduction of regular corn starch in a twin screw extruder is predicted using results of chapter 4 as well as flow simulations. It is explained in this chapter that for a better prediction in certain situations, the trajectories taken by starch particles during extrusion are needed to estimate a more accurate time-shear and time-temperature history. **Chapter 6** is a first step in that direction: mixing effects of different screw elements are measured using local Residence Time Distribution (RTD) determination in a completely filled twin screw extruder using a dilute solution of pre-gelatinized waxy corn starch as a model fluid. It is shown that most mixing takes place locally in the extruder and is not determined in global RTD measurements. Finally, **chapter 7** reviews the literature on starch molecular weight reduction. This chapter shows that many results of extrusion trials described in literature can actually be well understood using the findings of this thesis. Furthermore, suggestions for process design for selective degradation of starch are given and future research needs are addressed.

References

Akdogan, H. (1999). High moisture food extrusion. *International Journal of Food Science and Technology*, 34, 195-207.

Alves, R.M.L., Grossmann, M.V.E., & Silva, R.S.S.F. (1999). Gelling properties of extruded yam (Dioscorea alata) starch. *Food Chemistry*, 67, 123-127.

Barron, C., Buleon, A., Colonna, P., & Della Valle, G. (2000). Structural modifications of low hydrated pea starch subjected to high thermomechanical processing. *Carbohydrate Polymers*, 43, 171-181.

Barron, C., Bouchet, B., Della Valle, G., Gallant, D.J., & Planchot, V. (2001). Microscopical study of the destructuring of waxy maize and smooth pea starches by shear and heat at low hydration. *Journal of Cereal Science*, 33, 289-300.

Baud, B., Colonna, P., Della Valle, G., & Roger, P. (1999). Macromolecular degradation of extruded starches measured by HPSEC-MALLS. *Biopolymer Science: Food and Non Food Applications / Les Colloques de l'INRA*, 91, 217-221, 1999.

Berg, C. van den. Vapour sorption equilibria and other water-starch interactions; a physico-chemical approach. Wageningen Agricultural University, PhD thesis, 1981.

Bruemmer, T., Meuser, F., Lengerich, B. van, & Niemann, C. (2002). Expansion and functional properties of corn starch extrudates related to their molecular degradation, product temperature and water content. *Starch / Staerke*, 54, 9-15.

Buléon, A., Colonna, P., Planchot, V., & Ball, S. (1998). Starch granules: structure and biosynthesis. *International Journal of Biological Macromolecules*, 21, 85-112.

Camire, M.E. (1998). Chemical changes during extrusion cooking - recent advances. *Advances in experimental medicine and biology*, 434, 109-121.

Choudhury, G.S., & Gautam, A. (1998). Comparative study of mixing elements during twin-screw extrusion of rice flour. *Food Research International*, 31(1), 7-17.

Davidson, V.J., Paton, D., Diosady, L.L., & Larocque, G. (1984). Degradation of wheat starch in a single-screw extruder: characteristics of extruded starch polymers. *Journal of Food Science*, 49, 453-458.

Eco-foam.com (2003). http://www.eco-foam.com/production.asp

European Union (2002). Evaluation of the Community Policy for Starch and Starch Products. http://europa.eu.int/comm/agriculture/eval/reports/amidon/chap1.pdf

Fritz, H.G., Seidenstuecker, T., & Boelz, U. (1994). Use and modification of biological substances. In *Production of thermo-bioplastics and fibres based mainly on biological materials* (p. 10-108). European Commission Science Research Development.

Gérard, C., Planchot, V., Colonna, P., & Bertoft, E. (2000). Relationship between branching density and crystalline structure of A- and B-type maize mutant starches. *Carbohydrate Research*, 326, 130-144.

Gomez, M.H., & Aguilera, J.M. (1984). A physicochemical model for extrusion of corn starch. *Journal of Food Science*, 49, 40-63.

Govindasamy, S., Campanella, O.H., & Oates, C.G. (1996). High moisture twin-screw extrusion of sago starch: 1. Influence on granule morphology and structure. *Carbohydrate Polymers*, 30, 275-286.

Harper, J.M. (1986). Extrusion texturization of foods. *Food Technology*, 40, 70, 72, 74-76.

Mua, J.P., & Jackson, D.S. (1997). Relationships between functional attributes and molecular structures of amylose and amylopectin fractions from corn starch. *Journal of Agricultural and Food Chemistry*, 45, 3848-3854.

Oostergetel, G.T., & Bruggen, E.F.J. (1993). The crystalline domains in potato starch granules are arranged in a helical fashion. *Carbohydrate Polymers*, 21, 7-12.

Orford, P.D., Parker, R., & Ring, S.G. (1993). The functional properties of extrusion-cooked waxy-maize starch. *Journal of Cereal Science*, 18, 277-286.

Robin, J.P., Mercier, C., Charbonniere, R., & Guilbot, A. (1974). Lintenerized starches. Gel filtration and enzymatic studies of insoluble residue from prolonged acid treatment of potato starch. *Cereal Chemistry*, 51, 389-406.

Sebio, L. & Chang, Y.K. (2000). Effects of selected process parameters in extrusion of yam flour (Dioscorea rotundata) on physicochemical properties of the extrudates. *Nahrung*, 44(2), 96-101.

Starch.dk (1999). http://www.starch.dk/isi/stat/rawmaterial.html

Swinkels, J.J.M. (1985). Sources of starch, its chemistry and physics. In G.M.A. van Beynum, & J.A. Roels. *Starch conversion technology* (p. 15-46). New York: Marcel Dekker Inc.

Tegge, G. (1984). Staerke und Staerkederivate. Hamburg: Behr's Verlag.

Valle, G. Della, Quillien, L., & Gueguen, J. (1994). Relationships between processing conditions and starch and protein modifications during extrusion-cooking of pea flour. *Journal of the Science of Food and Agriculture*, 64, 509-517.

Willett, J.L., Millard, M.M., & Jasberg, B.K. (1997). Extrusion of waxy maize starch: melt rheology and molecular weight degradation of amylopectin. *Polymer*, 38(24), 5983-5989.

Zheng, X. & Wang, S.S. (1994). Shear induced starch conversion during extrusion. *Journal of Food Science*, 59(5), 1137-1143.

Yacu, W.A. (1985). Modelling a twin screw co-rotating extruder. *Journal of Food Engineering*, 8, 1-21.

Zuilichem, D.J. van, Kuiper, E., Stolp, W., & Jager, T. (1999). Mixing effects of constituting elements of mixing screws in single and twin screw extruders. *Powder Technology*, 106, 147-159.

Chapter 2

The effect of thermomechanical treatment on starch breakdown and the consequences for process design

Abstract

Macromolecular degradation of starch by heating and shear forces was investigated using a newly developed shear cell. With this equipment, waxy corn starch was subjected to a variety of heat and shear treatments in order to find the key parameter determining the degree of macromolecular degradation. A model based on the maximal shear stress during the treatment gave an improved prediction compared to existing models in literature based on specific mechanical energy input (SME) or shear stress multiplied by time ($\tau \cdot t$). It was concluded that molecular weight reduction of starch at the temperatures investigated (85-110°C) is a time-independent process, during which the starch molecules are broken down virtually instantaneously by high shear force within time scales investigated. Consequences for design of shear based processes (especially extrusion) are shortly discussed.

This chapter was published as: R.M. van den Einde, A. Bolsius, J.J.G. van Soest, L.P.B.M. Janssen, A.J. van der Goot, R.M. Boom, The effect of thermomechanical treatment on starch breakdown and the consequences for process design. (2004). *Carbohydrate Polymers*, 55(1), 57-63.

1. Introduction

Starch is an ingredient that determines product properties, such as cohesiveness, water solubility and cold paste viscosity of many food products. Previous studies have shown that the molecular weight of the starch is an important property in this respect (Bruemmer *et al.*, 2002; Bindzus *et al.*, 2002).

Production of starch based products often comprises a combination of shear and thermal treatment, for example in extrusion processes. It is well known that the combination of shear and thermal treatment leads to molecular breakdown, but the exact cause and control of this effect are still matters of uncertainties. This is partly due to the fact that the shear rates, shear stresses and temperatures are rather inhomogeneous in most process equipment and therefore difficult to control. Nevertheless, the use of extrusion trials led to development of empirical models describing the relation between molecular weight and process parameters. Parker *et al.* (1990) concluded that molecular breakdown relates to the specific mechanical energy input (SME) during extrusion, defined as the capacity transferred by the screws per unit of mass or volume (Meuser *et al.*, 1984). Diosady *et al.* (1985) obtained a first order correlation between the molecular weight reduction and shear stress multiplied by time ($\tau \cdot t$), thereby suggesting time-shear equivalence in molecular breakdown of starch.

Some authors presented a different approach by using equipment with more defined shear and temperature gradients. Vergnes *et al.* (1987) carried out an important study, describing the effect of well-defined shear and temperature on macromolecular degradation. They used a self-built rheometer with pre-shearing to simulate extrusion cooking and concluded that mechanical energy input during the treatment determined macromolecular degradation of the starch. Igura *et al.* (1997) used a flow tester equipped with a capillary tube to show qualitatively the impact of heating at 150°C and shearing on macromolecular degradation of various starches. They showed that longer time heating gave the same degree of degradation as a shorter time heating-shearing treatment, suggesting an equivalence of shear and heating time at this temperature.

Grandbois *et al.* (1999) and Beyer (2000) presented a fundamental approach. They investigated the molecular strength of the glucosidic bonds, and the effect of extensionally applied forces on these bonds using atomic force microscopy. One of their conclusions was that breakdown of a covalent bond in an amylose molecule takes place almost instantaneously in case the force applied exceeds the bond strength. If their outcome is applied to an extrusion process of a starch-containing product, it implies a dependency of the molecular weight reduction on the maximal force during the treatment, rather than on treatment time. This seems to be in contradiction with the empirical studies described above.

The aim of this study was therefore to investigate which fundamental process parameter determines starch macromolecular degradation during a heating-shearing treatment. For this purpose a new device was developed, which enabled the separation of the effects of shear force, shear rate, time and temperature. Experimental data of this device were used to find the key parameter to starch molecular weight reduction. The outcome of the key parameter study was used to explain the pattern of starch molecular weight reduction during extrusion cooking.

2. Theory

2.1. Measurement and quantification of starch degradation

Shear forces are known to induce endodegradation of the high molecular weight compounds in starch (Baud *et al.*, 1999; Davidson *et al.*, 1984). The intrinsic viscosity $[\eta]$ is especially sensitive to this type of degradation, even if the actual molecular weight reduction is limited and difficult to measure by chromatographic methods. Furthermore, a good correlation was found between the molecular weight of corn amylopectin as measured by chromatography in combination with laser light scattering and the intrinsic viscosity (Millard *et al.*, 1997), suggesting that $[\eta] \sim Mw^{0.29}$. Therefore, the intrinsic viscosity can be used as a measure for the molecular weight.

Some studies suggest that the crystalline part of the starch is not susceptible to a mechanical treatment. According to these investigations, only the molten parts can be degraded. As a result of this, the intrinsic viscosity needs to be corrected. Diosady *et al.* (1985) suggested the following correction:

$$X = \frac{[\eta]_i}{[\eta]_{rs}} \qquad [1]$$

$$[\eta]_i = \frac{[\eta] - (1-f)[\eta]_{rs}}{f} \qquad [2]$$

where f denotes the fraction crystalline starch; $[\eta]$ and $[\eta]_{rs}$ denote the intrinsic viscosity of the treated and of the native starch respectively. X represents the relative intrinsic viscosity

($0 < X < 1$) and can be used as a measure for starch degradation. $X = 1$ denotes that starch was not degraded.

2.2. Modeling and key parameter study

Models relating the decrease in intrinsic viscosity and process parameters were developed by Parker *et al.* (1990) and Diosady *et al.* (1985). Parker and co-workers related the intrinsic viscosity to the specific mechanical energy during extrusion. Diosady and co-workers related the intrinsic viscosity to the product of shear stress and time. Their models can be written as:

$$X = C_{1a} \exp\left(-C_{2a} \cdot SME\right) \qquad [3]$$

and

$$X = C_{1b} \exp\left(-C_{2b} \cdot \tau t\right) \qquad [4]$$

respectively, where SME denotes the specific mechanical energy, τt denotes the product of shear stress and time and C_{1a} and C_{1b} are constants. Parker and co-workers did not include the melt correction described in section 2.1, which means that they assumed that $f = 1$.

Contrary to these studies, the fundamental investigations of Beyer (2000) and Grandbois *et al.* (1999) suggest the maximal shear stress to be the key parameter. In analogy with the models described above, the following correlation can be derived:

$$X = C_{1c} \exp\left(-C_{2c} \cdot \tau_{\max}\right) \qquad [5]$$

The value of the constant C_{1a}, C_{1b} or C_{1c} depends on whether or not thermal breakdown takes place and on whether or not native starch can handle a certain shear stress or mechanical energy input before breaking down (figure 1). If thermal breakdown takes place, the value is expected to be lower than 1. If no thermal breakdown takes place and the native starch can handle a certain shear stress or mechanical energy input before breaking down, the constant is higher than 1. In this case, $X = 1$ if the stress or mechanical energy input level is lower than minimally required for breakdown (figure 1). If the native starch breaks down at any shear stress or mechanical energy level but no thermal breakdown takes place, the constant is equal to 1. The use of the shear cell described below allowed us to compare the different models and thus to find the key parameter to starch degradation.

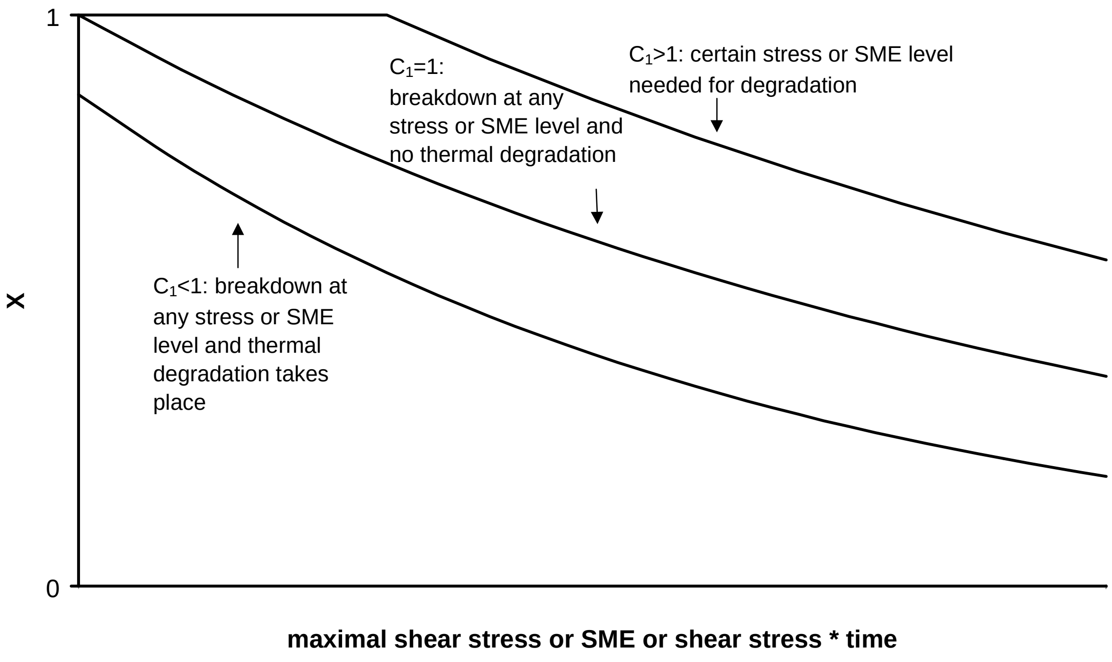

Figure 1: Effect of the value of parameter C_1 on the models described in the Theory section.

3. Materials and methods

3.1. Starch and water

Waxy corn starch was used in all experiments. Intrinsic viscosity and percentage of crystalline material of the native starch are given in table 1. Before processing, starch was pre-mixed with water to a moisture content of 30% (w water/w total). Experiments were carried out 1 day after pre-mixing in order to allow equilibrium of water over the starch.

3.2. Heating-shearing treatment in the shear cell

The starch-water mixture was thermomechanically treated in a newly developed shearing device. This new device was based on a cone and plate rheometer concept. It was designed and sized at pilot scale. Thickness of the product layer was kept small compared to the diameter of the cone, in order to apply the desired shear rates at relatively low rotation speeds, thereby avoiding circular flow and guarantee ideal flow conditions. The engine was chosen in such a way that shearing stresses up to $6 \cdot 10^4$ Pa, comparable to extrusion processes, were possible.

Table 1: Treatment conditions and results for a mixture of waxy corn starch and 30% water processed in the shear cell. Exp. no. = experiment number; N = rotation speed; T = temperature; t = treatment time; τ_{max} = maximal shear stress during the measurement; $\tau \cdot t$ = shear stress multiplied by time; *SME* = Specific Mechanical Energy; % crystalline = percentage of A-type crystals as measured by X-Ray diffraction; *[η]* = intrinsic viscosity.

Exp. no.	N (rpm)	T (°C)	t (s)	τ_{max} (10^4 Pa)	$\tau \cdot t$ (10^6 Pa·s)	*SME* (10^8 J/m^3)	% crystalline	*[η]* (ml/g)
Native	-	-	-	-	-	-	26.0	165
1	10	110	900	1.11	2.49	0.42	13.5	126
2	35	110	900	1.94	1.98	0.58	14.8	114
3	75	110	750	1.97	6.89	4.89	11.2	97
4	35	100	900	1.76	2.40	0.93	17.2	128
5	35	100	900	1.88	2.12	0.96	17.2	113
6	75	100	1200	2.96	5.50	4.58	11.2	81
7	75	100	900	3.89	3.10	3.18	14.6	82
8	75	85	960	3.68	5.29	4.22	15.3	89
9	75	85	1200	3.94	8.69	10.52	12.5	80
10	75	85	960	4.58	6.72	8.82	12.2	71

The shearing device and its dimensions are shown in figure 2. After the shearing zone (1) was filled, the starch-water mixture was heated by the electrical heating elements (2) in the cone and sheared between the rotating plate (3) and the non-rotating cone (4). A thermocouple (5) monitored the sample temperature. As soon as the temperature set point was reached, the engine was started. During the treatment of sample 1, rotation speed was kept constant at 10 rpm, corresponding to a shear rate of 24 s^{-1}. During the treatment of samples 2, 4 and 5, a rotation speed of 35 rpm was applied. To avoid slip and inhomogeneous samples, the rotation speed was obtained in the following steps: the rotation speed was first set at 10 rpm for 300 s, and then at 35 rpm until the end of the run. During the treatment of samples 3 and 6-10, a rotation speed of 75 rpm was applied, again obtained in steps: the rotation speed was first at 10 rpm for 300 s, then at 35 rpm for 250 s, then at 50 rpm for 110 s and finally at 75 rpm until the end of the run. The use of different rotation speed combinations made it possible to change the shear stress and mechanical energy input. Sample size was 130 g in all experiments. Times and temperatures are shown in table 1.

Shear stress during the treatment was determined by measuring the torque (6). The specific mechanical energy input during the treatment in the shear cell (SME_{SC}) was calculated according to (based on Meuser *et al.*, 1984):

$$SME_{SC} = \frac{\int_0^t torque \cdot \omega \cdot dt}{V} \qquad [6]$$

Also shear stress (τ) and shear stress multiplied by time (τ · t) were calculated from the torque measurements.

After the thermomechanical treatment the shear cell was opened and the heated-sheared sample was directly frozen. Prior to further analysis, samples were dried in an oven at 35°C to 10% water content. After drying, the samples were immersed in liquid nitrogen and ground to pass a 366 µm sieve.

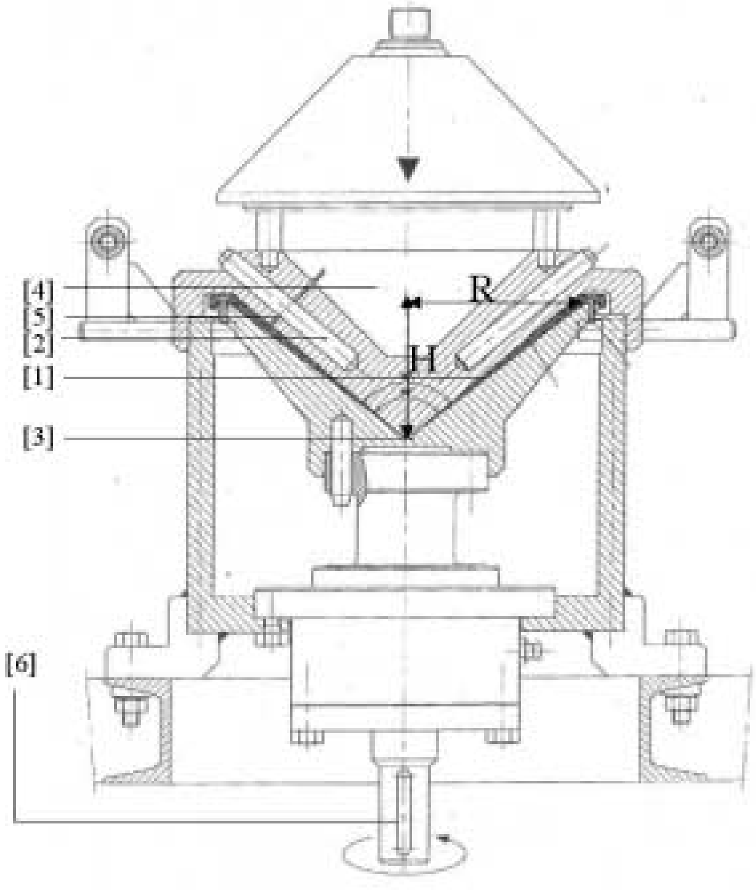

Figure 2: A newly developed shear cell for applying well-defined shear and temperature to low moistened starch. Cone angle = 100°, shear zone angle θ = 2.5°, R = 0.1 m, H = 0.082 m.

3.3. Analysis

Intrinsic viscosity *[η]* of the samples was measured at 25°C with an Ubbelohde viscometer (Fujio *et al.*, 1995). Starch was dissolved in 1 M KOH for 45 minutes and 6 concentrations in the range of 0.5-2 mg/ml were used (solvent flow time = 332 s). Values of the intrinsic viscosity measurement could be reproduced within a range of 5%.

Crystallite type of the starch and percentage of crystalline material was determined using a Philips PC-APD PW 3710 powder X-Ray diffractometer.

3.4. Mathematical comparison of models

In order to find the key parameter to starch degradation, the models described in the theory section were fitted to the data. In order to find the best model and thus the key parameter for starch degradation, two methods were used. As a first indication, the R^2 values were compared. Secondly, the Akaike information criterion was used (Akaike, 1973):

$$AIC = n\ln(s^2) + 2p + \frac{2p(p+1)}{n-p-1} \qquad [7]$$

$$s^2 = \frac{RSS}{n} \qquad [8]$$

The criterion states that if two models are compared, model 2 is considered to give a better fit than model 1 if $AIC_1 - AIC_2 > 5$.

Furthermore, the intercepts of the fits can be considered physically correct only if they are equal to or higher than 1 (see Theory section). Therefore, also the fitted values of the intercept were used to compare the models.

4. Results and discussion

4.1. Paste formation and melting

In all experiments, a melt with small powdery fractions was obtained, comparable to the results of Barron *et al.* (2000) on heating-shearing treatment of pea starch below the melting temperature. X-Ray diffraction measurements showed that indeed part of the material was not molten (table 1) and that all samples displayed A-type crystals, the same type as the native starch.

Development of the shear stress in time appeared to be sensitive to the exact conditions during preparation and filling. Therefore, starting with the same conditions could lead to a variety in shear stresses (τ, SME; table 1). Therefore, it was decided to relate the measured process data to the product properties.

4.2. Macromolecular degradation during heating-shearing treatment

In all samples, macromolecular degradation took place as evident from a decrease in intrinsic viscosity (table 1). In order to find the key factor to starch degradation, equations [3] to [5] were fitted to the data (figures 3, 4 and 5). The parameter values obtained, the correlation coefficients (R^2 values) and the values for the Akaike information criteria are shown in table 2. The first order SME and $\tau \cdot t$-based literature models yielded low R^2 values (<0.67), whereas an acceptable fit (R^2=0.933) could be obtained using a first order model based on the maximal shear stress τ_{max}. The calculated Akaike criteria showed that the τ_{max} based model described the data significantly better than the SME and $\tau \cdot t$ based models: the difference between the Akaike criteria was higher than 5. Thus, at the temperatures investigated the process of starch degradation on a macroscopic scale is time independent within time scales investigated, which is in agreement with the fundamental conclusion by Beyer (2000) for cleavage of covalent bonds.

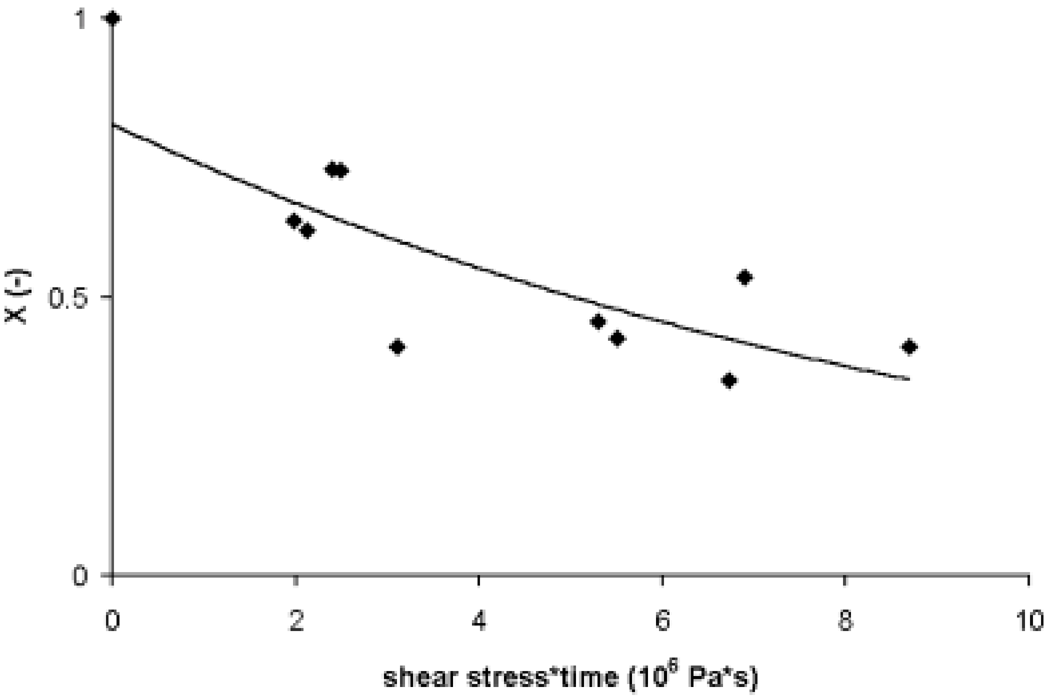

Figure 3: Relative intrinsic viscosity *X* of heated- and heated-sheared waxy corn starch as a function of $\tau \cdot t$. Points are the measurements, the line is the fitted first order model.

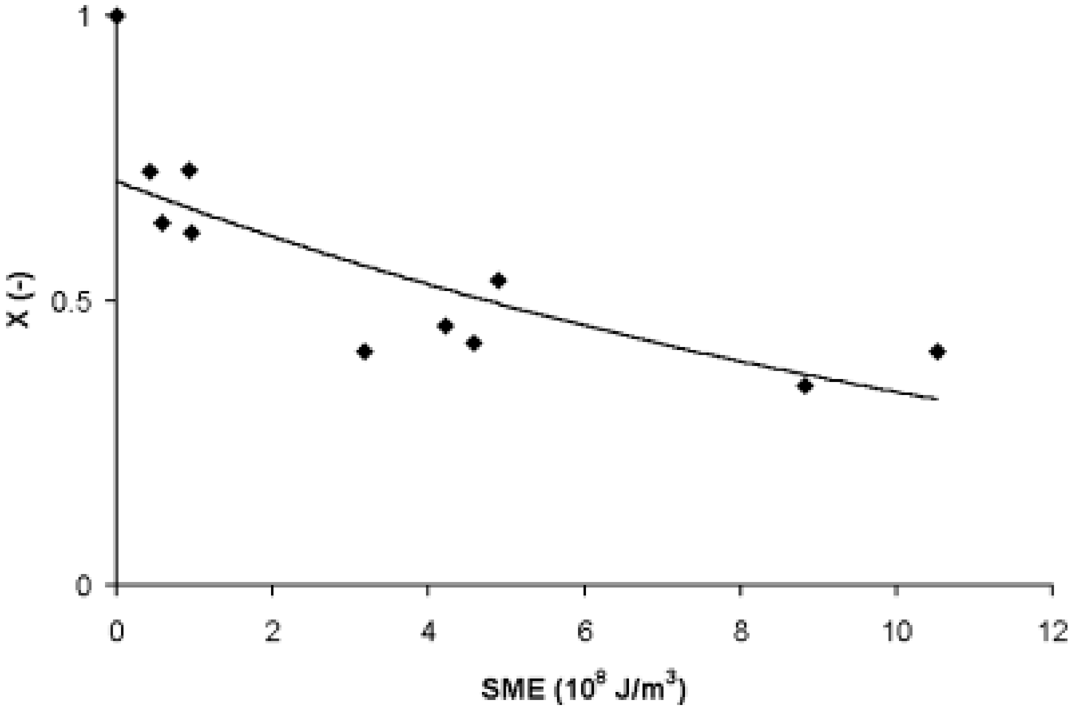

Figure 4: Relative intrinsic viscosity *X* of heated- and heated-sheared waxy corn starch as a function of *SME*. Points are the measurements, the line is the fitted first order model.

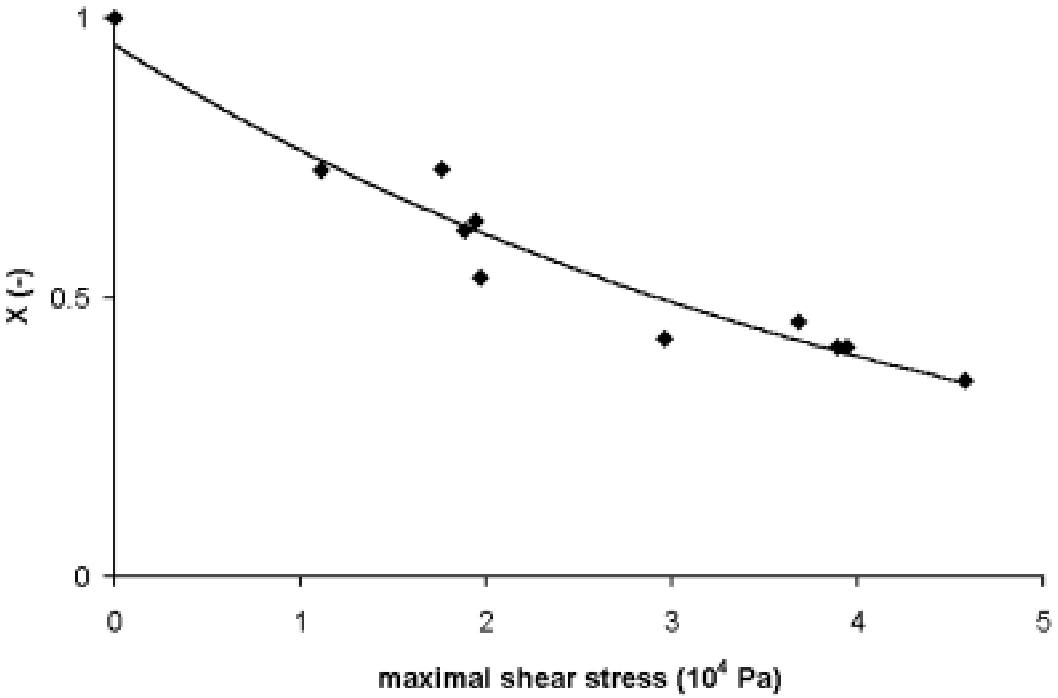

Figure 5: Relative intrinsic viscosity *X* of heated- and heated-sheared waxy corn starch as a function of maximal shear stress τ_{max}. Points are the measurements; the line is the fitted first order model.

Table 2: Fit parameters, R^2 and AIC values for different first order models including melt correction (see text) fitted to the data given in table 1.

Model	C_1	C_2	R^2	AIC
Diosady *et al.* (1985) $X = C_1 \exp(-C_2 \cdot \tau t)$	0.81	$9.60 \cdot 10^{-8}$	0.64	-46.6
Parker *et al.* (1990) $X = C_1 \exp(-C_2 \cdot \mathrm{SME})$	0.71	$7.37 \cdot 10^{-10}$	0.66	-44.8
New model $X = C_1 \exp(-C_2 \cdot \tau_{\max})$	0.95	$2.20 \cdot 10^{-5}$	0.93	-66.3

The value of the constant C_{1c} in the $\tau_{\max}$ based model was 0.95. As long as no thermal degradation takes place, one would expect the value to be at least 1 (see Theory). Although the uncertainty in the intrinsic viscosity experiments is such that the value is not significantly different from unity, it may be an indication that some thermal degradation took place. In order to check this, heating without shearing was applied both at 85 and 110°C for 15 minutes. The sample treated at 110°C had an intrinsic viscosity of 158 g/ml. This very small difference from the value of native starch might explain why the constant C_{1c} in the $\tau_{\max}$ based model was slightly below 1. Thermal treatment at 85°C decreased the intrinsic viscosity to 140 g/ml. This value was found in many replications of this experiment. This might be related to the solubility of the starch. After the thermal treatment at 85°C it was very difficult to dissolve the starch in a KOH solution. This might be responsible for the low intrinsic viscosity measured subsequently. However, these solubility problems were not observed on any of the thermomechanically treated samples. Comparison of samples 7 and 9, which have the same maximal shear stress but different treatment temperatures (table 1), clearly shows that the effect described above was not found in the heating-shearing experiments.

The constants C_{1a} and C_{1b} in the $\tau \cdot t$ and SME based models respectively were significantly lower than 1 (table 2). The thermal effects described above can not account for these low values of the constants, showing that the physical background of these models can not be correct. Again, this indicates that the time independent model should be used to predict starch degradation at the temperatures and process times investigated.

The fact that Vergnes *et al.* (1987) found a good correlation between SME in a rheometer, implying a kind of time-shear equivalence, may be explained from the applied higher temperatures (140 - 180°C). Thermal, time-dependent effects are not negligible anymore at these temperatures, so that a correlation with time is expected. Furthermore, possible interactions between thermal and shear effect might occur at these temperatures as well, which could further induce an effect of time on the results.

4.3. Explanation of degradation effects during extrusion processes

From the measurements, we suggest the following degradation pattern during extrusion at the temperatures investigated.

As long as all material is powdery, no degradation takes place because no significant shear force is applied to the starch molecules, as also found by Colonna *et al.* (1983). As the material begins to melt, shear stress is applied to the starch, causing the larger molecules in the molten parts to be degraded. The degradation pattern now becomes more complex as viscosity and shear stress on one hand decrease due to the breakdown of the macromolecules, but on the other hand increase due to further melting of the material. Furthermore, the breakdown will be inhomogeneous, because the shear rate, and thus the shear stress, varies locally in the extruder. Thus, it is expected that the degradation continues in time along the length of the extruder, although the degradation process itself is time-independent.

During extrusion trials, the SME is coupled to the shear stresses along the barrel. Typically, higher maximal shear stresses in the extruder lead to a higher torque on the engine and thus to a higher SME. Therefore, it is not surprising that in extrusion processes a good correlation between SME and starch breakdown can be obtained as for example found by Parker *et al.* (1990) and Willett *et al.* (1997).

Using the degradation pattern described above, we are now able to formulate how to prevent undesired degradation during extrusion (at the temperatures investigated in this paper) and to review how well the extruder performs if molecular weight reduction is a desired process.

According to our insights, undesired macromolecular degradation during extrusion processes can be reduced by decreasing the screw speed or increasing the depths of the gaps, so that the maximal shear stress is lower. The expected effect of screw speed is in accordance with data of Della Valle *et al.* (1995) on extrusion of potato starch. It is also in agreement with data of Della Valle *et al.* (1996) on extrusion of waxy corn starch and with data of Colonna and Mercier (1983) on extrusion of manioc starch, although in these two studies the effect of screw speed was investigated at higher temperatures, so that thermal effects may have to be taken into account. Increasing the moisture content will also lower the maximal shear stress and thus reduce the macromolecular degradation, although thermal effects might be more important at higher moisture content, as indicated by Igura *et al.* (2001). The expected effect of moisture content is in accordance with data of Chinnaswamy and Hanna (1990) on extrusion of corn starch and with data of Davidson *et al.* (1984) on extrusion of wheat starch.

On the other hand, if molecular reduction is desirable, the inhomogeneity of conditions in an extruder is a source of inefficiency, as only the high shear spots in the extruder are effective.

5. Concluding summary

At the temperatures investigated, the maximal shear stress during heating-shearing treatment was found to be the key parameter determining the degree of macromolecular degradation of starch. This conclusion could be drawn only by means of separating the effects of shear and time showing that the newly developed shear cell is a useful tool in understanding effects of shear, temperature and time on the properties of low moistened starch and probably other materials.

The degree of macromolecular degradation during extrusion processes can be reduced by decreasing the maximal shear stresses by decreasing screw speed or increasing the depths of the gaps, but the residence time does not play a role for the breaking process itself. Increasing moisture content also decreases the maximal shear stress, although it might also affect thermal breakdown effects. The results presented can form a basis to develop predictive models enabling exact description of starch degradation.

List of symbols

C_1	first fit parameter in first order model (-)
C_{1a}	first fit parameter in first order *SME* model (-)
C_{1b}	first fit parameter in first order $\tau \cdot t$ model (-)
C_{1c}	first fit parameter in first order τ_{max} model (-)
C_{2a}	second fit parameter in first order *SME* model (m^3/J)
C_{2b}	second fit parameter in first order $\tau \cdot t$ model ($m^2/(N \cdot s)$)
C_{2c}	second fit parameter in first order τ_{max} model (m^2/N)

f	fraction of molten material (-)
H	height of the cone (m)
MC	moisture content (%)
Mw	molecular weight (Da)
n	number of experiments (-)
N	rotation speed (rpm)
p	number of parameters (-)
R	radius of the cone at the top of the shearing zone (m)
RSS	residual sum of squares (-)
s	standard deviation
SME	specific mechanical energy (J/m^3)
SME_{SC}	specific mechanical energy as calculated for the new shearing device (J/m^3)
t	time (s)
V	volume (m^3)
X	relative intrinsic viscosity of the molten fraction of the treated starch compared to native starch (-)

Greek symbols

γ	shear rate (s^{-1})
$[\eta]$	intrinsic viscosity (ml/g)
$[\eta]_i$	intrinsic viscosity of the molten starch fraction (ml/g)
$[\eta]_{rs}$	intrinsic viscosity of the unmolten starch fraction (equals intrinsic viscosity of native starch (ml/g)
θ	angle of the shear zone of the newly developed shearing device (˚)
τ	shear stress (N/m^2)
τ_{max}	maximal shear stress (N/m^2)
ω	angular velocity [= $2\pi N/60$] (rad/s)

References

Akaike, H. (1973). Information theory and an extension of the maximum likelihood principle. In N. Petrov, & F. Csaki. *Proceedings of the 2nd international symposium on information theory* (p. 267-281). Budapest: Akademiai Kiado.

Barron, C., Buleon, A., Colonna, P., & Valle, G. Della (2000). Structural modifications of low hydrated pea starch subjected to high thermomechanical processing. *Carbohydrate Polymers*, 43, 171-181.

Baud, B., Colonna, P., Valle, G. Della, & Roger, P. (1999). Macromolecular degradation of extruded starches measured by HPSEC-MALLS. *Biopolymer Science: Food and Non Food Applications / Les Colloques de l'INRA*, 91, 217-221.

Beyer, M.K. (2000). The mechanical strength of a covalent bond calculated by density function theory. *Journal of Chemical Physics*, 112(17), 7307-7312.

Bindzus, W., Fayard, G., Lengerich, B. van, & Meuser, F. (2002). Description of extrudate characteristics in relation to the shear stress of plasticised starches determined in-line. *Starch / Staerke*, 54, 252-259.

Bruemmer, T., Meuser, F., Lengerich, B. van, & Niemann, C. (2002). Expansion and functional properties of corn starch extrudates related to their molecular degradation, product temperature and water content. *Starch / Staerke*, 54, 9-15.

Chinnaswamy, R., & Hanna, M.A. (1990). Macromolecular and functional properties of native and extrusion cooked starch. *Cereal Chemistry*, 67(5), 490-499.

Colonna, P., & Mercier, C. (1983). Macromolecular modifications of manioc starch components by extrusion-cooking with and without lipids. *Carbohydrate Polymers*, 3, 87-108.

Colonna, P., Melcion, J.P., Vergnes, B., & Mercier, C. (1983). Flow, mixing and residence time distribution of maize starch within a twin-screw extruder with a longitudinally split barrel. *Journal of Cereal Science*, 1, 115-125.

Davidson, V.J., Paton, D., Diosady, L.L., & Larocque, G. (1984). Degradation of wheat starch in a single-screw extruder: characteristics of extruded starch polymers. *Journal of Food Science*, 49, 453-458.

Diosady, L.L., Paton, D., Rosen, N., Rubin, L.J., & Athanassoulias, C. (1985). Degradation of wheat starch in a single-screw extruder: mechano-kinetic breakdown of cooked starch. *Journal of Food Science*, 50, 1697-1699, 1706.

Fujio, Y., Igura, N., & Hayakawa, I. (1995). Depolymerization of molten-moisturized-starch molecules by shearing force under high temperature. *Starch/Staerke*, 47(4), 143-145.

Grandbois, M., Beyer, M.K., Rief, M., Clausen-Schaumann, H., & Gaub, H.E. (1999). How strong is a covalent bond? *Science*, 283, 1727-1730.

Igura, N., Hayakawa, I., & Fujio, Y. (1997). Effect of longer heating time on depolymerization of low moisturized starches. *Starch / Staerke*, 49(1), 2-5.

Igura, N., Katoh, T., Hayakawa, I., & Fujio, Y. (2001). Degradation profiles of potato starch melts through a capillary type viscometer. *Starch / Staerke*, 53(12), 623-628.

Meuser, F., Lengerich, B. van, & Reimers, H. (1984). Kochextrusion von Staerken. Vergleich experimenteller Ergebnisse zwischen Laborextrudern und Produktionsextrudern mittels Systemanalyse. *Starch / Staerke*, 36(6), 194-199.

Millard, M.M., Dintzis, F.R., Willett, J.L., & Klavons, J.A. (1997). Light-scattering molecular weights and intrinsic viscosities of processed waxy maize starches in 90% dimethyl sulfoxide and H_2O. *Cereal Chemistry*, 74(5), 687-691.

Parker, R., Ollett, A.L., & Smith, A.C. (1990). Starch melt rheology: measurement, modelling and applications to extrusion processing. In P. Zeuthen. *Processing and quality of foods* (pp. 1.290-1.295). London: Elsevier.

Valle, G. Della, Boché, Y., Colonna, P., & Vergnes, B. (1995). The extrusion behaviour of potato starch. *Carbohydrate Polymers*, 28, 255-264.

Valle, G. Della, Colonna, P., Patria, A., & Vergnes, B. (1996). Influence of amylose content on the viscous behavior of low hydrated molten starches. *Journal of Rheology*, 40(3), 347-362.

Vergnes, B., Villemaire, J. P., Colonna, P., & Tayeb, J. (1987). Interrelationships between thermomechanical treatment and macromolecular degradation of maize starch in a novel rheometer with preshearing. *Journal of Cereal Science*, 5, 189-202.

Willett, J.L., Millard, M.M. & Jasberg, B.K. (1997). Extrusion of waxy maize starch: melt rheology and molecular weight degradation of amylopectin. *Polymer*, 38(24), 5983-5989.

Chapter 3

A mechanistic model on the relation between molecular structure of amylopectin and macromolecular degradation during heating-shearing processes

Abstract

A molecular scale model describing the molecular breakdown of low moisture amylopectin melts by shear forces was derived and compared to engineering scale experiments. The model is based on the assumption that the maximum shear stress on the polymer equals the effective surface stress on that polymer, which is related to the strength of the glycosidic bonds. The molecules are approximated as spheres, with a radius that exhibits fractal scaling with molecular weight. The molecular weight reduction as a function of applied shear stress as deduced from the model agrees satisfactorily with the results from experimentally obtained engineering scale data. The results show a successful example of a coupling between engineering scale experiments and micro-scale models and contribute to the understanding of fundamental changes in properties of starch during industrial scale heating-shearing processes.

This chapter was accepted for publication in *Polymer Degradation and Stability* as: R.M. van den Einde, E. van der Linden, A.J. van der Goot, R.M. Boom, A mechanistic model on the relation between molecular structure of amylopectin and macromolecular degradation during heating-shearing processes.

1. Introduction

The use of biopolymers for both food and non-food products is gaining more attention, partly because of ever stricter demands on product quality, partly for sustainability reasons. For industrial use, these products should meet high quality demands, leading to a need for new and flexible processes. Therefore, obtaining quantitative understanding of the phenomena that are taking place is essential for rational design of new processes.

Practical biopolymer systems are usually complex systems, being mixtures of components that may have complex molecular structures themselves. This often leads to a more or less semi-empirical approach to the design of processes and process equipment. Unfortunately, this also leads to a gap between fundamental, molecular scale mechanistic studies and the larger scale semi-empirical models.

This paper aims to interpret some aspects of the widely applied process of heating shearing treatment of low moistened starch, for example in the form of extrusion processes, into a mechanistic, molecular scale model. One of the phenomena that take place during heating shearing treatment is the degradation of starch to smaller fragments. This degradation has considerable impact, which can be positive as well as negative, on the properties of the end product, such as product cohesiveness (Harper, 1986), expansion at the extruder die (Chinnaswamy and Hanna, 1990; Bruemmer *et al.*, 2002), cold paste viscosity and water solubility (Bruemmer *et al.*, 2002).

Despite the importance of macromolecular degradation, its mechanism is still largely unknown. This is partly due to the fact that the shear rate and temperature are difficult to control in most engineering scale equipment handling high viscosity products. Another reason might be that the behavior of low moistened starch during heating and shearing is complex (Vergnes *et al.*, 1987), among others due to the changes in rheological properties as a consequence of the combination of melting of crystallites and molecular breakdown.

In earlier work, a pilot-scale shear cell was developed in which temperature, shear rate and time were well-defined and could be controlled independently (Van den Einde *et al.*, 2004). We showed that at temperatures between 85 and 110°C the maximally attained value of the shear stress during a heating-shearing treatment of moistened waxy corn starch determines the degree of macromolecular degradation. In this paper, the engineering scale experiments are coupled to a quantitative micro scale model describing the molecular weight reduction of starch as a function of the maximum shear stress applied. The results allow a molecular scale explanation of the starch breakdown phenomena occurring during heating shearing treatment.

2. Theory

We propose a model that relates the shear stress in a polymer melt, in our case molten amylopectin, during heating-shearing treatment, to the maximally allowed molecular weight of the polymer at these shear stress conditions. The structure of amylopectin is (in 2D) schematically shown in figure 1.

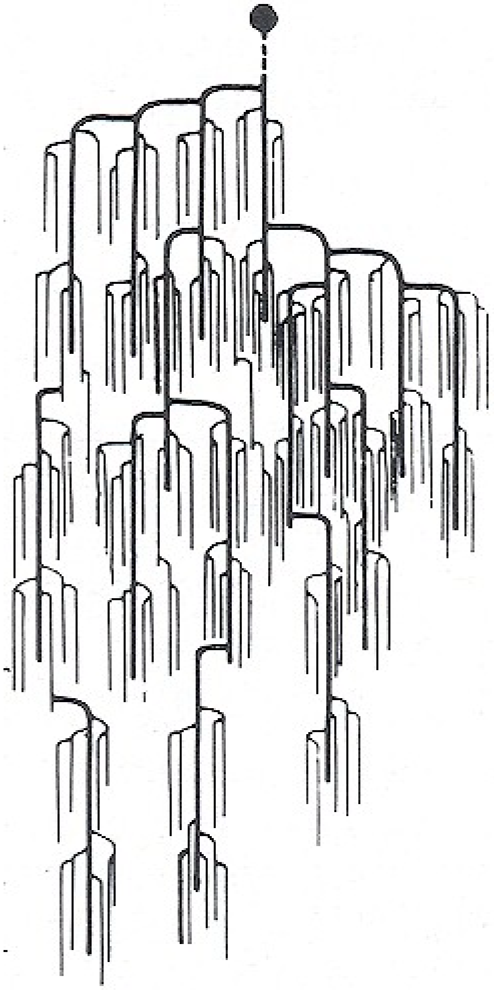

Figure 1: Structure of amylopectin (Robin *et al.*, 1974).

We start with the hypothesis that shear stress on a polymer material translates into an effective surface stress on that polymer molecule. For a sphere of radius R and surface tension σ, this surface stress can be written as $2\sigma/R$ and hence, the shear stress results in an equivalent surface tension $\sigma = 0.5\ \tau\ R$. This effective surface tension is internally counteracted by the total internal elastic energy of the polymer projected onto its surface (defined as the surface of the sphere with radius r that just encloses the polymer) per unit of surface area. The idea of using an effective surface tension equivalent to the total internal elastic energy of a material in a spherical geometry has been proposed for spherically symmetric lamellar liquid crystalline phases or layered, spherical structures, also called “onions” (Van der Linden and Dröge, 1993). The according effective surface tension was subsequently used to evaluate the surface stress and to explain the size of the onions as a function of the shear stress exerted on the lamellar liquid crystalline phase (Van der Linden *et al.*, 1996). Analogously, in our current case of a polymer under shear stress, the maximal shear stress $\tau_{\max}$ just before breakup is described as:

$$\tau_{\max} = b\frac{\sigma_{eff}}{r} \qquad [1]$$

where b was found to be a constant of order unity for linear macromolecules (Silberberg and Kuhn, 1952, 1954), whereas for lamellar droplets in a liquid crystalline phase, $b = 2$ was found to be a plausible value (Van der Linden *et al.*, 1996). Applying a force balance between the surface stress and the elastic forces inside the molecule results in:

$$-\frac{1}{b}\tau r + \frac{n_b E_b}{4\pi r^2} = 0 \qquad [2a]$$

and hence:

$$\sigma_{eff} = \frac{n_b E_b}{4\pi r^2} \qquad [2b]$$

where n_b is the number of bonds with energy E_b in the amylopectin molecule. Considering the inflexibility of the chair-shaped glucose unit, only the energy of the glycosidic C-O bonds is assumed to be important. We assume that the energy is divided equally over all glycosidic bonds and that rupture occurs only if the total force exceeds a certain value. Thus, the following relation was obtained:

$$n_b E_b = \frac{Mw}{M_{glu}} E_{C-O} = DP \cdot E_{C-O} \qquad [3]$$

where Mw denotes the molecular weight, M_{glu} denotes the mass of a glucose unit and DP is the degree of polymerization. Using the fact that the radius has been found to obey fractal scaling with molecular weight (Bello-Perez *et al.*, 1998), one finds:

$$\frac{r}{a} = \left(\frac{Mw}{DP_0 M_{glu}} \right)^{1/D_f} = \left(\frac{DP}{DP_0} \right)^{1/D_f} \qquad [4]$$

where a and DP_0 are the radius and the degree of polymerization of a statistical unit in the fractal structure respectively, D_f denotes the fractal dimension and DP is the degree of polymerization of the whole amylopectin molecule. It was assumed that the length of a statistical unit equals the average chain length in between branches. Hence, DP_0 is equal to 17.3 for starch with A-type crystals such as waxy corn (Gerard *et al.*, 2000). The radius of a glucose unit is about 0.295 nm and thus $a = 5.1$ nm.

Roger and co-workers found that the fractal dimension of corn amylopectin dissolved by microwave heating in aqueous solution was 1.8-2.2 (Roger *et al.*, 1999). Hanselmann and co-workers found that the fractal dimension of waxy corn starch in aqueous solution after 20 minutes of heating at 175°C was 2.39, which increased upon longer heating (Hanselmann *et al.*, 1996).

Substituting equations [2b-4] into equation [1] and taking the logarithm on each side yields:

$$\log(\tau_{\max}) = \left(1 - \frac{3}{D_f} \right) \log Mw + \log \left(\frac{bE_{C-O} DP_0^{\frac{3}{D_f}}}{4\pi a^3 M_{glu}^{1-\frac{3}{D_f}}} \right) \qquad [5]$$

Thus, a log-log plot of τ_{max} vs. Mw is expected to yield a straight line. The slope of the line reveals the fractal dimension, whereas the intercept may reveal a value for the average energy of the C-O bond in the system.

3. Experimental section

3.1. Heating shearing treatment

Moistened waxy corn starch (moisture content 30%) was heated and sheared in our self-developed shear cell at temperatures 85-110°C, as described earlier (Van den Einde *et al.*, 2004). At these temperatures, the effect of heating on depolymerization is negligible and all degradation is induced by the shear force (Van den Einde *et al.*, 2004). Experiments used for the model were those described earlier (Van den Einde *et al.*, 2004). Temperatures and maximal shear stresses are given in table 1.

Table 1: Maximal shear stress and intrinsic viscosity for a mixture of waxy corn starch and 30% water processed in the shear cell. Exp. no. = experiment number, 0 = native starch, T = temperature (°C), τ_{max} = maximally attained shear stress during the treatment (10^4 Pa), $[\eta]$ = intrinsic viscosity (ml/g).

Exp. no.	T	τ_{max}	$[\eta]$
0	-	-	165
1	110	1.11	126
2	110	1.94	114
3	110	1.97	97
4	100	1.76	128
5	100	1.88	113
6	100	2.96	81
7	100	3.89	82
8	85	3.68	89
9	85	3.94	80
10	85	4.20	86
11	85	4.58	71

3.2. Analysis

Intrinsic viscosity of the samples was determined as described earlier (Van den Einde *et al.*, 2004). In order to check validity of the intrinsic viscosity as a measure for the molecular weight of the sample, molecular weight distribution of part of the samples was determined using an HPSEC MALLS RI system. Native starch and samples 6 and 9 were dissolved in a 90% DMSO solution in water, whereas samples 7 and 11 were dissolved in 1 M NaOH. Concentration was 8 mg/ml in all cases. One Beckmann PWL-PRE prepguard precolumn and six Spherogel TSK columns were used for separation. Flow rate was 1 ml/minute. Refractive Index was measured using a Waters 410 differential refractometer, whereas laser light scattering was measured using a Dawn D Laser Photometer (Wyatt Technology).

The obtained Mw distribution curves for sample 11 and native starch are shown in figure 2. Intrinsic viscosity of sample 11, as well as intrinsic viscosity of samples 6, 7 and 9, could be well correlated to the weight-averaged molecular weight obtained from HPSEC MALLS RI data using the equation earlier found by Millard *et al.* (1997):

$$[\eta] = 0.59 Mw^{0.29} \qquad [6]$$

For sample 11, *Mw* obtained from HPSEC MALLS RI (figure 2) was $1.25 \cdot 10^7$ g/mole, so that [η] according to equation [6] was 67, which is in good agreement with the measured value of 71 (table 1).

For native starch, equation [6] could be applied to correlate intrinsic viscosity with the molecular weight obtained from HPSEC MALLS RI data if a slightly higher exponent was used (0.30). This value of the exponent is still within the margins suggested by Millard *et al.* (1997). Although equation [6] is quite sensitive to the value of the exponent, the outcome of the model presented in the Results and discussion section is not. Therefore, the molecular weight of all heated-sheared samples was obtained from the measurement of the intrinsic viscosity using equation [6] with exponent 0.29.

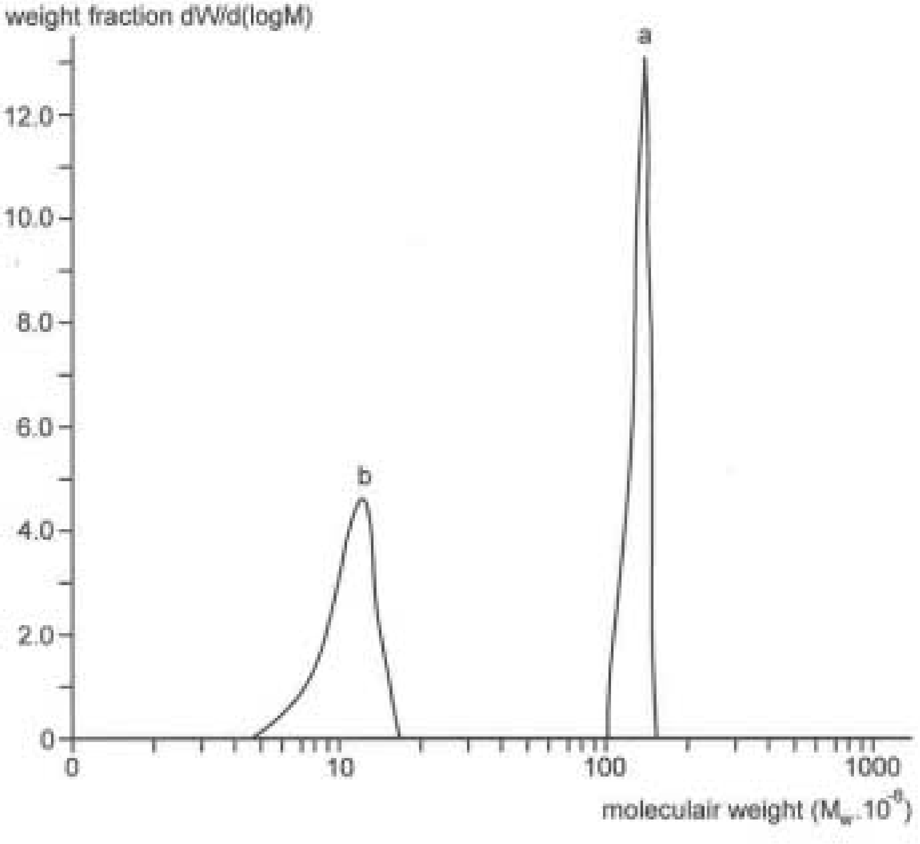

Figure 2: Example of HPSEC MALLS curves obtained from native waxy corn starch (a) and one of the heated-sheared waxy corn starch samples (experiment 11, b).

4. Results and discussion

4.1. Model fit and value of fractal dimension

Figure 3 shows the log-log plot of molecular weight as a function of the maximal shear stress τ_{max}. The model fitted all the data with $R^2 = 0.84$, which can be considered satisfactory. The residuals were distributed randomly.

Table 2 shows the calculated fractal dimension, the estimated average bond energy and the calculated energy of a glycosidic C-O bond, including expected values from literature.

The fractal dimension as deduced from applying our model to the data points was 1.9, which is in good agreement with the values of 1.8-2.2 as found by Roger *et al.* (1999). The larger difference between our value and the value obtained by Hanselmann *et al.* (1996) is probably due to the high temperature (175°C) that these authors used to dissolve the starch. Longer heating treatment at that temperature was shown to increase the fractal dimension (Hanselmann *et al.*, 1996).

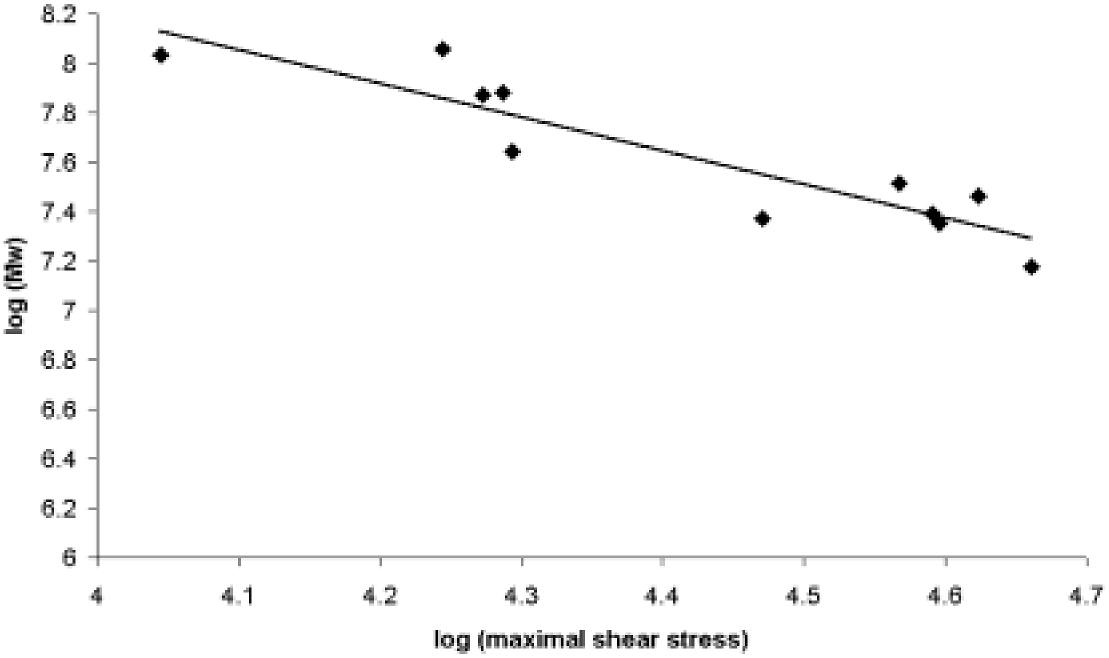

Figure 3: Logarithm of the molecular weight (calculated from intrinsic viscosity measurements) as a function of the applied maximal shear stress during heating-shearing treatment. Points are the measured data; the line is the fitted model (see theory section).

Table 2: Fitted and literature values of the fractal dimension D_f (-) and the average energy of the C-O bond $E_{C\text{-}O}$ (kJ/mole; see text).

	Fitted value	Literature values
D_f	1.9	1.8-2.2 (Roger *et al.*, 1999)
$E_{C\text{-}O}$	272	280 (Weast, 1979)

4.2. Value of bond energy

The average bond energy found when applying our model was $2.72 \cdot 10^5$ J/mole when taking b=2 (equation [1]). This is in accordance with the value for complete breakdown of the bond into radicals (= $2.8 \cdot 10^5$ J/mole (Weast, 1979)). Although it should be noted that all estimations made in the model lead to a degree of uncertainty, the value found suggests that the mechanism resembles breakdown by physical stress on the bonds, during which radicals may be formed. Furthermore, the fact that the energy found here is close to this literature value seems to imply that indeed the stress is divided more or less equally over all bonds, as was assumed in equation [3]. Hence, each bond is evenly likely to break. Bond breakage at the inside of the molecule (endodegradation) is effective in lowering the stress and will therefore stop further breakdown, leading to a shift in molecular weight distribution, as found in this work (figure 2). On the other hand, if a bond near the outside breaks (exodegradation), the stress will not become lower and therefore breakdown will continue until the molecule has become sufficiently smaller. However, although the number of small fragments that can arise from this exodegradation can be quite high, the total mass of these fragments (which is detected by the HPSEC MALLS system) will still be low. Hence, only the total mass of the high molecular weight components formed is sufficient for measuring, resulting in the molecular weight distribution shown in figure 2.

4.3. Extension of results to other systems

The model described in this paper relates molecular structure (a, D_f) to breakdown due to shear. The model hence reveals structure-function relationships for amylopectin and also possibly other polymers, as long as the polymer in the melt can be considered more or less as a sphere. Such relationships can be useful guidelines for initial process design. Two examples are given below.

Effect of solvent quality. Increasing solvent quality results in a lower fractal dimension as the molecule tends to adopt a less compact shape. For two solvents that are resulting in the same melt viscosity and that have the same degree of reactivity with the polymer, the better solvent will result in more degradation, as decreasing the fractal dimension reduces the maximally allowed shear stress before breakdown.

Effect of average chain length. A higher average branch length or in other words a more linear molecular structure implies a higher value of *a* and hence decreases the shear stress required to breakdown the polymer to a certain molecular weight. This means that a relatively less branched polymer will break down at lower shear stresses due to its higher hydrodynamic volume at the same molecular weight. However, this statement only holds if the more or less spherical shape of the polymer is not significantly affected.

During shear-induced starch degradation at the temperatures investigated the average statistical chain length *a* does not change (Bruemmer, 1999), so that the effect described above does not influence the outcome for amylopectin.

5. Conclusion

In this work, a model has been proposed that relate the molecular breakdown of starch with the maximum shear stress. The model is based on a stress balance projected onto the outer shell of the molecule. Important parameters are the C-O bond strength and the fractal dimension of amylopectin. The application to our experimental data yielded a fractal dimension of 1.9, which was in good agreement with literature data. The value obtained for the bond energy was close to the value for physical bond rupture.

The model developed here provides a tool for choosing the correct process parameters in order to induce breakdown of starch to the desired molecular weight. Some implications could be formulated for processes operating at different conditions, or with materials having different molecular structure. Our results suggest that coupling molecular scale phenomena to these types of complex processes improves understanding of the fundamental changes in properties of starch during engineering scale processes and will be essential in future process design.

Acknowledgement

The authors thank A. Postma for carrying out part of the HPSEC MALLS measurements and J.J.G. van Soest for his kind assistance with the HPSEC MALLS measurements.

Symbols list

a	radius of a statistical unit in the fractal type structure (m)
b	constant relating the surface stress to the effective surface tension divided by the radius (-)
D_f	fractal dimension (-)
DP	degree of polymerization (-)
DP_0	degree of polymerization of a statistical unit in the fractal type structure (-)
E_b	bond energy (J)
E_{C-O}	energy of a C-O bond (J or J/mole)
M_{glu}	molecular weight of a glucose unit (=162 Da)
Mw	molecular weight (Da)
n_b	number of bonds contributing to the effective surface energy in a molecule (-)
r	radius (m)

Greek symbols

$[\eta]$	intrinsic viscosity (g/ml)
σ_{eff}	effective surface tension (J/m^2)
τ_{max}	maximal shear stress (Pa)

References

Bello-Perez, L.A., Roger, P., Colonna, P., & Paredes-Lopez, O. (1998). Laser light scattering of high amylose and high amylopectin materials, stability in water after microwave dispersion. *Carbohydrate Polymers*, 37, 383-394.

Bruemmer T. (1999). Charakterisierung molekularer Strukturparameter kochextrudierter Maisstaerken und Ermittlung von Struktur-Eigenschaftsbeziehungen. Berlin: Technische Universitaet Berlin.

Bruemmer, T., Meuser, F., Lengerich, B. van, & Niemann, C. (2002). Expansion and functional properties of corn starch extrudates related to their molecular degradation, product temperature and water content. *Starch / Staerke*, 54, 9-15.

Chinnaswamy, R., & Hanna, M.A. (1990). Macromolecular and functional properties of native and extrusion cooked starch. *Cereal Chemistry*, 67(5), 490-499.

Einde, R.M. van den, Bolsius, A., Soest, J.J.G. van, Janssen, L.P.B.M., Goot, A.J. van der, & Boom, R.M. (2004). The effect of thermomechanical treatment on starch breakdown and the consequences for process design. *Carbohydrate Polymers*, 55(1), 57-63. (Chapter 2 of this thesis).

Gérard, C., Planchot, V., Colonna, P., & Bertoft, E. (2000). Relationship between branching density and crystalline structure of A- and B-type maize mutant starches. *Carbohydrate Research*, 326, 130-144.

Hanselmann, R., Burchard, W., Ehrat, M., & Widmer, H.M. (1996). Structural properties of fractionated starch polymers and their dependence on the dissolution process. *Macromolecules*, 29, 3277-3282.

Harper, J.M. (1986). Extrusion texturization of foods. *Food Technology*, 40, 70-76.

Linden, E. van der, & Dröge, J.H.M. (1993). Deformability of lamellar droplets. *Physica A*, 193, 439-447.

Linden, E. van der, Hogervorst, W.T., & Lekkerkerker, H.N.W. (1996). Relation between the size of lamellar droplets in onion phases and their effective surface tension. *Langmuir*, 12, 3127-3130.

Millard, M.M., Dintzis, F.R., Willett J.L., & Klavons, J.A. (1997). Light-scattering molecular weights and intrinsic viscosities of processed waxy maize starches in 90% dimethyl sulfoxide and H_2O. *Cereal Chemistry*, 74(5), 687-691.

Robin, J.P., Mercier, C., Charbonnière, R., & Guilbot, A. (1974). Lintenerized starches. Gel filtration and enzymatic studies of insoluble residue from prolonged acid treatment of potato starch. *Cereal Chemistry*, 51, 389-406.

Roger, P., Bello-Perez, L.A., & Colonna, P. (1999). Contribution of amylose and amylopectin to the light scattering behaviour of starches in aqueous solution. *Polymer*, 40, 6897-6909.

Silberberg, A., & Kuhn, W. (1952). Miscibility of liquids influenced by rate of shear. *Nature*, 170, 450-451.

Silberberg, A., & Kuhn W. (1954). Size and shape of droplets of demixing polymer solutions in a field of flow. *Journal of Polymer Science*,13, 21-42.

Vergnes, B., Villemaire, J.P., Colonna, P., & Tayeb, J. (1987). Interrelationships between thermomechanical treatment and macromolecular degradation of maize starch in a novel rheometer with preshearing. *Journal of Cereal Science*, 5, 189-202.

Weast, R.C. (1979). CRC Handbook of chemistry and physics, 59th ed. (p. F-239). Florida: CRC Press Inc.

Chapter 4

Molecular breakdown of corn starch by thermal and mechanical effects

Abstract

The molecular weight reduction of corn starch at 30-43% moisture during thermal treatment at temperatures 90-160°C and during well-defined thermomechanical treatment at temperatures 90-140°C was investigated. Thermal treatment resulted during the first 5 minutes in a decrease in molecular weight as measured by intrinsic viscosity, after which longer heating had no significant effect. Higher moisture contents and temperatures generally resulted in more breakdown, although the effect diminished at higher temperatures. The decrease in intrinsic viscosity during thermomechanical treatment at relatively low temperatures and moisture contents was shown to be only dependent on the maximal shear stress. At higher temperatures, thermomechanical breakdown could be split into a mechanical part depending on maximal shear stress and a thermal breakdown part, which was again time-dependent in the shorter time-scales only. Higher moisture content during thermomechanical treatment resulted in more thermal breakdown and lowered the shear stresses required for mechanical breakdown. Consequences for process design are discussed briefly.

This chapter was submitted as: R.M. van den Einde, C. Akkermans, A.J. van der Goot, R.M. Boom, Molecular breakdown of corn starch by thermal and mechanical effects.

1. Introduction

The molecular weight of starch influences many properties of starch-based products, such as expansion rate, cold paste viscosity, water solubility and absorption, the degree of retrogradation and gelling properties (Bindzus *et al.*, 2002; Bruemmer *et al.*, 2002; Chinnaswamy and Bhattacharya, 1986; Mua and Jackson, 1997). The production of starch-based products often involves the application of a combination of (shear) stresses and thermal treatment, for example during extrusion. It is known that this combination leads to starch molecular weight reduction (Baud *et al.*, 1999; Willett *et al.*, 1997).

Recently, it was shown that the extent of mechanical degradation of waxy corn starch is determined by the maximal shear stress during a thermomechanical treatment, in the situation that thermal breakdown effects can be neglected (Van den Einde *et al.*, 2004). However, in many practical situations, the temperature is such that thermal degradation is important as well, next to shear-based effects. Fujio *et al.* (1995) and Igura *et al.* (1997) showed that 15 minutes heating at 150°C resulted in a decrease of molecular weight of corn and sweet potato starch. Byars (2003) found that thermal degradation effects were important during jet cooking of waxy corn starch.

The combined and simultaneous effects of heating and shearing on starch have not yet been clarified completely. Many studies conducted so far have focussed on the degradation of starch during extrusion and molecular weight reduction was explained quantitatively in terms of mechanical degradation only (Parker *et al.*, 1990; Diosady *et al.*, 1985; Willett *et al.*, 1997). Effects of more defined shear and temperature on starch degradation so far also resulted in quantitative explanations in terms of mechanical degradation only (Vergnes *et al.*, 1987).

The influence of moisture content on molecular weight reduction is another effect that has not been investigated thoroughly. It has been suggested that increasing moisture content decreases the degree of starch degradation during heating and shearing processes such as extrusion (Chinnaswamy and Hanna, 1990; Wen *et al.*, 1990) due to the reduction of the stresses occurring (Davidson *et al.*, 1984) since the melt viscosity is reduced. On the other hand, water might be involved in the chemical reactions that are leading to (thermal) degradation of starch, as suggested in a recent review by Van den Einde *et al.* (2003). Igura *et al.* (2001) found that the effect of time-temperature history becomes large when processing starch at high moisture content. This suggests that the effect of moisture content might be more complex than only its effect through shear stresses.

In this study, a shear cell enabling a well-defined plain shear field was used to investigate the effects of simultaneous heating and shearing treatment on the molecular weight of regular corn starch at different moisture contents and temperatures in experiments in which both thermal and mechanical effects were important. The relative importance of heating was studied in separate experiments.

2. Materials and methods

2.1. Starch

Regular corn starch was obtained from Cargill BV. Starch was premixed with water as described earlier (Van den Einde *et al.*, 2004).

2.2. Heating treatment

Mixtures of corn starch were heat-treated in a mold with inner dimensions 100 *x* 150 *x* 2 mm (l *x* w *x* h) or in a rotating sterilizing device. The mold was pressurized to avoid steam leakage. Pressure was in all cases put onto the outer raised edge of the mold, not on the sample, to avoid pressure effects. Further details on the mold used can be found elsewhere (Van Soest and Kortleve, 1999). Heat treatment in the mold and in the rotating sterilizing device was shown to reveal the same results in terms of degradation (results not shown). Temperatures, times and moisture contents are given in table 1.

2.3. Heating-shearing treatment

Mixtures of corn starch and water were heated and sheared in the shearing device described earlier (Van den Einde *et al.*, 2004). Temperatures, times and rotation speeds are given in table 2. Due to the steam pressure, no temperatures higher than 125°C were possible at 37 and 43% moisture, whereas at 30% moisture the maximum temperature was 140°C. At higher temperatures, steam leakage took place, which was shown to have a large influence on all results obtained.

After the thermomechanical treatment, samples were dried and ground to fine powder under liquid nitrogen as described earlier (Van den Einde *et al.*, 2004).

Table 1: Time (*t*), temperature (*T*) and moisture content (*MC*) during heat treatment and absolute (*[η]*) and relative (*X*) intrinsic viscosity of heat-treated corn starch. Exp. no. = experiment number.

Exp. no.	*t* (s)	*T* (°C)	*MC* (%)	*[η]* (ml/g)	*X* (-)
native	-	-	-	225	1
1	900	85	30	224	0.99
2	900	100	30	229	1.02
3	300	110	30	220	0.98
4	600	110	30	225	1.00
5	900	110	30	209	0.93
6	900	110	30	207	0.92
7	900	110	30	209	0.93
8	900	120	30	192	0.85
9	900	130	30	177	0.79
10	300	140	30	171	0.76
11	600	140	30	165	0.73
12	900	140	30	154	0.68
13	900	140	30	166	0.74
14	300	160	30	156	0.69
15	600	160	30	160	0.71
16	900	160	30	147	0.65
17	300	110	43	178	0.79
18	600	110	43	168	0.75
19	900	110	43	174	0.77
20	300	140	43	152	0.68
21	600	140	43	145	0.64
22	900	140	43	140	0.62
23	300	160	43	144	0.64
24	600	160	43	141	0.63
25	900	160	43	152	0.68

2.4. Analysis

Intrinsic viscosity was determined as described earlier (Van den Einde *et al.*, 2004). The degree of degradation was calculated as the relative intrinsic viscosity *X* (Diosady *et al.*, 1985). X-Ray diffraction measurements on a Philips PC-APD PW 3710 powder X-Ray diffractometer showed that no native crystalline could be found anymore in almost all samples (results not shown). Only samples heat-treated at $T \leq 140$°C and 30% moisture showed some A-type crystals (approximately 12%), but as these samples were hardly degraded at all, the effect on *X* was minimal (maximally 0.01). Therefore, the calculation method described by Diosady *et al.* (1985) could be simplified to:

$$X = \frac{[\eta]}{[\eta]_0} \qquad [1]$$

Table 2: Total treatment time (*t*), time after maximal shear stress (t_{th}), temperature (*T*), moisture content (*MC*), rotation speed (*N*), maximal shear stress (τ_{max}), absolute ($[\eta]$) and relative (*X*) intrinsic viscosity, and relative intrinsic viscosity of thermal part (X_{th}; see text) of thermomechanically treated starch. Exp. no. = experiment number.

Exp. no.	t (s)	t_{th} (s)	T (°C)	MC (%)	N (rpm)	τ_{max} (10^4 Pa)	$[\eta]$ (ml/g)	X (-)	X_{th} (-)
26	960	130	90	30	75	5.11	147	0.65	1.03
27	1051	857	90	30	50	4.86	154	0.68	1.04
28	480	127	100	30	35	3.87	165	0.73	0.95
29	360	88	110	30	75	4.56	143	0.64	0.92
30	272	122	110	30	25	3.32	192	0.85	1.01
31	540	140	110	30	35	3.51	186	0.83	1.00
32	600	260	110	30	35	3.11	172	0.76	0.87
33	510	149	120	30	75	3.67	191	0.85	1.06
34	600	268	120	30	35	3.27	161	0.72	0.84
35	270	120	125	30	50	4.13	169	0.75	1.01
36	600	268	130	30	35	2.44	171	0.76	0.78
37	847	687	130	30	50	3.45	136	0.60	0.73
38	1153	1015	130	30	50	3.45	131	0.58	0.70
39	581	444	140	30	50	2.85	151	0.67	0.73
40	900	558	140	30	50	1.51	148	0.66	0.66
41	300	120	90	37	25	3.16	167	0.74	0.85
42	300	120	90	37	75	4.00	157	0.70	0.92
43	273	121	90	37	50	3.75	177	0.79	0.99
44	600	462	90	37	50	4.20	147	0.65	0.89
45	285	88	110	37	25	2.25	179	0.80	0.80
46	273	229	110	37	10	2.40	170	0.76	0.77
47	720	568	110	37	50	2.85	131	0.58	0.64
48	226	86	125	37	50	1.95	173	0.77	0.77
49	606	564	125	37	50	2.25	136	0.60	0.60
50	280	124	90	43	50	2.80	148	0.66	1.02
51	270	130	90	43	25	2.14	162	0.72	0.97
52	270	148	110	43	50	1.99	166	0.74	0.96
53	270	232	110	43	10	1.45	143	0.64	0.74
54	270	562	110	43	10	1.54	122	0.54	0.64
55	270	126	125	43	50	1.64	194	0.86	1.04
56	600	250	125	43	25	1.09	135	0.60	0.64

3. Results and discussion

All the measured values are shown in tables 1 (heat-treated samples) and 2 (heated-sheared samples).

3.1. Breakdown by thermal effects only

Figure 1 shows the measured relative intrinsic viscosity X as a function of temperature and moisture content after 15 minutes heat treatment. A higher temperature generally resulted in more starch breakdown, although the effect diminished at both high temperature and high moisture content. At 30% moisture, heat treatment at temperatures ≤ 110°C induced only a small amount of starch degradation within 15 minutes ($X \geq 0.92$), which can probably be neglected in short-time experiments. Increasing moisture content generally resulted in more degradation. This effect of moisture content is in accordance with the hypothesis mentioned in the introduction that water may be involved in the chemical reactions occurring. The effect became less pronounced at the higher temperatures (table 1).

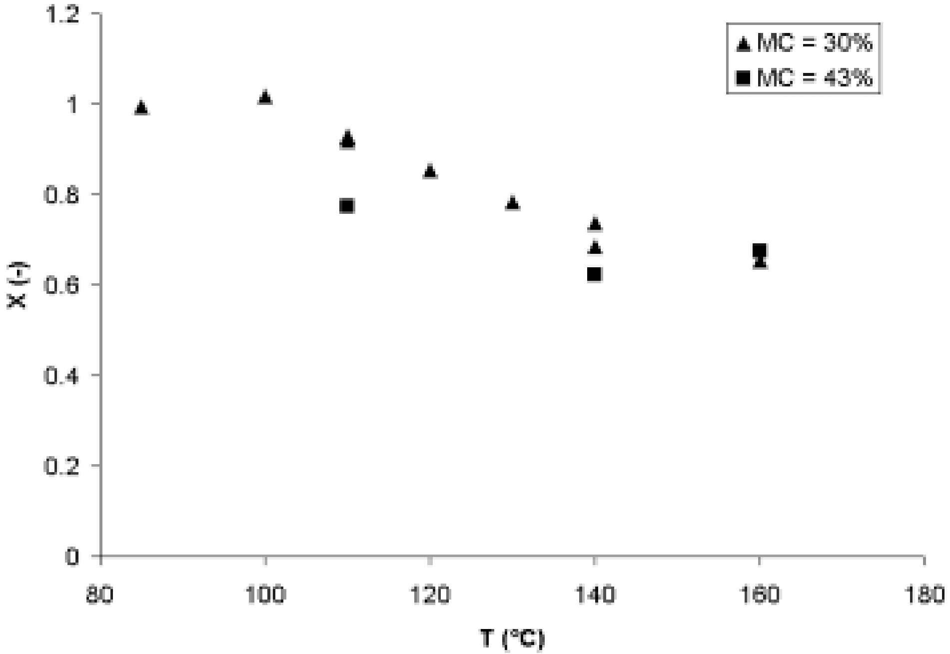

Figure 1: Relative intrinsic viscosity X of low moistened starch heat-treated at different moisture contents as a function of temperature. Treatment time was in all cases 15 minutes.

Figure 2 shows that different treatment times (5, 10 or 15 minutes) did not result in significantly different degrees of breakdown at 30% moisture. Comparable results were obtained for 43% moisture. It seems that thermal treatment resulted in initial starch degradation only, after which the intrinsic viscosity remained approximately constant. As intrinsic viscosity measurements are only sensitive to endodegradation, it was also checked whether or not increase of time led to the formation of more water soluble products, which are a measure for exodegradation. Water solubility of the product was in all cases low (0-7%) and different treatment times resulted in only very small differences, suggesting that also exodegradation was not significantly dependent on time. Although one would intuitively expect a first order degradation process, recent investigations by other researchers have revealed comparable results. Byars (2003) studied degradation of waxy corn starch during heating in a jet cooker. The first few passes through the jet cooker resulted in significant decrease in intrinsic viscosity, whereas little additional breakdown was observed during further passes. Dintzis and Bagley (1995) found that the intrinsic viscosity value of waxy corn starch autoclaved at 120°C remained constant with increasing holding time (21 to 60 minutes). Although the treatment time investigated was much longer than in this paper, their results also suggest time independence after an initial breakdown, in agreement with the results reported here.

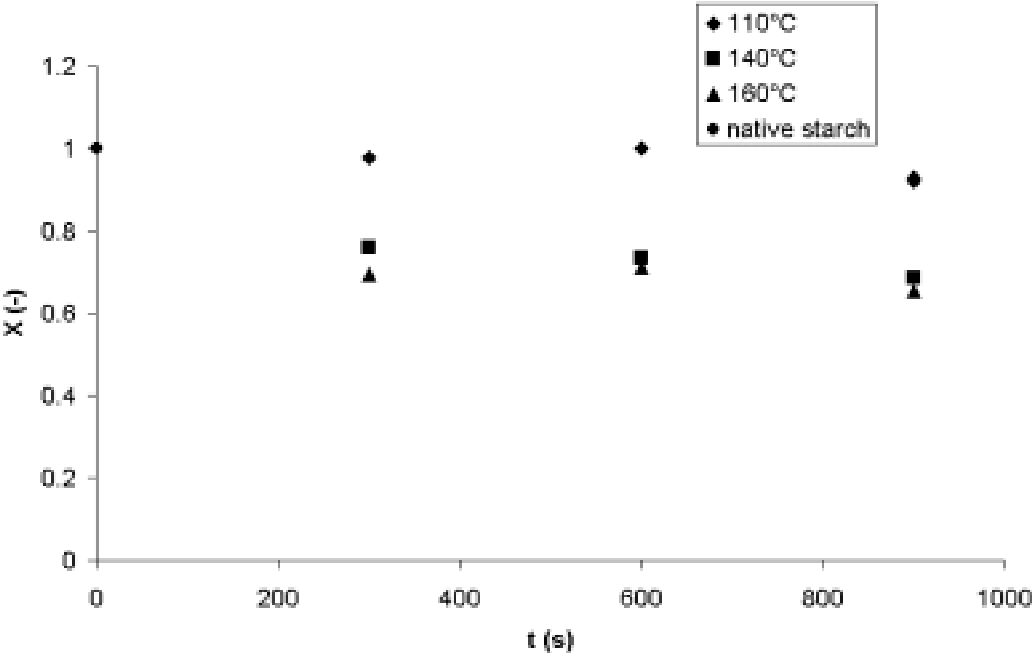

Figure 2: The effect of treatment time on the relative intrinsic viscosity *X* of heat-treated low moistened starch at different temperatures. *MC* = 30%.

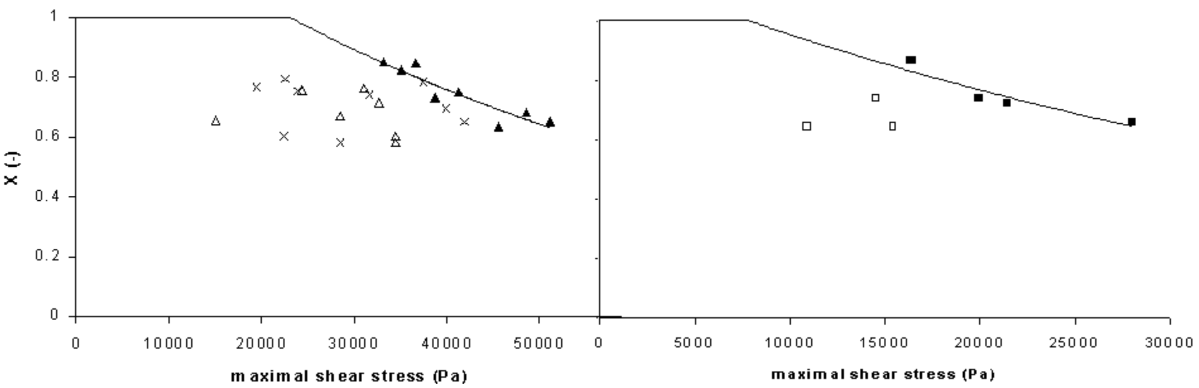

Figure 3: Relative intrinsic viscosity *X* of thermomechanically treated low moistened starch as a function of maximally applied shear stress $\tau_{\max}$ and moisture content. ▲ and Δ: *MC* = 30%. *x*: *MC* = 37%; ■ and □: *MC* = 43%. Closed symbols are used for experiments in which only mechanical effects are significant; open symbols indicate results from experiments in which thermal effects played a significant role. Lines indicate the fitted first order models.

3.2. Breakdown by shear

Figure 3 shows the relative intrinsic viscosity *X* of thermomechanically treated low moistened starch as a function of maximally applied shear stress τ_{max} and moisture content. In our earlier work (Van den Einde *et al.*, 2004), it was shown that when thermal effects were avoided, the mechanical breakdown of waxy corn starch at 30% moisture could be well described by a first order equation with the maximal shear stress τ_{max} as the key parameter:

$$X_m = C_1 \exp(C_2 \tau_{\max}) \qquad [1]$$

As explained in the previous section, the heating experiments showed that thermal effects play a role within 15 minutes at temperatures higher than 110°C if moisture content = 30%. Equation [1] could indeed be fitted well to all the data at temperatures ≤ 110°C, but also to the data obtained from short time experiments at 120 and 125°C (table 2, exp. no. 33 and 35). Thermal effects at 120 and 125°C were found negligible due to the short times used in these two experiments and therefore these data could be used for fitting as well. Fitted parameters were $C_1 = 1.46$ and $C_2 = -2.45\ 10^{-5}$ m^2/N. C_1 was higher than 1 suggesting that there is a threshold value for shear stress before regular corn starch breaks down (Van den Einde *et al.*, 2004). If the shear stress applied is lower than this threshold value, X_m remains at 1. The minimally required stress can be calculated by equaling equation [1] to 1. Thus, the degradation equations become:

$$X_m = 1 \qquad \text{if } \tau_{max} < 2.32\ 10^4 \text{ N/m}^2 \qquad [5a]$$

$X_m = 1.46\exp\left(-1.63 \cdot 10^{-5} \tau_{\max}\right)$ if $\tau_{max} \geq 2.32\ 10^4$ N/m^2 [5b]

The R^2 value was 0.83, which suggests that a first order correlation, as found for waxy corn starch at 30% moisture content, can be also be applied to regular corn starch at 30% moisture content. Samples treated for a longer time at 120 or 125°C and samples treated at 130 or 140°C clearly showed an additional thermal effect (table 2), as was expected from the heating experiments.

At 43% moisture, the situation was somewhat different (figure 3). As stated in the introduction, water may be involved in the occurring reactions. It is also known that the rupture force of a covalent bond depends on the chemical environment of the bond (Röhrig and Frank, 2001). Therefore, it was expected that a higher fraction of water might destabilize the glycosidic bond and that the shear stresses required for breaking down the starch might be lower at higher moisture content. For this reason, a separate first order equation with the maximal shear stress τ_{max} was fitted to those data that had received a relatively short treatment time after the maximal shear stress was reached (so that thermal effects were supposed to be almost negligible), resulting in:

$X_m = 1$ if $\tau_{\max} < 7.74\ 10^3$ N/m^2 [6a]

$X_m = 1.18\exp\left(-2.18 \cdot 10^{-5} \tau_{\max}\right)$ if $\tau_{\max} \geq 7.74\ 10^3$ N/m^2 [6b]

(R^2 = 0.88). The temperature at and above which thermal effects are important is approximately 110°C. As expected, this is lower than at 30% moisture. Thermal effects during thermomechanical treatment are further discussed in the next section.

At 37% moisture, data obtained at 90°C were more or less comparable in breakdown to 30% moisture, although they were somewhat more scattered (figure 3 and table 2). At higher temperatures, in all cases more breakdown took place than expected from the 30% moisture shear-induced breakdown line (figure 3). This could be due to thermal effects during the thermomechanical treatment, as further explained in the next section.

3.3. Breakdown by shear and heat

As explained in the previous section, part of the breakdown of starch in thermomechanically treated samples was due to thermal effects. As was found earlier, effects of shear stress are time-independent and the molecular weight of starch after shearing treatment is determined by the maximal shear stress applied. It was therefore assumed that mechanical breakdown is dominant during thermomechanical treatment until the time that this maximal shear stress is encountered. After this time, thermal effects may result in further degradation of the starch. The mechanisms of breakdown by heat and shear were assumed to be independent. Therefore, it is logical to assume the following relation:

$$X = X_m X_{th} \rightarrow X_{th} = \frac{X}{X_m} \qquad [7]$$

X_m was calculated according to equations [5a] and [5b] for 30 and 37% moisture and according to equations [6a] and [6b] for 43% moisture.

Figure 4a shows X_{th} as a function of temperature at 30% moisture. The data points close to $X_{th} = 1$ are the ones of which thermal effects were supposed to be negligible and that were used for fitting the first order models described in the previous section (figure 3). The other data in this figure clearly suggests that the data obtained from thermal experiments are not highly different from those derived from the thermomechanical experiments. This suggests that thermomechanical treatment can indeed be approximated as an independent combination of a mechanical treatment with main parameter τ_{max} and a thermal treatment. Combining figure 4a and table 2 reveals that, in analogy with the heat-treated samples, all samples with $t_{th} > 300$ s could be described as dependent on temperature only and not significantly on treatment time (compare for example experiments 37 and 38). This finding can simplify the description of the effects of thermomechanical treatment: if time after the maximal shear stress exceeds a threshold, the treatment can be described as an addition of an effect of τ_{max} and an effect of the temperature.

Figure 4b shows X_{th} as a function of temperature at 43% moisture. The shape of the curve is comparable to the one obtained from the data at 30% moisture. In line with the expectations, the downward trend in X_{th} with temperature occurs at lower temperatures than at 30% moisture. The data obtained from the purely thermal experiments are not highly different from the ones derived from the thermomechanical treatment. This suggests that also at 43% moisture, a heating-shearing treatment can be approximated as a mechanical treatment with main parameter τ_{max} and an independent thermal treatment. The somewhat lower value found for X_{th} in experiment 54 (110°C; table 2) might be due to the following. Figure 4b clearly shows that the difference in breakdown between 110 and 125°C is high. Although temperature control during the experiment was reasonably accurate, a local increase of temperature to approximately 114°C was shown to be possible. Taking into account the large dependence of breakdown on temperature in this regime, it may be possible that this higher temperature caused the additional breakdown.

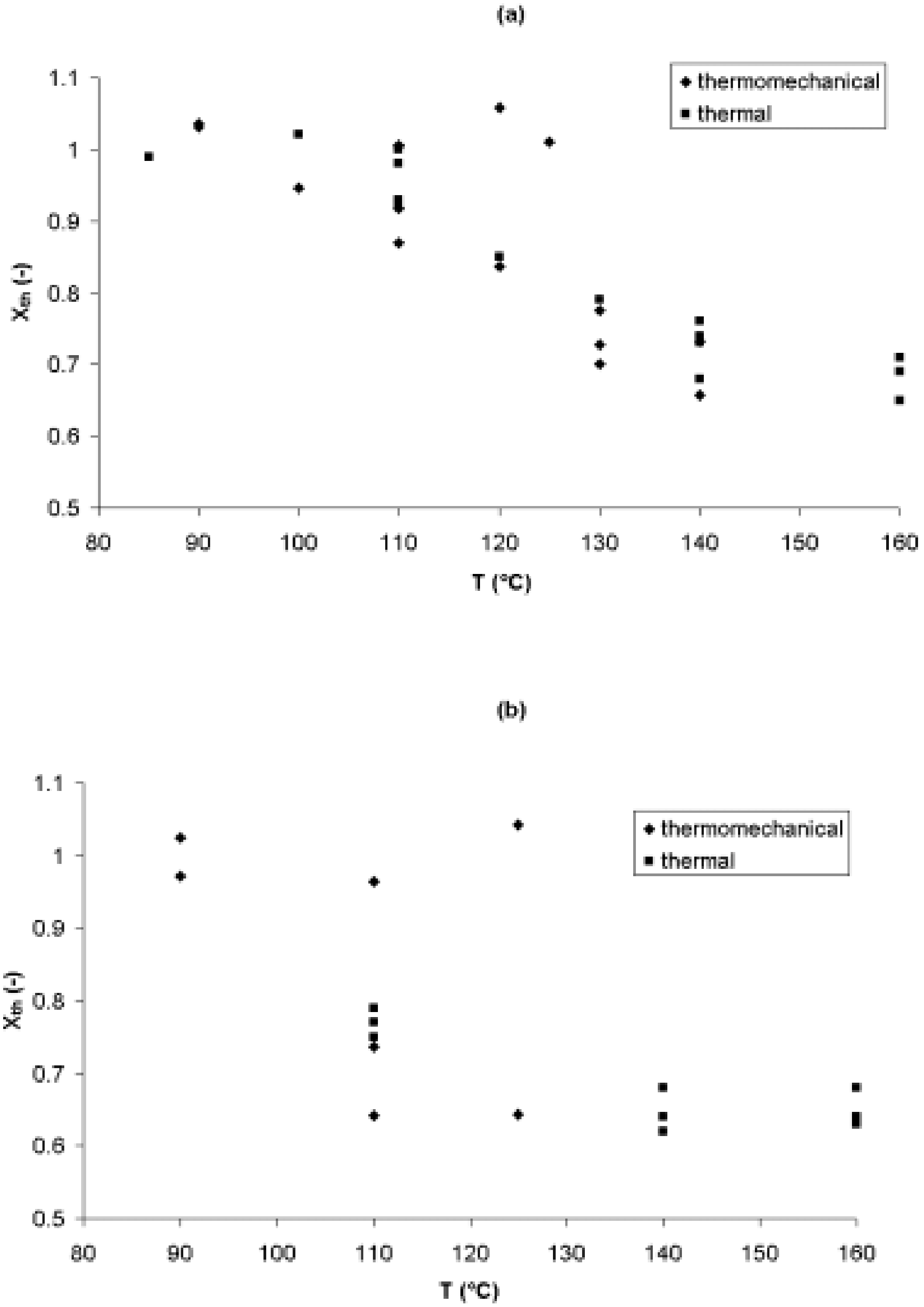

Figure 4: Relative intrinsic viscosity due to thermal effects X_{th} of thermally and thermomechanically treated corn starch at (a) 30% and (b) 43% moisture as a function of temperature. Data points with X_{th} close to 1 were those being used for fitting the first order mechanical degradation lines in figure 3 (negligible thermal effects; see text).

At 37% moisture, reproducibility was less than at 30 and 43% moisture (table 2) and data were highly scattered (figure 3). It seems that 37% is in the intermediate area between the two regimes. The behavior in this region appears to be complex as small changes in conditions will cause several effects to occur simultaneously, such as bond destabilization, effects on viscosity and thermal breakdown. Therefore, the behavior of the starch-water mixture in this region seems to be highly sensitive to small deviations in temperature or moisture content. In order to obtain a complete view of all the influences on the starch degradation at 37% moisture, a higher accuracy than possible with the current experimental setup may be necessary.

3.4. Consequences for product and process design

The role of water in starch breakdown. As described in the introduction, previous studies suggested that increasing moisture content decreased the degree of starch degradation during heating-shearing processes, due the effect of lower stresses. Our study indicates that this statement is not always valid. As figures 2 to 4 and tables 1 and 2 show, increasing moisture content has three different effects. It decreases the shear stresses, but it also increases the degree of thermal breakdown and it destabilizes the bond so that smaller stresses are required for mechanical breakdown. Hence, the relation between moisture content and degree of degradation is not linear, but more complex. It can even be expected that an optimum occurs in breakdown at a certain moisture content, as changing moisture content will probably affect melt viscosity to a different extent than it will affect the degree of degradation. This is in accordance with results by Govindasamy *et al.* (1996). They found that increasing moisture content from 34 to 42% decreased the degree of starch degradation, but that increasing moisture content from 42 to 50% increased the degree of starch degradation during extrusion of sago starch. However, these authors suggested this to be caused by gelatinization, resulting in various extents of granular structure relaxation, rather than by thermal breakdown effects. Baud *et al.* (1999) found that degree of degradation after extrusion could not be related directly to the moisture content, which could be in accordance with the current results. These authors did not explain their result in terms of thermal degradation either.

Time (in)dependence of thermal breakdown. Another interesting result for process design is the unexpected partial time dependence of starch breakdown during heat treatment. Apparently, once a certain heating time is reached, no further starch breakdown will take place. This can be a useful feature, as it might be possible to change various product properties or inactivate undesired components without significantly affecting the starch molecular weight.

4. Concluding remarks

Effects of shear and thermal treatment on low moistened corn starch were unraveled in this work. Thermal breakdown was shown to have an effect during a limited time only. Upon further increasing thermal treatment time, no additional breakdown takes place. Thermomechanical degradation could be divided clearly into a mechanical effect, depending on maximal shear stress, and an independent thermal effect, which was for (thermal) treatment times > 300 s only dependent on temperature and not on time. These findings suggest a convenient way to estimate the effect of thermomechanical treatment on starch molecular weight and can therefore be a useful tool in process design.

Increasing moisture content had three separate effects on starch molecular weight reduction: it decreased the stresses, increased thermal breakdown and decreased the stresses required for breakdown. This makes the effect of moisture content quite difficult to predict, but the findings described in this paper can provide a first guideline for estimating the effects of changing moisture content on starch molecular weight reduction.

The finding that shear and temperature effects can be considered independent may open up the possibility for relatively simple, but accurate models that could be used for design of processes that are more effective and efficient than the thermomechanical processes available today.

Acknowledgement

The authors thank H. Bosman for carrying out part of the heat treatment experiments, J.J.G. van Soest for his kind assistance during part of the heat treatment experiments and during the X-Ray diffraction measurements and S. van Brenk for carrying out part of the intrinsic viscosity measurements.

List of symbols

C_1	first fit parameter in first order τ_{max} model (-)
C_2	second fit parameter in first order τ_{max} model (m^2/N)
MC	moisture content (%)
t	time (s)
t_{th}	time after the maximal shear stress was reached [time during which thermal effects were dominant compared to mechanical effects] (s)
X	relative intrinsic viscosity of the molten fraction of the treated starch compared to native starch (-)
X_m	relative intrinsic viscosity of the molten fraction of the treated starch due to mechanical breakdown (-)
X_{th}	relative intrinsic viscosity of the molten fraction of the treated starch due to thermal breakdown (-)

Greek symbols

$[\eta]$	intrinsic viscosity (ml/g)
$[\eta]_0$	intrinsic viscosity of native starch (ml/g)
τ_{max}	maximal shear stress (N/m^2)

References

Baud, B., Colonna, P., Valle, G. Della, & Roger, P. (1999). Macromolecular degradation of extruded starches measured by HPSEC-MALLS. *Biopolymer Science: Food and Non Food Applications / Les Colloques de l'INRA*, 91, 217-221.

Bindzus, W., Fayard, G., Lengerich, B. van, & Meuser, F. (2002). Description of extrudate characteristics in relation to the shear stress of plasticised starches determined in-line. *Starch / Staerke*, 54, 252-259.

Bruemmer, T., Meuser, F., Lengerich, B. van, & Niemann, C. (2002). Expansion and functional properties of corn starch extrudates related to their molecular degradation, product temperature and water content. *Starch / Staerke*, 54, 9-15.

Byars, J.A. (2003). Jet cooking of waxy maize starch: solution rheology and molecular weight degradation of amylopectin. *Cereal Chemistry*, 80(1), 87-90.

Chinnaswamy, R., & Bhattacharya, K.R. (1986). Characteristics of gel-chromatographic fractions of starch in relation to rice and expanded rice-product quality. *Starch / Staerke*, 38(2), 51-57.

Chinnaswamy, R., & Hanna, M.A. (1990). Macromolecular and functional properties of native and extrusion cooked starch. *Cereal Chemistry*, 67(5), 490-499.

Davidson, V.J., Paton, D., Diosady, L.L., & Larocque, G. (1984). Degradation of wheat starch in a single-screw extruder: characteristics of extruded starch polymers. *Journal of Food Science*, 49, 453-458.

Dintzis, F.R., & Bagley, E.B. (1995). Effects of thermomechanical processing on viscosity behavior of corn starches. *Journal of Rheology*, 39(6), 1483-1495.

Diosady, L.L., Paton, D., Rosen, N., Rubin, L.J., & Athanassoulias, C. (1985). Degradation of wheat starch in a single-screw extruder: mechano-kinetic breakdown of cooked starch. *Journal of Food Science*, 50, 1697-1699,1706.

Einde, R.M. van den, Goot, A.J. van der, & Boom, R.M. (2003). Understanding molecular weight reduction of starch during heating shearing processes. *Journal of Food Science*, 68(8), 2396-2404. (Chapter 7 of this thesis).

Einde, R.M. van den, Bolsius, A., Soest, J.J.G. van, Janssen, L.P.B.M., Goot, A.J. van der, & Boom, R.M. (2004). The effect of thermomechanical treatment on starch breakdown and the consequences for process design. *Carbohydrate Polymers*, 55(1), 57-63. (Chapter 2 of this thesis).

Fujio, Y., Igura, N., & Hayakawa, I. (1995). Depolymerization of molten-moisturized-starch molecules by shearing force under high temperature. *Starch / Staerke*, 47(4), 143-145.

Govindasamy, S., Campanella, O.H., & Oates, C.G. (1996). High moisture twin-screw extrusion of sago starch: 1. Influence on granule morphology and structure. *Carbohydrate Polymers*, 30, 275-286.

Igura, N., Hayakawa, I., & Fujio, Y. (1997). Effect of longer heating time on depolymerization of low moisturized starches. *Starch / Staerke*, 49(1), 2-5.

Igura, N., Katoh, T., Hayakawa, I., & Fujio, Y. (2001). Degradation profiles of potato starch melts through a capillary type viscometer. *Starch / Staerke*, 53(12), 623-628.

Mua, J.P., & Jackson, D.S. (1997). Relationships between functional attributes and molecular structures of amylose and amylopectin fractions from corn starch. *Journal of Agricultural and Food Chemistry*, 45, 3848-3854.

Parker, R., Ollett, A.L., & Smith, A.C. (1990). Starch melt rheology: measurement, modelling and applications to extrusion processing. In P. Zeuthen. *Processing and quality of foods* (pp. 1.290-1.295). London: Elsevier.

Röhrig, U.F., & Frank, I. (2001). First-principle molecular dynamics study of a polymer under tensile stress. *Journal of Chemical Physics*, 115, 8670-8674.

Soest, J.J.G. van, & Kortleve, P.M. (1999). The influence of maltodextrins on the structure and properties of compression-molded starch plastic sheets. *Journal of Applied Polymer Science*, 74, 2207-2219.

Vergnes, B., Villemaire, J.P., Colonna, P., & Tayeb, J. (1987). Interrelationships between thermomechanical treatment and macromolecular degradation of maize starch in a novel rheometer with preshearing. *Journal of Cereal Science*, 5, 189-202.

Wen, L.F., Rodis, P., & Wasserman, B.P. (1990). Starch fragmentation and protein insolubilization during twin-screw extrusion of corn meal. *Cereal Chemistry*, 67(3), 268-275.

Willett, J.L., Millard, M.M., & Jasberg, B.K. (1997). Extrusion of waxy maize starch: melt rheology and molecular weight degradation of amylopectin. *Polymer*, 38(24), 5983-5989.

Chapter 5

Modeling macromolecular degradation of corn starch in a twin screw extruder

Abstract

Macromolecular degradation of starch in a twin screw extruder was modeled. A shear cell having well-defined flow conditions described earlier was used to measure peak viscosity of corn starch melts at various moisture contents and temperatures. Shear rate and elongation rate distributions in the extruder were estimated from numerical calculations from literature and elongational viscosity was estimated using the Trouton ratio. In this way, stresses in the extruder were calculated and, using relations on maximum stress vs. intrinsic viscosity obtained in earlier work, the expected relative intrinsic viscosity was calculated. The model gave a good prediction of relative intrinsic viscosity after extrusion at various temperatures (97-130°C), moisture contents (23–45%) and screw speeds (90 or 140 rpm). This suggests that the use of pilot scale equipment having a well-defined flow pattern can be useful for understanding complex processes such as extrusion.

This chapter was submitted for publication as: R.M. van den Einde, M.E. van der Veen, H. Bosman, A.J. van der Goot, R.M. Boom, Modeling macromolecular degradation of corn starch in a twin screw extruder.

1. Introduction

Extrusion cooking is known to modify starch at all structural levels: the granular structure disappears, the crystals melt and macromolecules depolymerize (Barron *et al.*, 2001). Molecular breakdown of starch is known to influence various product characteristics such as water solubility, cold paste viscosity and extrudate expansion (Bruemmer *et al.*, 2002; Bindzus *et al.*, 2002). The effects of screw speed, temperature, moisture content and amylose content on molecular breakdown of starch during extrusion have been investigated (Cai *et al.*, 1995; Davidson *et al.*, 1984a; Govindasamy *et al.*, 1996; Orford *et al.*, 1993). However, these studies are extruder-type dependent and can not always easily be translated to other types (Harper, 1986). To obtain knowledge that is more generally applicable, a mechanistic approach to understand the effect of process conditions during extrusion cooking on molecular weight of starch is needed.

A challenge in understanding the effects of extrusion cooking on starch is the estimation of the correct stresses along the extruder barrel. In most studies only nominal values for the shear rate were used to describe the effect of extruder stress or strain on starch degradation (Davidson *et al.*, 1984b; Cai *et al.*, 1995) or on destruction of other components (Komolprasert and Ofoli, 1991; Ilo and Berghofer, 1998). However, in our previous work we have shown that the maximum rather than the average stress determines starch breakdown (Van den Einde *et al.*, 2004a). Slit dies can be used to determine melt viscosity at the end of the extruder (Della Valle *et al.*, 1995), but these measurements are already influenced by product transformations during its residence in the barrel. Hence, it is difficult to estimate the maximum shear stresses during the treatment from those experiments.

The use of equipment having more defined shear and temperature gradients was shown to be successful for understanding changes in starch by thermomechanical treatment (Vergnes *et al.*, 1987; Barron *et al.*, 2000; Barron *et al.*, 2001; Van den Einde *et al.*, 2004a, 2004b). Therefore, the purpose of this work was to construct a model describing the molecular weight reduction of starch in a twin screw extruder, based on experiments carried out in well-defined shear and thermal conditions. A shear cell described earlier (Van den Einde *et al.*, 2004a) was used together with extrusion trials. Shear cell torque data were used to calculate the peak melt viscosity of the starch. The shear and elongation rates at different places in a paddle section in the extruder were estimated and the corresponding shear and elongational stresses were calculated. Paddle sections are, compared to (sections of) transport and single lead elements,

Table 1: Treatment conditions and rheological results for a mixture of corn starch and 30% water processed in the shear cell. Exp. no. = experiment number; T = temperature; MC = moisture content; N = rotation speed; τ_{max} = maximum shear stress; K_{max} = calculated consistency factor at $\tau = \tau_{\max}$. New samples are marked A1 to A8. Other samples were described earlier (Van den Einde *et al.*, 2004b); numbers are the same as used in the earlier work.

Exp. no.	T (°C)	MC (%)	N (rpm)	τ_{max} (10^4 Pa)	K_{max} (10^3 Pa s$^{0.3}$)
26	90	30	75	5.11	10.8
27	90	30	50	4.86	11.6
A1	90	30	25	5.25	15.4
A2	90	30	50	4.76	11.3
28	100	30	35	3.87	10.2
29	110	30	75	4.56	9.6
30	110	30	25	3.32	9.7
31	110	30	35	3.51	9.3
32	110	30	35	3.11	8.2
A3	110	30	50	4.25	10.1
A4	110	30	50	4.25	10.1
33	120	30	75	3.67	7.7
34	120	30	35	3.27	8.7
35	125	30	50	4.13	9.8
A5	125	30	50	4.10	9.8
A6	125	30	50	3.67	8.7
36	130	30	35	2.44	6.5
37	130	30	50	3.45	8.2
38	130	30	50	3.45	8.2
A7	130	30	75	3.66	7.7
39	140	30	50	2.85	6.8
A8	140	30	35	3.45	9.1
40	140	30	50	1.51	3.6
41	90	37	25	3.16	9.3
42	90	37	75	4.00	8.4
43	90	37	50	3.75	8.9
44	90	37	50	4.20	10.0
45	110	37	25	2.25	6.6
46	110	37	10	2.40	9.3
47	110	37	50	2.85	6.8
48	125	37	50	1.95	4.6
49	125	37	50	2.25	5.4
50	90	43	50	2.80	6.7
51	90	43	25	2.14	6.3
52	110	43	50	1.99	4.7
53	110	43	10	1.45	5.6
54	110	43	10	1.54	6.0
55	125	43	50	1.64	3.9
56	125	43	25	1.09	3.2

known to be flow restricting and high shear as for example indicated by their effect on the mechanical energy input (Choudhury and Gautam, 1998). These sections are therefore determining maximal stresses and hence the degree of breakdown. The expected degree of degradation in the extruder was calculated and compared to the extrusion experiments.

2. Materials and methods

2.1. Starch and water

Regular corn starch was obtained from Cargill BV (Bergen op Zoom, The Netherlands). For practical reasons, starch and water were pre-mixed one day before the shear cell experiments. Starch and water were mixed inside the extruder during the extrusion experiments.

2.2. Determination of melt viscosity

Our shear cell was used to determine melt viscosity at different temperatures and moisture contents (defined on wet basis). Maximum shear stress was 36 kPa. Further details on this equipment can be found elsewhere (Van den Einde *et al.*, 2004a).

Experiments used to describe the rheology of the starch melt were part of the ones described earlier (Van den Einde *et al.*, 2004b). Furthermore, some extra experiments were carried out to get a more complete view on the rheology of the starch melt and the reproducibility of the torque measurements. All experiments are summarized in table 1. From the torque measurement during the treatment, the peak viscosity of the starch melt was calculated. In accordance with Vergnes and Villemaire (1987), Willett *et al.* (1997) and Remsen and Clark (1978), a power law type behavior of the starch melt was assumed. The pseudoplastic index n was assumed to be 0.3 (Vergnes *et al.*, 1987). The peak consistency factor K_{max} was calculated according to:

$$K_{\max} = \frac{\tau_{\max}}{\gamma^{n}} \qquad [1]$$

The K_{max}-values were then fitted to the following equation (Vergnes and Villemaire, 1987):

$$K_{\max} = K_0 \exp\left(k_1 MC + k_2 T\right) \qquad [2]$$

2.3. Extrusion cooking

Mixtures of corn starch and water were extruded using a co-rotating twin screw extruder (APV Baker MPF 50, *L/D* = 25). The screw configuration is shown in figure 1. This

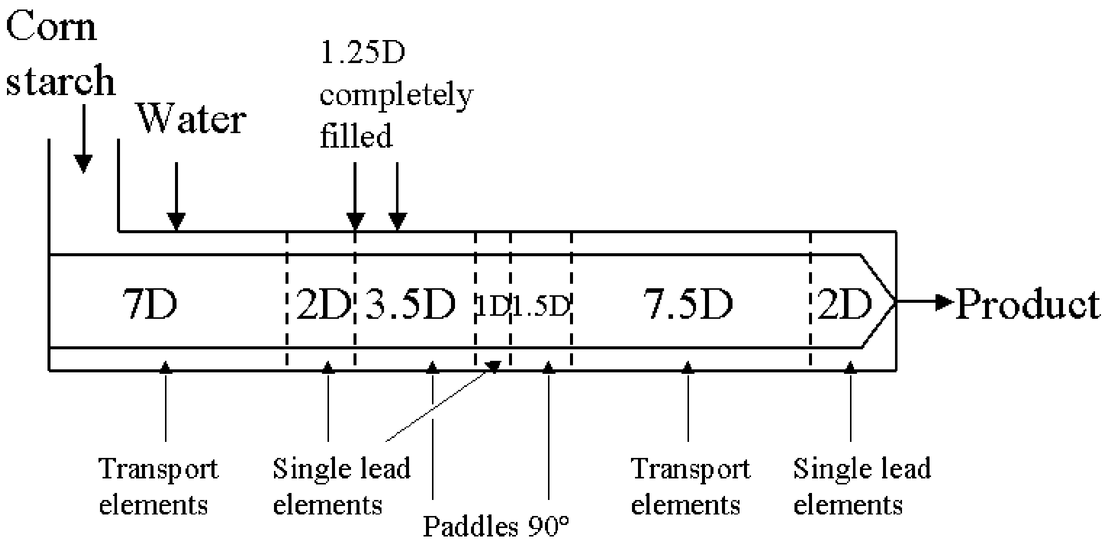

Figure 1: Screw configuration used in the extrusion experiments.

configuration was chosen in order to facilitate comparison with other results (not shown in this paper). Our earlier finding that the maximum shear stress determines breakdown suggests that the first set of restrictive elements induces all breakdown so that the screw configuration after this set of elements is only of minor importance. Table 2 gives moisture contents, temperatures, throughputs and screw speeds. The range of moisture contents was chosen

Table 2: Treatment conditions and results for a mixture of corn starch and water processed in the co-rotating twin screw extruder. Exp. no. = experiment number, *MC* = moisture content, *T* = temperature, *N* = screw speed, *[η]* = intrinsic viscosity, *X* = measured relative intrinsic viscosity, X_{model} = relative intrinsic viscosity predicted by the model for *Tr* = 6.5.

Exp. no.	*MC* (%)	*T* paddles (°C)	*T* barrel (°C)	throughput (kg/hour)	*N* (rpm)	*[η]* (ml/g)	*X* (-)	X_{model} (-)
E1	37	98	100	32.7	140	150	0.67	0.66
E2	28	119	100	28.4	140	130	0.58	0.59
E3	23	125	100	26.7	140	113	0.50	0.51
E4	37	113	130	32.7	140	170	0.76	0.74
E5	28	130	130	28.4	140	139	0.62	0.65
E6	45	97	100	25.2	140	155	0.69	0.60
E7	30	113	100	19.7	140	140	0.62	0.59
E8	23	126	100	23.0	140	110	0.49	0.52
E9	30	109	100	24.0	90	150	0.67	0.59
E10	30	114	100	24.8	140	136	0.60	0.60
E11	30	123	130	24.2	90	147	0.65	0.67
E12	30	122	130	24.9	140	144	0.64	0.65

somewhat broader than in the shear cell to obtain a significant range in degradation values. No die was applied, since the focus was on the effect of the high-shear paddle section without other resistances being present. The first 5 pairs of paddles were shown to be the only elements of the extruder that were completely filled. Temperature in the paddle section was measured continuously during the experiment; values are given in table 2.

Extruded samples were dried and ground to fine as described earlier (Van den Einde *et al.*, 2004a).

2.4. Analysis

Intrinsic viscosity was determined as described earlier (Van den Einde et al., 2004a). The degree of degradation was calculated as the relative intrinsic viscosity *X* (Diosady *et al.*, 1985). X-Ray diffraction measurements on a Philips PC-APD PW 3710 powder X-Ray diffractometer showed that the native crystalline could not be found in any of the heated-sheared or extruded samples (results not shown). Therefore, the calculation method described by Diosady *et al.* (1985) could be simplified to:

$$X = \frac{[\eta]}{[\eta]_0} \qquad [3]$$

2.5. Estimation of shear and elongational stresses in the extruder

In order to calculate the local shear stresses in the extruder from the melt viscosity data, the shear rates in the paddle section of the extruder were estimated.

The shear rates and therefore shear stresses differ radially along a paddle. Therefore, the shear rate distribution was calculated. Van der Wal *et al.* (1996) simulated the flow of an incompressible Newtonian fluid in a paddle in an extruder identical to the one used in this work. Van der Wal & Klomp calculated the shear and elongation rate distributions at various axial positions along the paddle (unpublished). Although we were aware that the assumptions made in their paper (incompressible, Newtonian) were not entirely valid for our work, these simulations were, compared to others described in literature, closest to the situation described in this paper. Ideally, these data should be combined with information on the pathways that each particle is taking through the paddle section. Unfortunately there is not, to the best of our knowledge, any publication describing this. However, the velocity vectors calculated by Van der Wal *et al.* (1996) suggest that a high percentage of the particles stays more or less at the same radial distance from the middle point of the extruder axis. As an approximation, this was assumed to be the case for all particles. As the maximum shear rate determines the maximum shear stress and hence the degree of degradation, the figures of Van der Wal & Klomp (unpublished) were used to estimate the maximum shear rates. Using the rheological data from the shear cell experiments, the maximum shear stresses at the temperatures and moisture contents used in the extruder experiments were calculated, according to $\tau = K \cdot \gamma^n$ (equation [1]). K follows from equation [2] where T is in this case the temperature in the paddle section. The same procedure was applied to estimate maximum elongation rates. Both shear and elongation rates are linearly proportional to the screw speed N (Van der Wal *et al.*, 1996).

The elongational viscosity was calculated according to (Jones *et al.*, 1987):

$$\eta_e(\varepsilon) = \eta\left(\sqrt{3}\varepsilon\right) \cdot Tr \qquad [4]$$

Bhattacharya *et al.* (1994) measured the Trouton ratio of corn meal at the end of a single screw extruder at temperatures 160-180°C and moisture contents of 30-35%, resulting in $Tr \approx$ 20 to 55. They suggested that lower product moisture and especially lower barrel temperatures resulted in a decreased Tr. We assumed corn meal to be comparable to corn starch with respect to the Trouton ratio. In our work, the moisture content was comparable to the work of Bhattacharya and co-workers, but the temperature was much lower. Therefore, we expected the Trouton ratio to be lower than 20. For a Newtonian liquid, the Trouton ratio has a constant value of 4 (Bhattacharya, 1993). As no further data were available on the Trouton ratio of corn starch at the temperatures and moisture contents used, Tr was taken as a fit parameter with an expected value $4 < \mathrm{Tr} < 20$.

The elongational stress σ was calculated according to:

$$\sigma = \eta_e \cdot \varepsilon \qquad [5]$$

In this way, various zones in the paddle section were defined, each having a certain maximum shear and elongational stress.

2.6. Calculation of expected breakdown during extrusion cooking

Assuming that an elongational stress would result in the same degree of degradation as plain shear stress of the same magnitude (this assumption is further discussed in section 3.4), the expected relative intrinsic viscosity X of material after a maximum shear or elongational stress in zone i was calculated according to:

$$X_i = C_1 \exp\left(-C_2 \cdot \tau_{\max,i}\right) \qquad [6a]$$

or

$$X_i = C_1 \exp\left(-C_2 \cdot \sigma_{\max,i}\right) \qquad [6b]$$

respectively, whichever of the two gave the largest degree of degradation (i.e. the lowest value of *X*). The parameters C_1 and C_2 follow from our earlier work (Van den Einde *et al.*, 2004b):

$$X = 1 \qquad \text{if } \tau_{max} < 2.32\ 10^4 \text{ N/m}^2 \qquad [7a]$$

$$X = 1.46 \exp\left(-1.63 \cdot 10^{-5} \tau_{\max}\right) \qquad \text{if } \tau_{max} \geq 2.32\ 10^4 \text{ N/m}^2 \qquad [7b]$$

for $MC = 30\%$ and:

$$X = 1 \qquad \text{if } \tau_{\max} < 7.74\ 10^3 \text{ N/m}^2 \qquad [8a]$$

$$X = 1.18 \exp\left(-2.18 \cdot 10^{-5} \tau_{\max}\right) \qquad \text{if } \tau_{\max} \geq 7.74\ 10^3 \text{ N/m}^2 \qquad [8b]$$

for $MC = 43\%$. In both cases, these equations were only valid if treatment time after the maximum shear stress was reached was shorter than approximately 150 s, so that thermal effects were negligible (Van den Einde *et al.*, 2004b). This was the case in all shear cell experiments used in this work as well as in the extruder trials. The relative intrinsic viscosity of the end product was calculated according to:

$$X = \sum_{i=0}^{m} w_i X_i \qquad [9]$$

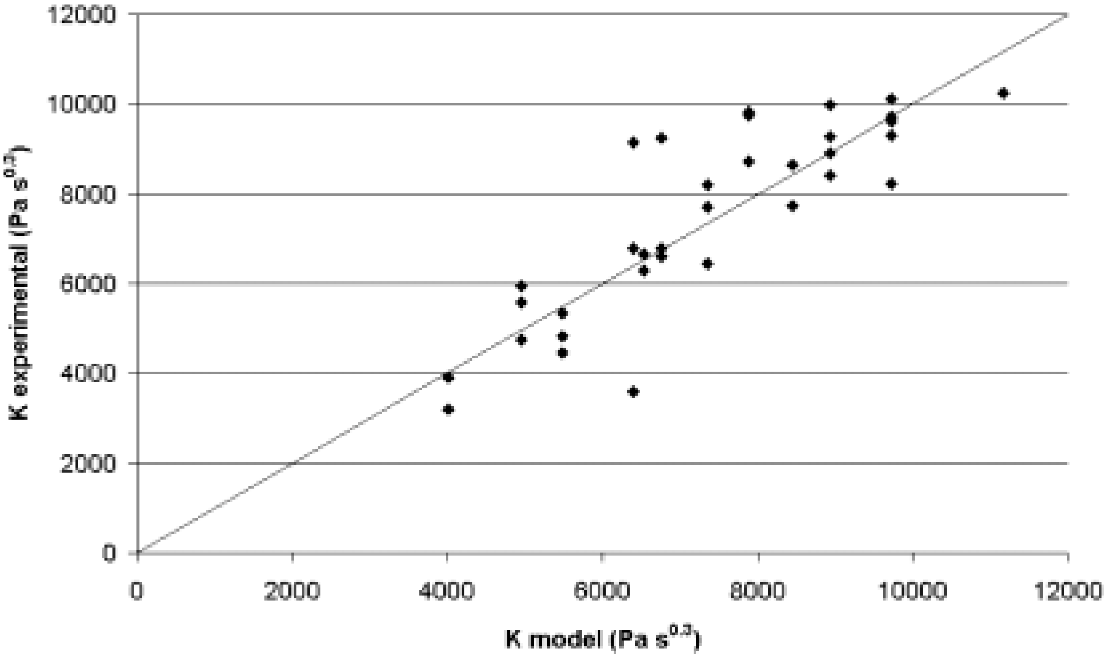

Figure 2: Consistency factors as determined in the experiments versus consistency factors calculated according to equation [10].

where w_i denotes the weight fraction of material passing zone i. w_i was calculated by dividing the area of each zone by the total area. Calculating an overall relative intrinsic viscosity X by averaging the relative intrinsic viscosities of the different fractions was earlier done by Diosady *et al.* (1985).

The predicted relative intrinsic viscosity X (equation [9]) was then compared to the experimentally determined value. It was assumed that samples extruded at MC<30% would behave according to the equations derived for $MC = 30\%$ (equations [7a] and [7b]; no thermal breakdown). The sample extruded at $MC = 45\%$ was assumed to behave according to the equations derived for $MC = 43\%$ (equations [8a] and [8b]). In our previous work (Van den Einde *et al.*, 2004b) it was demonstrated that the breakdown of starch at 37% moisture and $T = 90°\text{C}$ could be well described using the equations for $MC = 30\%$ (equations [7a] and [7b]) and therefore it was decided to calculate the relative intrinsic viscosity X of both samples extruded at 37% moisture using these equations.

3. Results

3.1. Melt viscosity

The maximum consistency factors K_{max} of the starch melts as calculated from the peak torque are shown in table 1. Fitting the data to equation [2] revealed:

$$K_{\max} = 2.13 \cdot 10^{5} \cdot \exp(-0.052 \cdot MC - 0.014 \cdot T) \qquad [10]$$

Figure 2 shows the consistency factor fitted with equation [10] and the measured consistency factor. R^2 value was 0.78, which is acceptable considering the accuracy of the torque measurement (± 10%), and residuals were divided randomly around zero.

3.2. Estimated shear and elongation rate division in paddle section

Figures 3a and 3b show the calculated maximum shear rate and elongation rate distribution respectively inside the paddle section, under the assumptions given in section 2.5. At the highest elongation rates, the corresponding stresses are much higher than the maximum shear stresses for all values of the Trouton ratio suggested in section 2.5. This suggests that these stresses are important, although the fraction of material exposed to them is low (figure 3b).

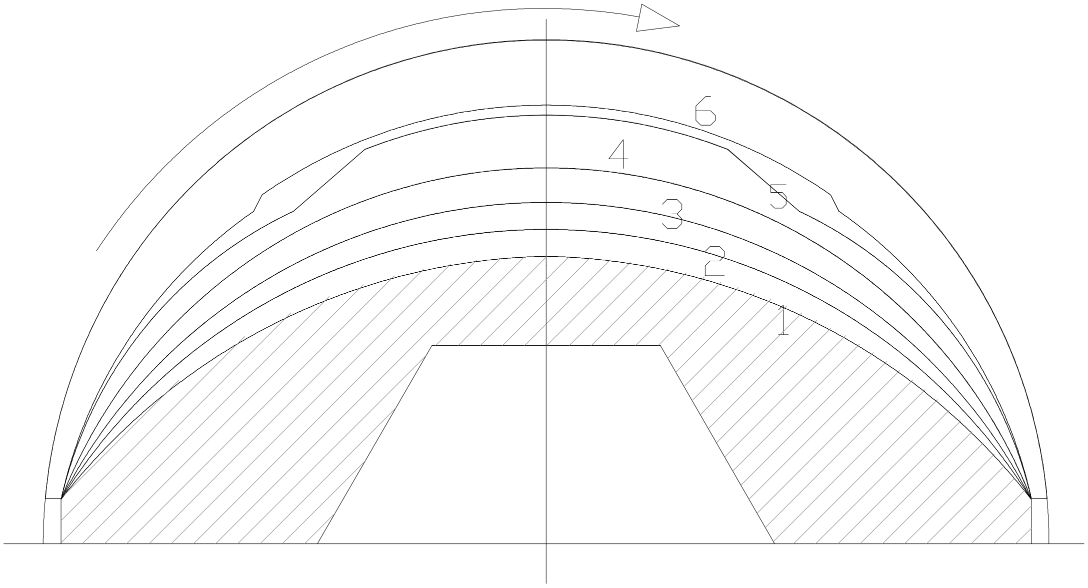

Figure 3a: Distribution of maximally encountered shear rates at the end of a paddle (derived from Van der Wal *et al.*, 1996 and Van der Wal, unpublished). Lines 1 to 6 indicate 0, 20, 40, 60, 80 and 100% of maximum shear rate respectively, calculated to be 122 s^{-1} at $N = 140$ rpm (derived from Van der Wal *et al.*, 1996 and Van der Wal, unpublished). The arrow indicates the rotation direction of the screw.

3.3. Comparison between model and extruder data

Figure 4 shows a parity plot of the experimental data vs. the model prediction for $Tr = 6.5$. In this case, all data are very close to the line $y = x$, indicating that the model described is able to predict the intrinsic viscosity after extrusion, with Tr within the expected range. It should be noted that the model was sensitive to the value of the Trouton ratio. Still, the fact that the Trouton ratio is within the expected range suggests the model to be physically relevant.

The use of a simplified, defined system (our shear cell) enabled us to describe the macromolecular degradation in a complex system (the co-rotating twin screw extruder). It is therefore expected that such a defined system in our future work will contribute to the understanding of development and change of product properties in various engineering scale processes.

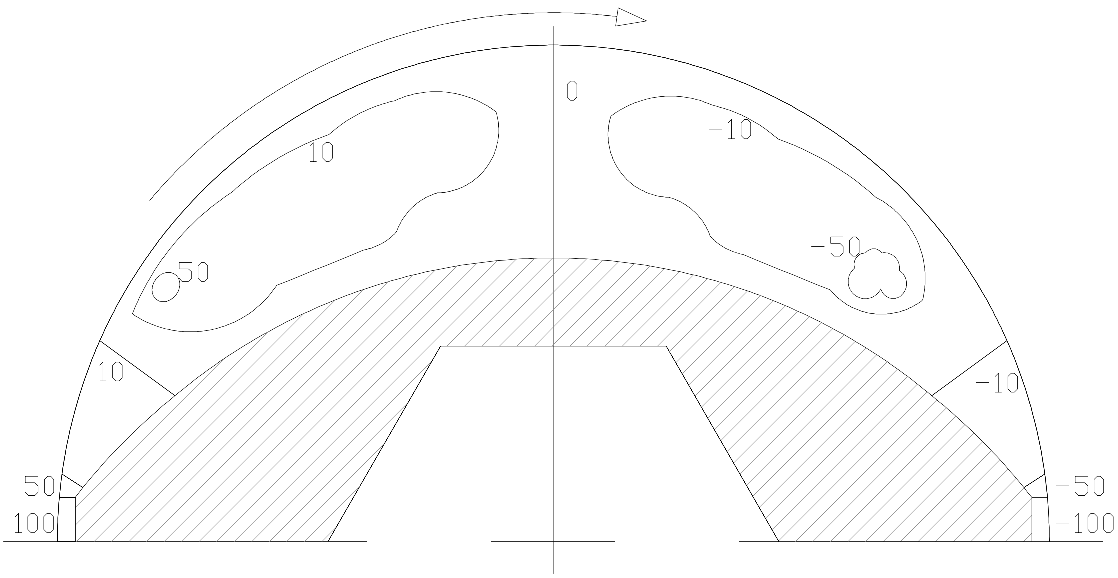

Figure 3b: Distribution of maximally encountered elongation rates at the end of a paddle (derived from Van der Wal *et al.*, 1996). Lines indicate 0, 10, 50 and 100% of maximum elongation rate due to constriction, calculated to be 129 s^{-1} at $N = 140$ rpm. Lines with negative values indicate 10, 50 and 100% of maximum elongation rate due to broadening.

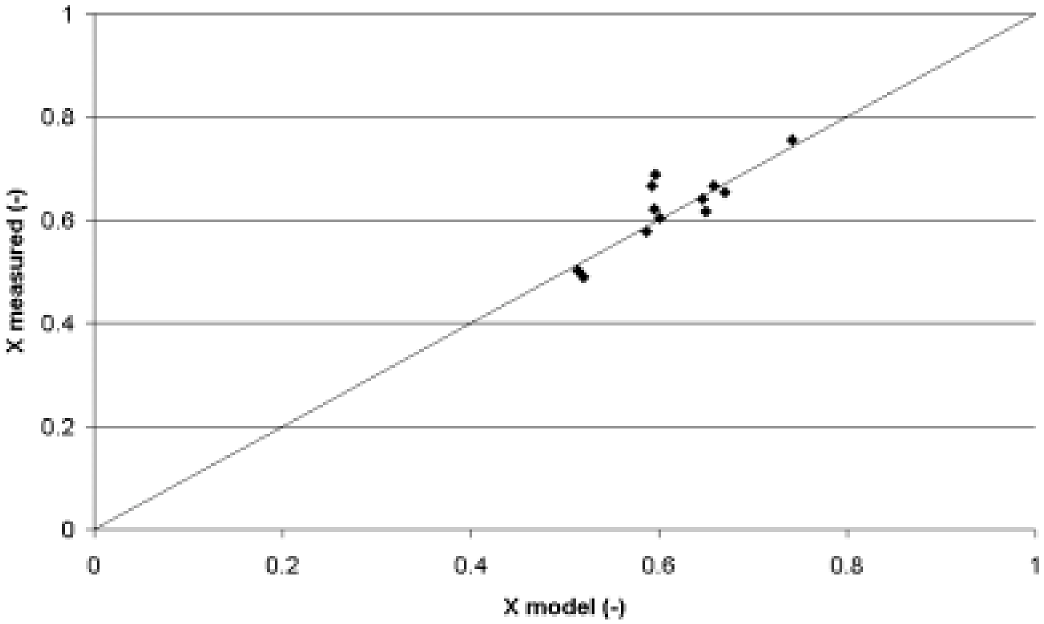

Figure 4: Experimental vs. fitted values for the relative intrinsic viscosity *X* of extruded corn starch. Fitted values were obtained from the model described in sections 2.5 and 2.6 at *Tr* = 6.5.

3.4. Discussion on model assumptions

In this modeling study, it was assumed that calculation of the maximum shear and elongation rate and hence stress distribution supplies the correct maximum stress distribution for the whole paddle section. It is possible that material that has not encountered high shear rates in the first pair of paddles is in fact encountering those high shear rates further on in the section, probably resulting in more breakdown of the starch. On the other hand, viscosity and therefore stresses may be reduced due to the macromolecular breakdown. The validity of the assumption stated above was checked in the following way. The reduction in consistency factor K_{max} in the first paddle due to starch breakdown was calculated from the predicted intrinsic viscosity value after the first paddle according to the equation derived by Parker *et al.* (1990):

$$K_{\max} \sim [\eta]^{3.4} \qquad [12]$$

Using the reduced consistency factor, the same procedure as used to calculate the degradation in the first paddle (sections 2.5 and 2.6) was applied. This was repeated for all 5 completely filled paddles. Results of this rough calculation showed that the other completely filled paddles decreased X maximally 0.0217 (on average 0.007), while the first ones result in a reduction of 0.26-0.49, suggesting that most degradation is likely to take place in the first paddle.

The calculation of the stress distribution is based on the assumption that shear and elongation have the same effect on the molecular breakdown and that the effect of simultaneous shear and elongation can be considered equal to the effect of the larger one of the two. In emulsion technology, it is known that elongation is more effective in breaking up droplets than shear and some relationships describing this effect exist (Walstra, 1983). However, this sort of relationships is unknown for the system described here. Still, as most studies used only nominal values for shear rate, as outlined in the introduction of this paper, the approach used here is a clear step forward, although further investigations on the effect of combined shear and elongation might improve understanding in this respect.

3.5. Consequences for extruder modeling and process design

In this work, the elongational flow regimes were shown to be important in some of the regions where this type of flow took place. So far, studies on extruder stress modeling focussed on shear stress only (Cai *et al.*, 1995). Our results suggest that elongational flow can not be neglected in extrusion studies.

Another interesting result is that our model was able to describe the molecular weight reduction in a complete extruder quite well by concentrating on a single paddle. This could imply that extruders are often oversized when considering molecular weight reduction and possibly other changes in product properties. Once that the first restrictive element is reached, breakdown (this paper) and melting (Colonna *et al.*, 1983) predominantly take place in this high-shear section. A larger length of the extruder is hence unnecessary to induce these transformations, suggesting that extruders may be designed in a more efficient way. This suggestion is more or less in agreement with the current trend towards the use of high screw speeds (see, for example, Qian *et al.*, 2002 and Bleiman *et al.*, 2002), as these high speeds result in short residence times in the high shear sections. On the other hand, high screw speeds will lead to extra breakdown due to the higher shear and elongational stresses occurring.

4. Conclusion

A model for the degradation of corn starch in a twin screw extruder was developed using viscosity data from our shearing device, shear and elongation rate estimations from numerical simulations from literature and the relations between mechanical breakdown and maximum stress derived in our earlier work. Using this model, the relative intrinsic viscosity after extrusion could well be described. The model can therefore be considered as a first step towards a more fundamental understanding of product modifications during the extrusion process by using more defined equipment. Therefore, it is a clear step towards a rational design of processes from the desired product properties.

Acknowledgement

The authors thank Professor A.E.P. Veldman of the University of Groningen, The Netherlands, for providing the flow simulation data, J. Schouten for carrying out part of the intrinsic viscosity measurements and for his assistance during the extrusion experiments, J.J.G. van Soest for his assistance during the X-Ray diffraction measurements and S. van Brenk for carrying out part of the intrinsic viscosity measurements.

Symbols list

C_1	first fit parameter in first order model (-)
C_2	second fit parameter in first order model (m^2/N)
D	extruder diameter (m)
f	fraction of molten material (-)
K	consistency factor ($Pa \cdot s^n$)
K_{max}	consistency factor at $\tau = \tau_{max}$ ($Pa \cdot s^n$)
K_0	consistency factor at (extrapolated) $MC = 0\%$ and $T = 0°C$ ($Pa \cdot s^n$)
k_1	factor describing the dependency of K on moisture content ($\%^{-1}$)
k_2	factor describing the dependency of K on temperature ($°C^{-1}$)
L	extruder length (m)
m	number of equal-stress zones (-)
MC	moisture content (%)
n	pseudoplastic index (-)
N	screw speed (rpm)
T	temperature (°C)
Tr	Trouton ratio (-)
X	relative intrinsic viscosity of the molten fraction of the treated starch compared to native starch (-)
w	weight fraction (-)

Greek symbols

γ	shear rate (s^{-1})
ε	elongation rate (s^{-1})
η	melt viscosity ($Pa \cdot s$)
η_e	elongational viscosity ($Pa \cdot s$)
$[\eta]$	intrinsic viscosity (ml/g)
$[\eta]_0$	intrinsic viscosity of native starch (ml/g)
θ	angle of the shear zone of the shear cell (˚)
σ	elongational stress (Pa)
σ_{max}	maximum elongational stress (Pa)

τ	shear stress (Pa)
τ_{max}	maximum shear stress (Pa)

References

Barron, C., Buleon, A., Colonna, P., & Valle, G. Della (2000). Structural modifications of low hydrated pea starch subjected to high thermomechanical processing. *Carbohydrate Polymers*, 43, 171-181.

Barron, C., Bouchet, B., Della Valle, G., Gallant, D.J., & Planchot, V. (2001). Microscopical study of the destructuring of waxy maize and smooth pea starches by shear and heat at low hydration. *Journal of Cereal Science*, 33, 289-300.

Bhattacharya, M. (1993). Slit rheometer studies of wheat flour dough. *Journal of Texture Studies*, 24(4), 391-409.

Bhattacharya, M., Padmanabhan, M., & Seethamraju, K. (1994). Uniaxial extensional viscosity during extrusion cooking from entrance pressure drop method. *Journal of Food Science*, 59(1), 221-226.

Bindzus, W., Fayard, G., Van Lengerich, B., & Meuser, F. (2002). Description of extrudate characteristics in relation to the shear stress of plasticised starches determined in-line. *Starch / Staerke*, 54, 252-259.

Bleiman, P., Bulters, M., Elemans, P., & Slot, H. (2002). Melting model for co-rotating twin-screw extruders. In SPE, *Proceedings of ANTEC 2002*. Brookfield, Society of Plastic Engineers, Inc.

Bruemmer, T., Meuser, F., Lengerich, B. van, & Niemann, C. (2002). Expansion and functional properties of corn starch extrudates related to their molecular degradation, product temperature and water content. *Starch / Staerke*, 54, 9-15.

Cai, W., Diosady, L.L., & Rubin, L.J. (1995). Degradation of wheat starch in a twin-screw extruder. *Journal of Food Engineering*, 26, 289-300.

Choudhury, G.S., & Gautam, A. (1998). Comparative study of mixing elements during twin-screw extrusion of rice flour. *Food Research International*, 31(1), 7-17.

Colonna, P., Melcion, J.P., Vergnes, B., & Mercier, C. (1983). Flow, mixing and residence time distribution of maize starch within a twin-screw extruder with a longitudinally split barrel. *Journal of Cereal Science*, 1, 115-125.

Davidson, V.J., Paton, D., Diosady, L.L., & Larocque, G. (1984a). Degradation of wheat starch in a single-screw extruder: characteristics of extruded starch polymers. *Journal of Food Science*, 49, 453-458.

Davidson, V.J., Paton, D., Diosady, L.L., & Rubin, L.J. (1984b). A model for mechanical degradation of wheat starch in a single-screw extruder. *Journal of Food Science*, 49, 1154-1157.

Diosady, L.L., Paton, D., Rosen, N., Rubin, L.J., & Athanassoulias, C. (1985). Degradation of wheat starch in a single-screw extruder: mechano-kinetic breakdown of cooked starch. *Journal of Food Science*, 50, 1697-1699, 1706.

Einde, R.M. van den, Bolsius, A., Soest, J.J.G. van, Janssen, L.P.B.M., Goot, A.J. van der, & Boom, R.M. (2004a). The effect of thermomechanical treatment on starch breakdown and the consequences for process design. *Carbohydrate Polymers*, 55(1), 57-63. (Chapter 2 of this thesis).

Einde, R.M. van den, Akkermans, C., Goot, A.J. van der, & Boom, R.M. (2004b). Molecular breakdown of corn starch by thermal and mechanical effects. Submitted to *Carbohydrate Polymers*. (Chapter 4 of this thesis).

Govindasamy, S., Campanella, O.H., & Oates, C.G. (1996). High moisture twin-screw extrusion of sago starch: 1. Influence on granule morphology and structure. *Carbohydrate Polymers*, 30, 275-286.

Harper, J.M. (1986). Extrusion texturization of foods. *Food Technology*, 40, 70, 72, 74-76.

Ilo, S., & Berghofer, E. (1998). Kinetics of thermomechanical destruction of thiamin during extrusion cooking. *Journal of Food Science*, 63(2), 312-316.

Jones, D.M., Walters, K., & Williams, P.R. (1987). On the extensional viscosity of mobile polymer solutions. *Rheologica Acta*, 26(1), 20-30.

Komolprasert, V., & Ofoli, R.Y. (1990). Effect of shear on thermostable alpha-amylase activity. *Food Science and Technology / Lebensmittel Wissenschaft und Technologie*, 23, 412-417.

Orford, P.D., Parker, R., & Ring, S.G. (1993). The functional properties of extrusion-cooked waxy-maize starch. *Journal of Cereal Science*, 18, 277-286.

Parker, R., Ollett, A.L., & Smith, A.C. (1990). Starch melt rheology: measurement, modelling and applications to extrusion processing. In P. Zeuthen. *Processing and quality of foods* (pp. 1.290-1.295). London: Elsevier.

Qian, B., Gogos, C.G., & Todd, D.B. (2002). The melting behavior of amorphous polyester in a co-rotating twin screw extruder. In SPE. *Proceedings of ANTEC 2002*. Brookfield, Society of Plastic Engineers, Inc.

Remsen, C.H., & Clark, J.P. (1978). A viscosity model for a cooking dough. *Journal of Food Process Engineering*, 2, 39-64.

Valle, G. Della, Boche, Y., Colonna, P., & Vergnes, B. (1995). The extrusion behaviour of potato starch. *Carbohydrate Polymers*, 28, 255-264.

Vergnes, B., Villemaire, J.P., Colonna, P., & Tayeb, J. (1987). Interrelationships between thermomechanical treatment and macromolecular degradation of maize starch in a novel rheometer with preshearing. *Journal of Cereal Science*, 5, 189-202.

Vergnes, B., & Villemaire, J.P. (1987). Rheological behaviour of low moisture molten maize starch. *Rheologica Acta*, 26, 570-576.

Wal, D.J. van der, Goffart, D., Klomp, E.M., Hoogstraten, H.W., & Janssen, L.P.B.M. (1996). Three-dimensional flow modeling of a self-wiping corotating twin-screw extruder. Part II: the kneading section. *Polymer Engineering and Science*, 36(7), 912-924.

Walstra, P. (1983). Formation of emulsions. In P. Becher. *Encyclopedia of emulsion technology, volume 1: basic theory* (pp. 57-127). New York, Marcel Dekker Inc.

Willett, J.L., Millard, M.M., & Jasberg, B.K. (1997). Extrusion of waxy maize starch: melt rheology and molecular weight degradation of amylopectin. *Polymer*, 38(24), 5983-5989.

Chapter 6

Local mixing effects of screw elements during extrusion

Abstract

An in-line method was applied to determine local residence time distribution (RTD) at two places in a completely filled co-rotating twin screw extruder. Axial mixing effects of different types of elements were evaluated. Elements were found to induce mixing downstream, but also upstream of them. Therefore, it was concluded that global RTD measurements provide too little information on the local mixing. Each element could be characterized by an equivalent additional mixing length λ, which may be practically useful for extrusion applications.

This chapter was submitted for publication as: R.M. van den Einde, P. Kroon, A.J. van der Goot, R.M. Boom, Local mixing effects of screw elements during extrusion.

1. Introduction

In the last decades, interest has steadily grown in the use of co-rotating twin screw extruders in both food- and non-food applications (De Ruyck, 1997; Oberlehner *et al.*, 1994; Puaux *et al.*, 2000). The extruder can be used for various functions, such as mixing, cooking or chemical reactions.

To meet today's product specifications, accurate control over process conditions is required. Insight into flow and mixing in the extruder is essential in this respect. Residence time distribution (RTD) measurements are often used to determine the extent of mixing and flow phenomena inside the extruder. In various studies in literature, the RTD was measured at the end of the extruder, as recently reviewed by Ganjyal and Hanna (2002).

In case of extrusion, the RTD is determined by a combination of degree of fill, which mainly influences mean residence time, and the screw design, which influences the degree of axial mixing. Therefore, the RTD is useful for a first, overall impression of the mixing behavior, but it hardly provides detailed information on the local flow phenomena (Carneiro *et al.*, 1999). Measurement of mixing in a single element would allow improved understanding of the different mechanisms of mixing that are taking place locally in the extruder. Therefore, it is interesting to determine local RTD over a screw element in order to characterize the effect of a screw element on the flow directly.

To our knowledge, few attempts to measure local RTD curves are described in literature. In general, two types of studies can be distinguished. In some studies local RTD is defined as the global RTD measured over a very short part of the extruder with die. Jager *et al.* (1991) injected the tracer at various points along a co-rotating twin screw extruder and measured the RTD at the die. Oberlehner *et al.* (1994) measured RTD at the die of a short part of an intermeshing co-rotating twin screw extruder.

In other studies the RTD is measured locally along the screw. Chalamet *et al.* (2000) measured the local RTD during reactive extrusion using an in-line ultrasonic technique. Jager *et al.* (1988, 1989) measured local RTD of the various zones of a counter-rotating twin screw extruder using a radioactive tracer and two scintillation detectors and modeled the effect of each zone. Gao *et al.* (1999) measured local RTD along the screw with an optical probe, but only used the RTD measured at the die for further analysis. An interesting study was carried out by Carneiro *et al.* (1999). They showed that a mixing block with discs offset 90° in a partially filled co-rotating twin-screw extruder induces (back) mixing locally, upstream of the block.

It can therefore be concluded that the mixing in a twin screw extruder is more complex than can be deduced from the overall RTD curve. This mixing behavior determines the typical distribution of processing histories that a product stream will experience and thus strongly influences overall product quality. Therefore, it is interesting to investigate the local mixing effects of elements and the distance or volume over which back flow can occur. The aim of this study was therefore to measure in-line the effects of different types of screw elements (transport, single lead, paddles 90° forward, paddles 30° reverse) on the local RTD both upstream and downstream the element in a co-rotating twin screw extruder with a completely filled measurement section.

2. Materials and methods

2.1. Material

The fluid used for RTD measurements was a 6% (w/v) solution of pre-gelatinized waxy corn starch in water. Tracer was prepared by mixing this starch solution (88.75%) with NaCl (10%) and water (1.25%).

The viscosity of both tracer and flow material was after preparation 1.8 Pa·s at the average shear rate in the channel of a transport element at the process conditions investigated in this study (= 18 s^{-1}, calculated according to Martelli (1983) and Yacu (1985)).

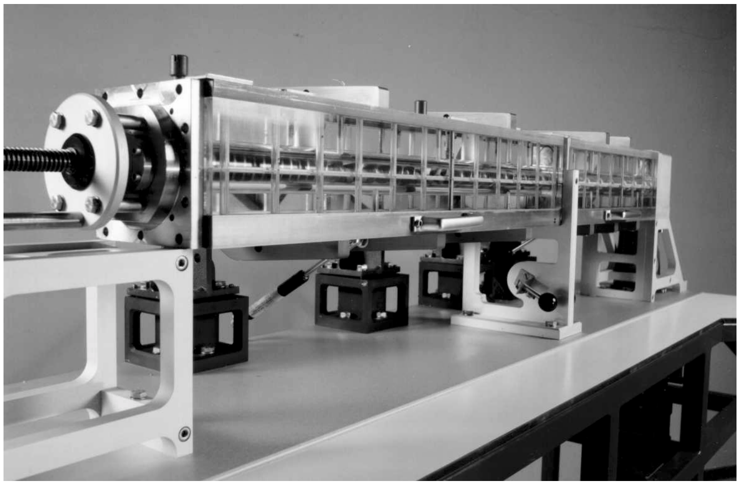

Figure 1: Full size translucent co-rotating twin screw model extruder (dimensions equal to APV MPF 50 extruder).

2.2. Extruder

The extruder used was a transparent full size model of a co-rotating APV MPF 50 twin screw extruder (*L/D* of used part = 14.5; *D* = 50 mm). A picture of this extruder is shown in figure 1. The flow rate was $11.7 \cdot 10^{-6}$ m^3/s (± 5%). Flow rate was measured using an Endress & Hauser Promag 50 measuring device. Screw speed was 60 rpm. The model material was fed to the extruder through a gear pump. The theoretical flow rate Q_{th} of the transport elements was calculated to be $11 \cdot 10^{-5}$ m^3/s, which means that the extruder gave rise to an additional pumping effect, as usual under practical conditions.

Apart from the measurement section, the screw configuration was the same in all experiments, as schematically outlined in figure 2. The extruder was completely filled with fluid during all measurements.

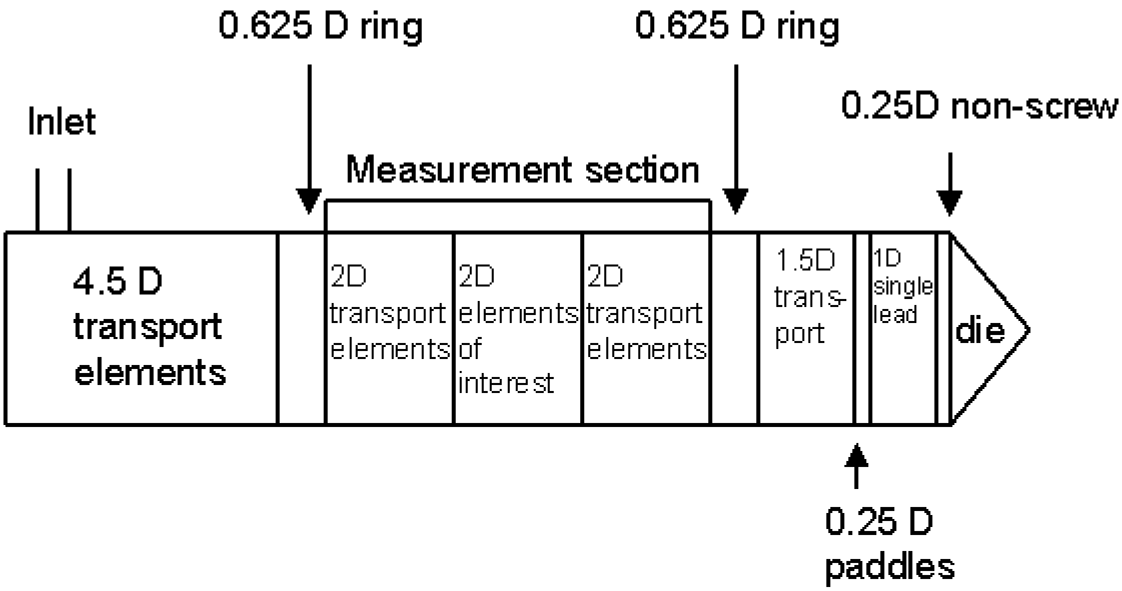

Figure 2: Extruder configuration.

Tracer was fed into the extruder by means of an injection system shown in figure 3. The injection system consisted of two electronically adjusted valves and a digital timer, allowing an exact tracer block pulse of 1 second. The tracer injection system was connected to the extruder via a tube (length = 85 cm, diameter = 14 mm). The complete setup is schematically shown in figure 4 (tracer injection system not shown).

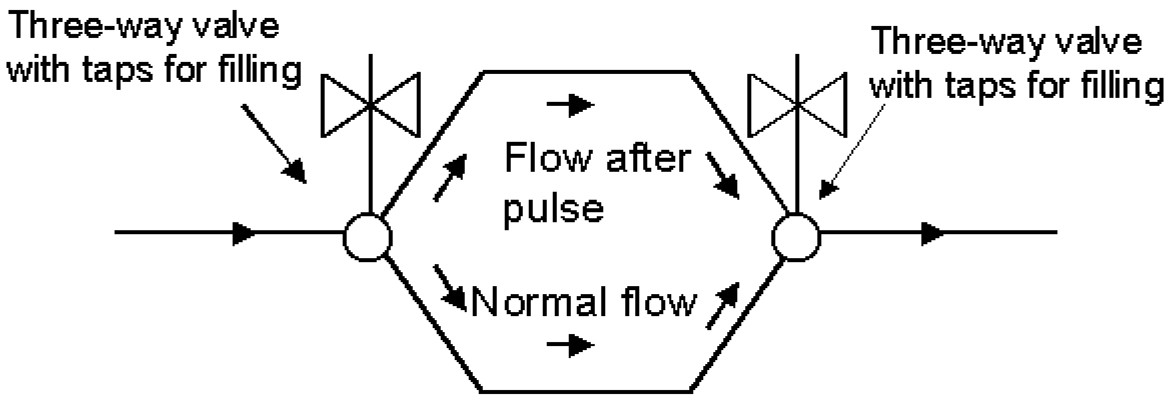

Figure 3: Tracer injection system.

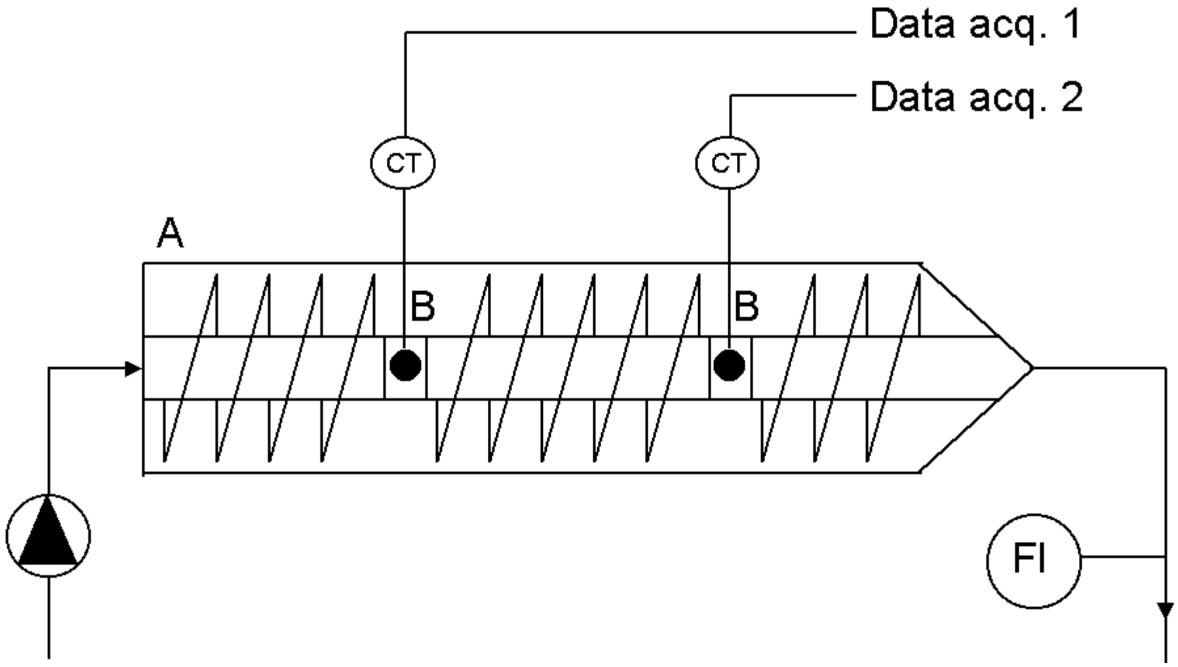

Figure 4: Extruder with system for local RTD measurement: A = extruder; B = conductivity probes; CT = conductivity transmitters; FI = flow rate measuring device.

2.3. In-line measurement system

The technique investigated was based on the measurement of the electrical conductivity of the material at two points in the extruder. This type of technology was earlier used by Castelain and co-workers for determination of RTD curves in spatially chaotic 3D flow (Castelain *et al.*, 2000). The method described here is based on the measurement system used by Van den Einde *et al.* (2002) with various modifications allowing simultaneous measurements of both RTD functions.

The two measurement points were located before and after a 6 D element section (figure 2). To avoid damage of the conductivity probes (WTW TetraCon 325) by the screw, a plastic spacer ring (0.625 D) was placed around the axis near the probes. The main wire of each probe was exactly halfway at the ring. The element section of interest (2 D) was placed in between two sections of transport elements (each 2 D) so that effects further upstream and downstream of the element could be measured (as explained in the Introduction of this chapter).

Electrical influences on the measurements (via extruder screw, sockets or connected measurement devices) turned out to be critical. Therefore, the signals of the probes were transformed to volt signals completely independently from each other as described below.

The signal of the first probe was transferred to a volt signal by a WTW LF 340 battery-operated conductivity transmitter. This volt signal was recorded by a FLUKE 89 IV multimeter. The signal of the second probe was transferred to a volt signal by a WTW LF 538 conductivity transmitter. Between the transmitter and the socket, an isolating transformer was placed to avoid disturbances of the conductivity signal by external factors. The volt-signal was then recorded on a data logging system connected to a computer with Viewdac 2.10 software (Keithley Instruments Inc.). Both systems were independently calibrated. Measurement of both *E(t)* curves was now possible within one experiment.

2.4. Determination of local RTD by in-line method

At steady state conditions, the in-line measurement system was started and at the same moment the tracer was injected as a 1 second block pulse. The signals of both probes were recorded until they were back at base line.

The conductivity responses from the probes were smoothed according to a 3 point moving average method:

$$k(n) = \frac{k(n-1) + k(n) + k(n+1)}{3} \qquad [1]$$

The base line was then subtracted from the measurement points and salt concentrations were calculated. The *E(t)* function was calculated according to:

$$E(t) = \frac{c_i(t)}{\int_0^{\infty} c_i(t)dt} = \frac{c_i(t)}{\sum_0^{\infty} c_i(t)\Delta t} \qquad [2]$$

Quality of the measurement was tested by checking the total amount of salt detected by each of the probes. Furthermore, the mean residence time τ of both measurement points was calculated from the measurement according to:

$$\tau = \frac{\int_0^\infty c(t) \cdot t \cdot dt}{\int_0^\infty c(t) \cdot dt} \qquad [3]$$

The measured mean residence time was compared to the theoretical mean residence time (τ_{th}), calculated according to:

$$\tau_{th} = \frac{V}{Q_v} \qquad [4]$$

where V is the extruder volume from the tracer injection system until the measurement probe.

3. Results and discussion

3.1. Quality of measurement

Percentages of detected salt compared to the salt in the inlet pulse are shown in table 1. All values are close to 100%, suggesting a reliable measurement. For unknown reasons, the percentage detected by the second probe was consistently somewhat lower in the experiments with forward 90° paddles.

Table 1 also shows that the measured mean residence time τ was well reproducible within a series of experiments with the same element of interest (± at most 2.5%).

3.2. RTD curve and mean residence time

As expected, different screw elements gave rise to differences in RTD downstream of the elements. However, for some elements also upstream effects were observed (figure 5). Strongest effects were found after incorporation of paddles. Paddles –30° resulted in a broad RTD curve upstream of this element section. Paddles +90° resulted in a broad RTD curve downstream of this element section.

The theoretical value of the mean residence time was always lower than the measured one (equations [3-4] and table 2), suggesting circular flows inside the extruder. A result of these circular flows is an increased apparent volume over which the mean residence time is actually measured (figures 6 and 7). Hence, the measured mean residence time is equal to this apparent

Table 1: Flow rates (Q_v), average percentages detected NaCl and measured mean residence times (τ) in the experiments for both probes. Subscripts 1 and 2 indicate the first and second measurement point respectively; exp. no. = experiment number.

Element of interest	Exp. no.	Q_v (10^{-6} m^3/s)	% probe 1	τ_1 (s)	% probe 2	τ_2 (s)
transport	1	11.6	107	67.2	100	125.7
	2	11.8	107	68.5	98	124.9
	3	11.9	109	68.8	100	126.4
	4	11.9	100	71.3	90	126.5
single lead	1	11.5	110	70.0	97	118.0
	2	11.1	108	70.0	96	118.8
paddles +90°	1	12.2	107	74.3	83	144.2
	2	12.0	109	75.2	83	144.6
	3	12.1	109	74.4	82	146.1
paddles –30°	1	11.6	104	101.8	96	131.1
	2	11.7	104	97.8	97	125.3
	3	11.7	105	99.2	99	130.5
	4	11.6	106	99.7	97	128.5
	5	11.6	104	97.7	95	127.2
	6	11.6	102	97.9	96	127.7

volume divided by the flow rate. This can be written as:

$$\tau_1 = \frac{V_0 + q_1 \cdot V_1}{Q_v} \qquad [5a]$$

where q_1 ($0 \leq q_1 \leq 1$) denotes the fraction of the volume between the first and the second measurement point that is actually part of the apparent volume, and:

$$\tau_2 = \frac{V_0 + V_1 + q_2 \cdot V_2}{Q_v} \qquad [5b]$$

respectively, where q_2 denotes the fraction of volume of the section downstream of the second probe that is part of the apparent volume over which the mean residence time is measured. Because the volume of elements differs, the downstream volumes were defined in terms of the corresponding additional mixing length λ, the length of the section downstream of the

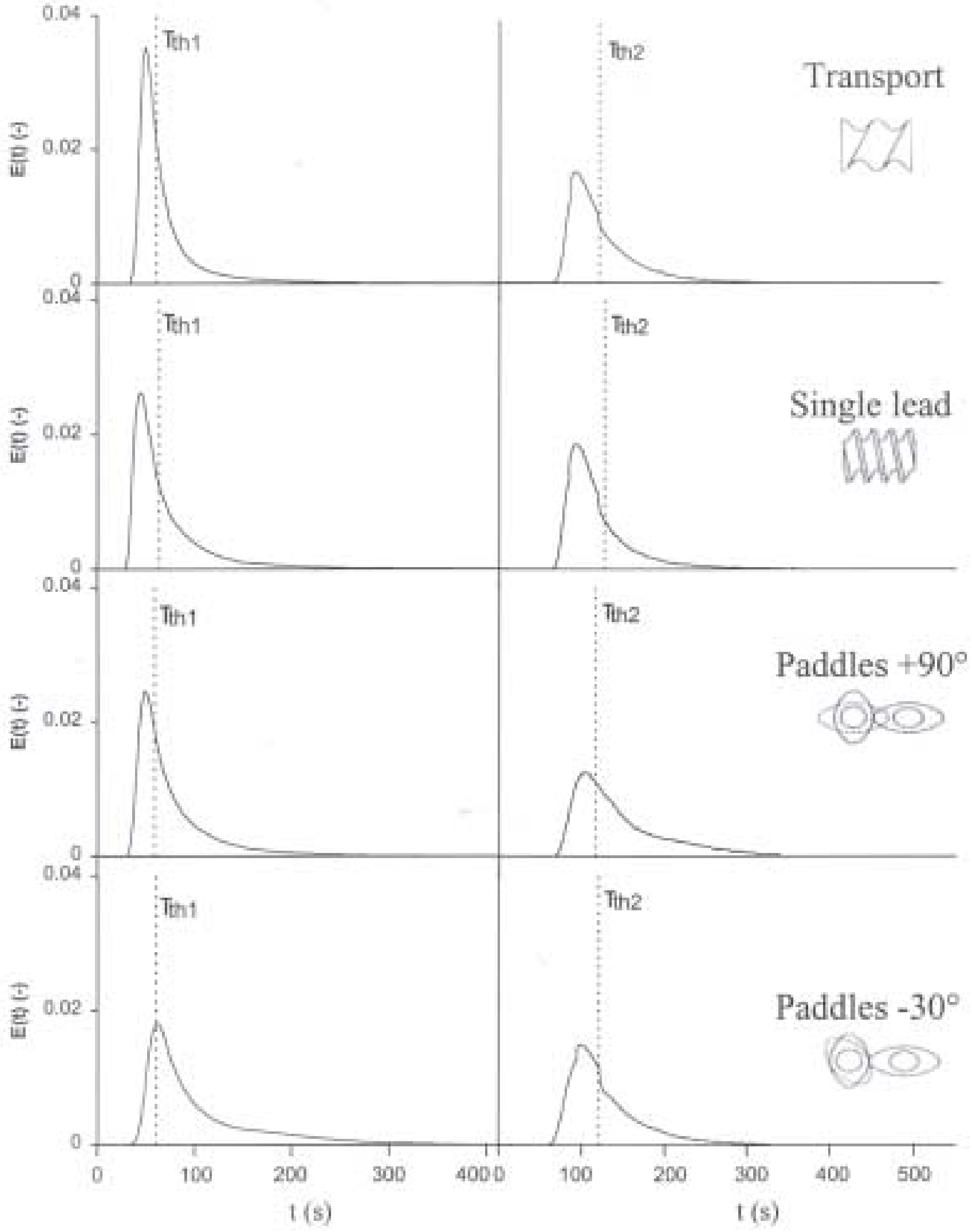

Figure 5: Local residence time distribution curves obtained at the two measurement points (η = 1.8 Pa·s, 60 rpm) for different mixing elements.

probe that is part of the apparent volume over which the mean residence time is measured. As extruder lengths are often defined as a function of the diameter of the screw D, λ was divided by D, resulting in the dimensionless additional mixing length (λ/D). This can be written as:

$$\frac{\lambda_1}{D} = \frac{q_1 \cdot V_1}{v} \qquad [6a]$$

and

$$\frac{\lambda_2}{D} = \frac{q_2 \cdot V_2}{v} \qquad [6b]$$

where v denotes the extruder volume (m^3) of a section with length D. v differs slightly for each element type. Table 2 shows that additional mixing length of the material at both measurement points was highly influenced by the elements in the measurement section.

Part of the additional mixing length could be caused by two factors. Firstly, the ring around the screw axis that avoids damage of the probe probably behaves as a perfect mixer, resulting in circular flow from both upstream and downstream with λ/D = at most 0.3 (see subsection: In-line measurement system). Secondly, the accuracy of the flow rate measurement was ± 3%, causing a possible deviation in λ/D of 0.2 at the first measurement point and of 0.4 at the second measurement point. Therefore, only if the absolute value of λ/D was larger than 0.5 at the first probe or larger than 0.7 at the second probe, it was concluded that significant circular flow as a result of screw elements took place.

Table 2 shows that transport elements did not induce any significant circular flow at the second probe. However, at the first probe some circular flow took place. To explain this, the model of Jager *et al.* (1991) was used, who interpreted the extruder as a row of moving CSTRs with back flow. The number of CSTRs downstream of the second probe is much lower than the number downstream of the first probe, resulting in less circular flow to the second probe. The use of single lead elements resulted in the same type of flow pattern. No significant circular flow was induced at the second probe, whereas some circular flow towards the first probe took place. The negative value of λ/D at the second probe was probably a result of the maximum measurement accuracy due to variation in throughput.

The main difference between transport or single lead elements and paddles is the lack of drag flow towards the die in paddles. This implies that transport towards the die is a result of pressure flow, as shown in figure 6.

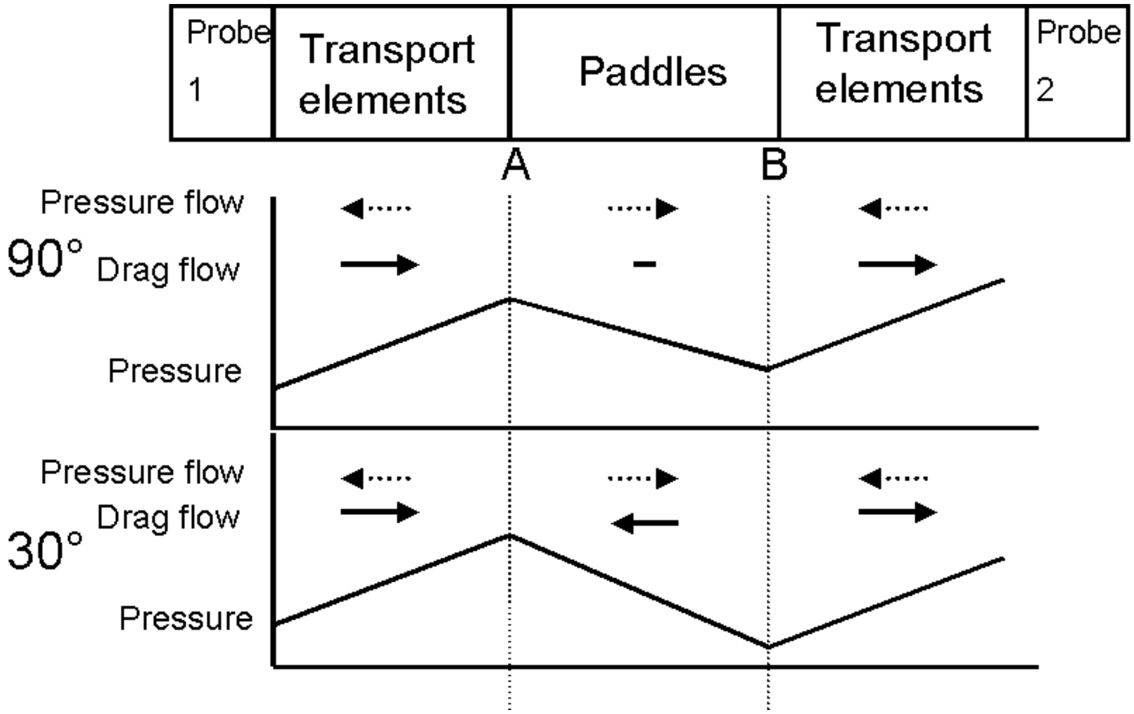

Figure 6: Schematic description of the pressure flow and drag flow as suggested to take place in paddles +90° and paddles –30° and in the transport elements upstream and downstream of them. Arrows indicate the direction of the flow only. - = no flow expected. Dashed arrows indicate pressure flow; solid arrows indicate drag flow.

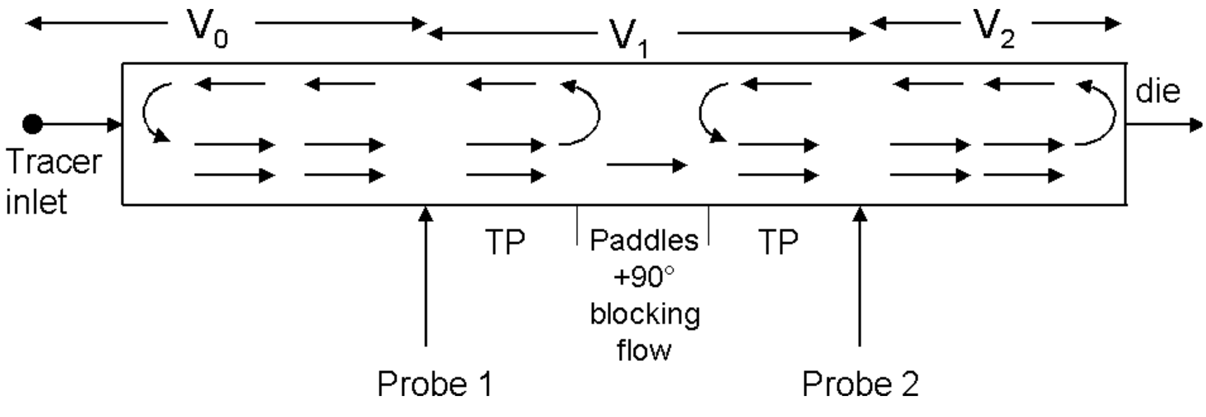

Figure 7: Visualization of circular flow patterns as induced by paddles +90°. The use of two arrows instead of one indicates that a relatively larger amount of flow is suggested.

Table 2: Theoretical mean residence time (τ_{th}, equation [4]), downstream volume fractions q_1 and q_2 that are part of the apparent volume and additional mixing length λ/D (see text). Subscripts 1 and 2 indicate the first and second measurement point respectively, exp. no. = experiment number.

Element	Exp. no.	τ_{1th} (s)	q_1 (-)	λ_1/D (-)	τ_{2th} (s)	q_2 (-)	λ_2/D (-)
transport	1	58.4	0.13	0.81	124.1	0.05	0.12
	2	57.5	0.17	1.07	122.0	0.08	0.23
	3	57.0	0.19	1.16	121.0	0.16	0.48
	4	57.0	0.22	1.43	121.0	0.16	0.49
single lead	1	59.0	0.18	1.04	122.1	-0.12	-0.32
	2	61.1	0.14	0.79	126.5	-0.21	-0.66
paddles +90°	1	55.6	0.32	1.95	114.4	0.89	3.17
	2	56.6	0.31	1.91	116.3	0.83	3.07
	3	56.0	0.31	1.89	115.4	0.91	3.20
paddles –30°	1	58.4	0.70	4.20	120.3	0.31	1.02
	2	57.9	0.65	3.91	119.3	0.17	0.53
	3	57.9	0.67	4.04	119.3	0.32	1.08
	4	58.4	0.67	4.00	120.3	0.23	0.75
	5	58.4	0.63	3.82	120.3	0.20	0.62
	6	58.4	0.64	3.84	120.3	0.21	0.67

The lack of drag flow in paddles +90° leads to a virtual block of the flow at the position marked A in figure 6. This block results in circular flow towards the first probe. At position B, no material can stream upwards. This leads to circular flow towards the second probe, as material flowing back from the transport element section downstream of the paddles can not enter the paddles +90° section due to the lack of drag flow and the pressure gradient in these paddles (figure 6). The complete resulting flow pattern is visualized in figure 7. Due to this pattern, a large additional mixing length was found both at the first and the second measurement point (table 2).

Finally, the large negative conveying drag flow induced by paddles –30° makes that particles passing position A are actively transported back, resulting in a large additional mixing length at the first measurement point. Although the pressure drop in these elements does not favor back flow, the negative conveying drag flow allows material that is flowing back from the transport element section to flow upstream, so that circular flow towards the second probe is limited. Hence, only a relatively small additional mixing length was measured at the second measurement point.

3.3. Consequences for process design and flow measurements and modeling

The local mixing effects upstream of elements found in this work can not be determined using global RTD measurements, because the additional mixing length is in that case not included. This means that there is a clear risk that measurements of RTD carried out at the end of the extruder underestimate the mixing inside the extruder and thus provide incorrect information for process design.

The measurements showed that the mixing effect of transport and single lead elements was dependent on the available downstream volume. As far as we can see now, it is likely that this effect also holds for the other types of elements. This means that positioning of these elements influences the local mixing effect. It is known that the positioning of elements determines their effect in a partially filled twin screw extruder, due to effects on the degree of fill (Gautam and Choudhury, 1999), but the effect that we found has not yet been reported.

Our results may also have important consequences for modeling of extruder flow, as they clearly show the complexity of the extruder flow pattern and the interactions between elements. Some modeling studies have focused on detailed numerical calculation of the flow profile in a single element or in a block of elements of the same type (Van der Wal *et al.*, 1996; Ishikawa *et al.*, 2000). The effects described in this paper suggest that taking into account a larger section of elements would significantly increase the relevance of flow modeling.

4. Conclusion

The local mixing effect of different types of elements in a co-rotating twin screw extruder was successfully determined using local RTD measurements. Elements in a completely filled twin screw extruder were found to induce mixing downstream, but also upstream. This means that the positioning of elements is important, not only from the well known effects on the degree of fill, but even in a completely filled system. Comparison between the measured mean residence time and the theoretical one showed the following differences between the elements with respect to circular flow:

- Paddles +90° induce circular flow both downstream and upstream of these elements, due to the pressure drop in these elements without drag flow.
- Paddles –30° induce circular flow upstream of these elements, due to the combination of the pressure drop in these elements and their negative conveying effect.
- Single lead and transport elements induce limited circular flow upstream of them.

The circular flow of each element could well be characterized using the additional mixing length λ, suggesting that this parameter is important in extrusion applications. The additional mixing length is depending on the remaining length of the screw and the type of element.

The effect of elements on RTD upstream clearly shows that more attention should be paid to local flow phenomena, which in many cases can not be extracted from global residence time distribution measurements. Since these local flow phenomena were found to have a large effect on global flow patterns inside the extruder, the result indicates that for further understanding it is essential to consider the local flow phenomena as part of the complete extruder.

Acknowledgement

The authors thank J. Peters and C. de Regt for their contributions during the early stages of this work.

Symbols

$c(t)$	concentration of NaCl at time = t (kg/m^3)
D	extruder diameter (m)
$E(t)$	residence time distribution function (1/s)
$k(n)$	nth data point for screw configuration k (-)
L	length (m)
q_1	the fraction of volume of the section downstream of the first probe that is part of the apparent volume over which mean residence time is measured by this probe (-)
q_2	the fraction of volume of the section downstream of the second probe that is part of the apparent volume over which mean residence time is measured by this probe (-)

Q_{th}	theoretical maximal throughput (m^3/s)
Q_v	extruder throughput (m^3/s)
t	time (s)
V	volume (m^3)
V_0	extruder volume until the first measurement point (m^3) [including tube connecting tracer injection system to extruder]
V_1	extruder volume between first and second measurement point (m^3)
V_2	extruder volume downstream of second measurement point (m^3)

Greek symbols

λ	additional mixing length (D)
v	extruder volume with length D (m^3)
τ	mean residence time as calculated from the measurements (s)
τ_{th}	theoretical mean residence time (s)

References

Carneiro, O.S., Caldeira, G., & Covas, J.A. (1999). Flow patterns in twin-screw extruders. *Journal of Materials Processing Technology*, 92-93, 309-315.

Castelain, C., Berger, D., Legentilhomme, P., Mokrani, A., & Peerhossaini, H. (2000). Experimental and numerical characterisation of mixing in a steady spatially chaotic flow by means of residence time distribution measurements. *International Journal of Heat and Mass Transfer*, 43, 3687-3700.

Chalamet, Y., Taha, M., & Vergnes, B. (2000). Carboxyl terminated polyamide 12 chain extension by reactive extrusion using a dioxazoline coupling agent. *Polymer Engineering and Science*, 40(1), 263-274.

Einde, R.M. van den, Peters, J., Goot, A.J. van der, & Boom, R.M. (2002). In-line measurement of local residence time distribution in a twin screw extruder. In: *Proceedings of ANTEC 2002 San Francisco, vol. 1 Processing* (p. 28-30). Brookfield: Society of Plastics Engineers, Inc.

Ganjyal, G., & Hanna, M. (2002). A review on Residence Time Distribution (RTD) in food extruders and study on the potential of neural networks in RTD modeling. *Journal of Food Science*, 67(6), 1996-2002.

Gao, J., Walsh, G.C., Bigio, D., Briber, R.M., & Wetzel, M.D. (1999). Residence time distribution model for twin-screw extruders. *AIChE Journal*, 45(12), 2541-2549.

Gautam, A., & Choudhury, G.S. (1999). Screw configuration effects on residence time distribution and mixing in twin-screw extruders during extrusion of rice flour. *Journal of Food Process Engineering*, 22, 263-285.

Ishikawa, T., Kihara, S. I., & Funatsu, K. (2000). 3-D Numerical simulations of nonisothermal flow in co-rotating twin screw extruders. *Polymer Engineering and Science*, 40(2), 357-364.

Jager, T., Zuilichem, D.J. van, Stolp, W., & Riet, K. van ’t (1988). Residence time distributions in extrusion-cooking. IV. The feed zone of a conical, counter-rotating, twin-screw extruder processing maize grits. *Journal of Food Engineering*, 8(3), 157-172.

Jager, T., Zuilichem, D.J. van, Stolp, W., & Riet, K. van ’t (1989). Residence time distributions in extrusion-cooking. V. The compression zone of a counter-rotating, twin-screw extruder fed with maize grits. *Journal of Food Engineering*, 9(3), 203-218.

Jager, T., Zuilichem, D.J. van, Swart, J.G. de, & Riet, K. van ’t (1991). Residence time distributions in extrusion-cooking. VII. Modelling of a corotating, twin-screw extruder fed with maize grits. *Journal of Food Engineering*, 14(3), 203-239.

Martelli, F.G. (1983). *Twin-screw extrusion*, New York: Van Nostrand Reinhold Company.

Oberlehner, J., Cassagnau, P. & Michel, A. (1994). Local residence time distribution in a twin screw extruder. *Chemical Engineering Science*, 49(23), 3897-3907.

Puaux, J.P., Bozga, G., & Ainser, A. (2000). Residence time distribution in a corotating twin-screw extruder. *Chemical Engineering Science*, 55(9), 1641-1651.

Ruyck, H. de (1997). Modelling of the residence time distribution in a twin-screw extruder. *Journal of Food Engineering*, 32(4), 375-390.

Wal, D.J. van der, Goffart, D., Klomp, E.M., Hoogstraten, H.W., & Janssen, L. P. B. M. (1996). Three-dimensional flow modeling of a self-wiping corotating twin-screw extruder. Part II: the kneading section. *Polymer Engineering and Science*, 36(7), 912-924.

Yacu, W.A. (1985). Modelling a twin screw co-rotating extruder. *Journal of Food Engineering*, 8, 1-21.

Chapter 7

Understanding molecular weight reduction of starch during heating-shearing processes

Abstract

Recent understanding of the mechanisms underlying the changes in molecular weight of starch as a function of process parameters during thermomechanical treatment, for example extrusion, holds promise towards more effective optimization of thermomechanical processes according to the desired modification of molecular weight. This paper summarizes recent advances in theoretical understanding and experimental methods. Empirical observations from extruder experiments can be better understood on this basis.

The current status in this field has opened up potential for developing new equipment in which the main process parameters, which normally occur simultaneously, can be separated and optimized. This will create a much wider window for product-oriented process design and for new products.

This chapter was published as: R.M. van den Einde, A.J. van der Goot, R.M. Boom, Understanding molecular weight reduction of starch during heating-shearing processes. (2003). *Journal of Food Science*, 68(8), 2396-2404.

1. Introduction

Food products are required to have specific properties. Examples are crispiness, strength, brittleness, stringiness and fracturability. In many cases, obtaining the correct properties is still trial and error. In today's fast-moving market, there is clearly a demand for "reverse process engineering", the design of process and product formulation according to the desired properties (Meeuwse *et al.*, 1999).

In many food products, starch is the major carbohydrate component, thereby determining the product properties. Therefore, it is important to understand the effects of processing and process parameters on the starch. Many starch-based foods are produced using processes involving heating and shearing, for example extrusion. Thermomechanical treatment induces various changes, such as melting of crystallites, disruption of granules and molecular breakdown of amylopectin (Vergnes *et al.*, 1987). A better understanding of these changes could lead to improved product quality and new process concepts.

Recent studies have indicated that the molecular weight (distribution) of starch determines product properties to a large extent (Bruemmer *et al.*, 2002). Thermomechanical breakdown has been shown to affect the molecular weight distribution significantly (figure 1). Recent advances in understanding the changes in molecular weight of starch as a function of process parameters bear potential for optimization of thermomechanical processes according to the desired product properties (Bruemmer, 1999; Van den Einde *et al.*, 2004a).

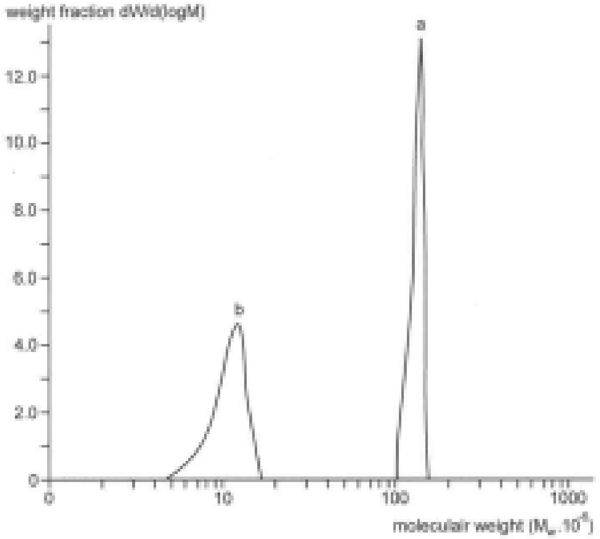

Figure 1: Molecular weight distribution of native (a) and heated-sheared waxy corn starch (b). (Van den Einde *et al.*, 2004b).

The objectives of this work were to review the thermally and thermomechanically induced molecular breakdown of starch, including the relevance for food product properties, recent advances in understanding breakdown mechanisms and relation of these mechanisms to extrusion processes, analytical methods and finally some recommendations for future research and process design.

2. Effects of macromolecular degradation on product properties

The impact of macromolecular degradation on the properties of the end product has recently gained more interest of researchers, because it strongly influences many properties. Bruemmer (1999) and Bindzus *et al.* (2002b) found that a lower molecular weight decreased the cold paste viscosity of the extrudate. Mua and Jackson (1997) studied the effect of molecular weight on functional properties of isolated amylose and amylopectin fractions. They concluded that molecular weight influenced pasting and gelling properties of the starch, as well as the degree of retrogradation (table 1).

A lot of work has been done on the effect of *Mw* on extrudate expansion. Already in the mid-70s, Mercier and Feillet (1975) found a relation between the amount of water-soluble carbohydrate after extrusion – which is related to degradation of the starch – and the expansion of the extruded product. Almost 10 years later, Chinnaswamy and Bhattacharya (1986) concluded that it was the mean molecular weight of starch that determined expansion of parboiled rice by heating at 250°C. Cai and Diosady (1993) found that more starch degradation led to less extrudate expansion. Bruemmer *et al.* (2002) found that a lower molecular weight led to less expansion of the extrudate at the die if the water content was higher than 16%. At 16% water content, a lower molecular weight increased the expansion of the extrudate.

Not only the average molecular weight, but also the polydispersity (Bruemmer, 1999) and the average chain length (Mua and Jackson, 1997) were found to influence the product properties. Table 1 schematically shows the correlation found between average molecular weight, polydispersity or average chain length and product properties. From table 1, it is clear that our knowledge at this moment is not yet complete. As molecular weight may influence various food product properties that are not noted in table 1, more investigations are required to further unravel structure-properties relations in starch.

Table 1: Correlation found between average molecular weight (Mw), polydispersity (pd) or average chain length (DP_c) and product properties. + = an increase of the independent variable results in an increase of the dependent variable, - implies the opposite dependency. 0 = no significant correlation was found.

		Product property																				
Authors	Starch type	Expansion			Cold paste viscosity			Water solubility			Water absorption			Gel fracturability			Gel stringiness			Retrogradation		
		Mw	pd	DP_c	Mw	pd	DP_c	Mw	pd	DP_c	Mw	pd	DP_c	Mw	pd	DP_c	Mw	pd	DP_c	Mw	pd	DP_c
Bindzus and others (2002b)	wheat, corn, rice				+a)			-			+											
Bruemmer (1999)	corn	b)			+	-		-	+			+	-									
Chinnaswamy and Bhattacharya (1986)	rice	+																				
Mua and Jackson (1997)	corn amylose				+		+							+		+	0		+			
Mua and Jackson (1997)	corn amylopectin				+		0							+		-	-		-	-		c)

a) For wheat starch: parabolic relation; for corn and rice starch linear positive correlation.

b) Depending on moisture content, see text.

c) Depending on measurement method either – or 0.

3. Mechanisms of thermal and shear-induced breakdown

One of the complicating factors in understanding the molecular weight reduction of starch-water mixtures by heating and shearing is that both thermal treatment without shear and thermomechanical treatment can induce breakdown. Igura *et al.* (1997) showed that long-time heating could lead to more or less the same average degree of breakdown as a short-time heating-shearing treatment. Although the exact mechanisms of the molecular weight reduction of starch are not completely clarified, some knowledge is available that provides a tool in understanding the degradation during thermomechanical treatment and extrusion.

In describing the mechanisms, this review focuses on the effects of heating with or without shear on starch in the presence of limited water. Dry heating of starch to 160°C or higher results in extensive depolymerization leading to the so-called “British gums”. This subject has been extensively reviewed by Tomasik and Wiejak (1989) and receives no further attention in this paper.

3.1 Thermal breakdown

Although it has been acknowledged that thermal breakdown of starch is important in various applications such as extrusion (Davidson *et al.*, 1984b), only a few studies have been conducted on the effect of heating of starch in the presence of a limited amount of water (<45% w/w). Fujio *et al.* (1995) and Igura *et al.* (1997) investigated the effect of heating of potato, corn and wheat starch at 150°C and 20 or 25 % (db) moisture content on molecular weight. They concluded that the effect of heating was dependent on heating time and starch type. A heating time of 15 minutes resulted in a significant decrease in molecular weight of corn and sweet potato starch. On the other hand, almost no change in molecular weight was found if potato or wheat starch was heated for 15 minutes. Steeneken and Woortman (2001) concluded that heating of potato starch at 16% moisture content to 210°C at 10°C/min in a DSC experiment resulted in appreciable molecular degradation.

The chemical reactions involved in thermal breakdown of low moistened starch are still largely unknown. It is possible that the same depolymerization reactions occur as during heating of dry starch. Tegge (1984) suggested that fragments with a 1,6-anhydro-β-D-glucopyranose end were formed during dry heating (figure 2). Theander and Westerlund (1987) found that these components were present in heat-processed (180°C for 1-4 hours) starch and wheat flour. The component was shown to react further with starch and starch

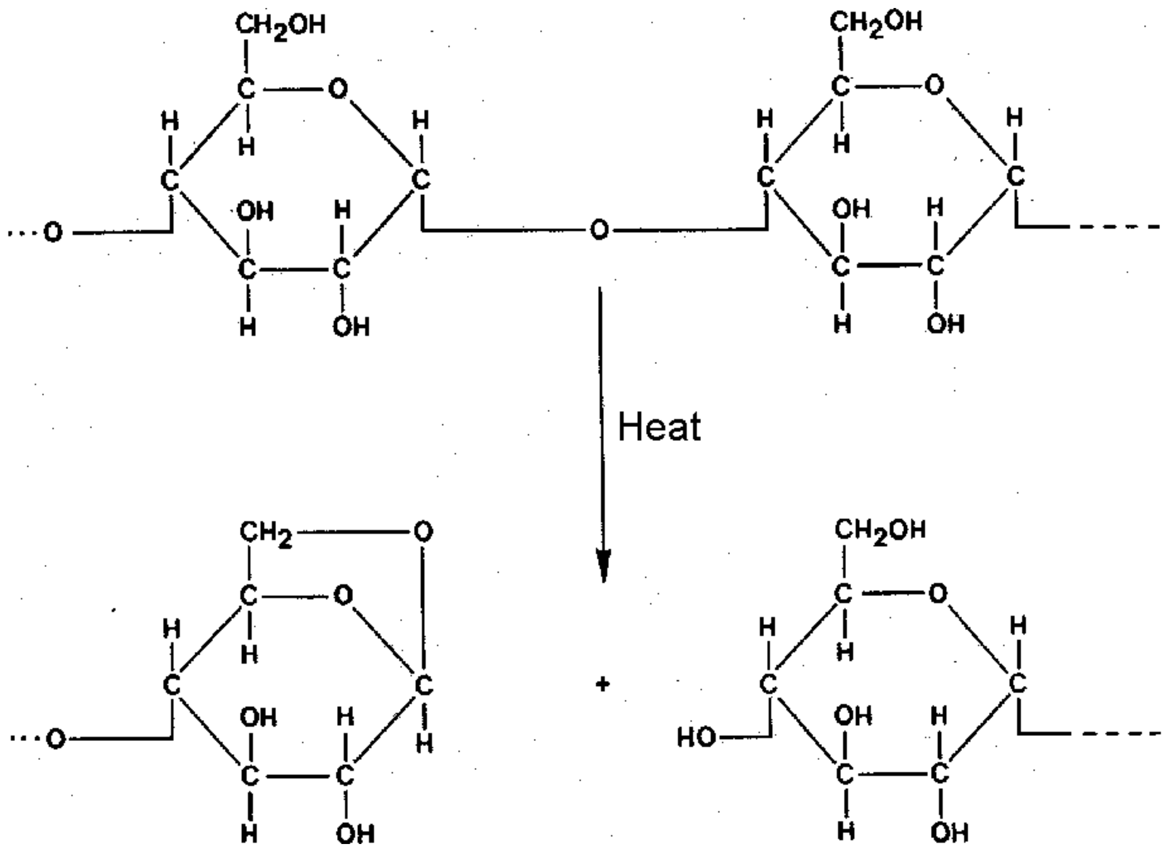

Figure 2: Mechanism of degradation of dry starch at high temperatures (Tegge, 1984).

fragmentation products to give branched structures, resistant to amylolytic enzymes. Other reactions may involve water. Hydrolysis reactions might occur during heating of low moistened starch. This hypothesis is in accordance with the results of a recent investigation by Igura *et al.* (2001), who concluded that time-temperature history was more effective on the depolymerization of potato starch at higher moisture content. Martinez-Bustos *et al.* (1998) found that addition of calcium hydroxide during extrusion resulted in a lower water solubility index if extrusion temperature and moisture content were high. Under these conditions, thermal reactions are expected to be dominant. Apart from lowering the water activity, the addition of calcium hydroxide might decrease the number of catalytic protons available and hence decrease the speed of hydrolysis. However, starch can also be broken down by the hydroxide itself. As no data were given on this aspect, no definite conclusions can be drawn, but the results obtained by Martinez-Bustos and co-workers might suggest that hydrolysis occurs. Finally, the increase in polydispersity of starch during extrusion at high temperature

(Bruemmer, 1999) is consistent with the exodegradation caused by acid hydrolysis (Van Soest *et al.*, 1996), which again suggests that this is indeed a possible reaction.

3.2. Mechanical breakdown

Subjecting low moistened starch to combined heating and shearing may induce a variety of physical and chemical changes. The granular structure is lost, native crystals are partially or completely molten and macromolecules can be disrupted (Barron *et al.*, 2000). Barron *et al.* (2001) gave a schematic representation of destructuring of waxy corn and smooth pea starch by shear and heat (figure 3). They concluded that shearing induced fragmentation of granules and that a homogeneous melt was obtained when temperature was above the melting temperature and mechanical energy input was higher than 100 J/g. No significant molecular breakdown was observed as long as no solid/melt transition had taken place.

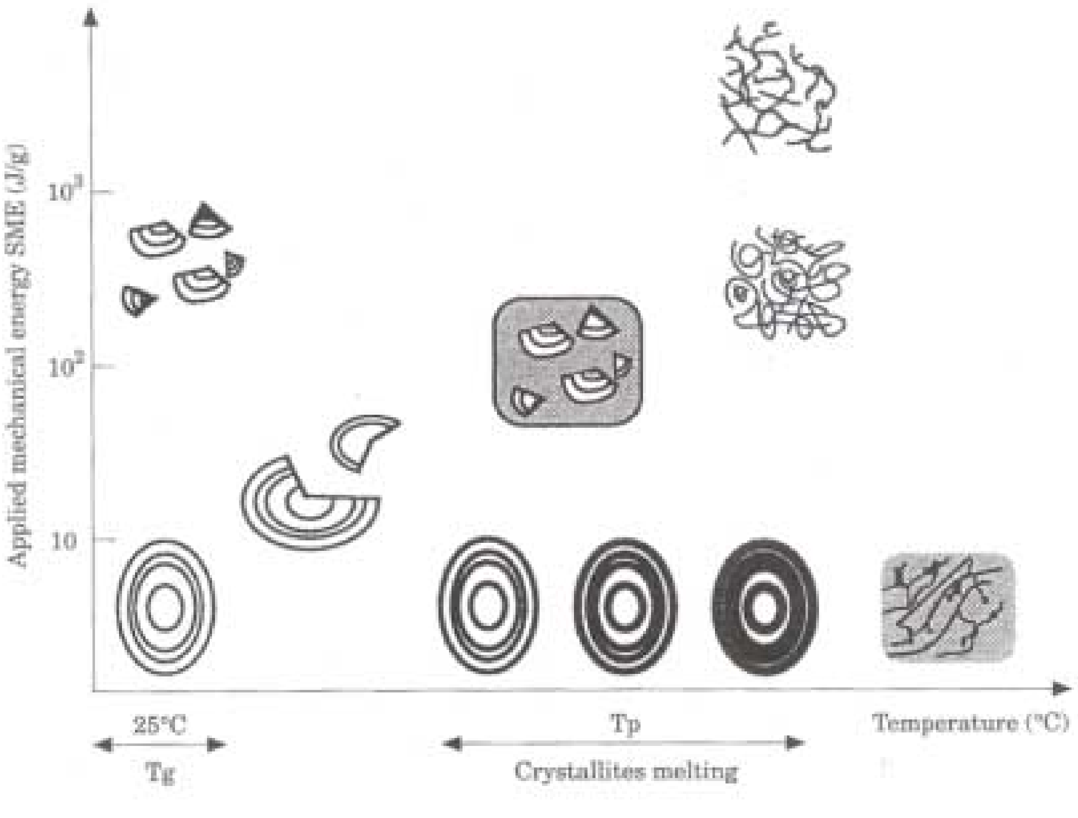

Figure 3: Schematic representation of starch destructuring under shear and temperature (Barron *et al.*, 2001).

Amylopectin is more susceptible to mechanical damage caused by shear than amylose. Davidson *et al.* (1984a) suggested that amylopectin can not align itself effectively in the streamlines of the flow in high shear equipment. Della Valle *et al.* (1996) suggested that the high sensitivity of amylopectin, compared to amylose, would be due to its higher molecular weight rather than to its branched structure. Various authors have demonstrated the susceptibility of amylopectin for extruder shear forces (examples are given further on in this paper).

As earlier mentioned for thermal breakdown, research done on thermomechanical degradation has mostly focussed on physical properties; knowledge on the actual chemical reactions occurring is much less complete. The fragments with a 1,6-anhydro-β-D-glucopyranose end that were found after dry heating of starch (as described above) were shown to be present in wheat starch extruded at 200°C and moisture content 10% only, but could not be found in wheat starch extruded at 105°C and 30% moisture or 150°C and 20% moisture (Theander and Westerlund, 1987). Again, it could be possible that under those circumstances hydrolysis reactions dominate, as described in the section on thermal breakdown.

3.3. Time-dependent and time-independent breakdown

Recently, Van den Einde *et al.* (2004a) showed that the peak stress during heating-shearing treatment of waxy corn starch with 30% water determines the degree of starch degradation, provided that thermal effects can be neglected. The suggested mechanism was that of (covalent) bond breakage by mechanical stress along the polymer chain. From studies using atomic force microscopy (Grandbois *et al.*, 1999; Beyer, 2000) it can be derived that the force required for breaking a covalent bond can be considered time-independent within the time scales generally encountered during heating-shearing processes.

Despite the demonstrated time independence of shear-induced bond breakage, in other studies the degree of starch breakdown was found to be dependent on or even linearly proportional to the treatment time (Vergnes *et al.*, 1987; Davidson *et al.*, 1984b; Diosady *et al.*, 1985). Two factors can be responsible for this. Firstly, thermal effects might play a role. These effects are time-dependent, as shown by Igura *et al.* (1997). Furthermore, combined effects of heat and shear might be important. The theory of Bueche (1960) on degradation of high molecular weight polymers suggested that applying shear could lower the activation energy for thermal bond rupture. Arisawa and Porter (1970) suggested in an investigation on breakdown of polystyrene that shear (mechanical energy) could change the potential energy function for thermal bond rupture. Another factor is the crystalline nature of the starch. It has been suggested that the unmolten crystalline parts of the starch are not susceptible to mechanical action (Diosady *et al.*, 1985) or that the solid melt transition is a prerequisite for extensive depolymerization by chain cleavage as for example observed under severe extrusion conditions (Barron *et al.*, 2001). The melting of these crystalline parts was shown to be time-, temperature- and shear dependent (Barron *et al.*, 2002; Barron *et al.*, 2000; Zheng and Wang, 1994). Therefore, although the degradation of starch itself is time-independent, increasing the processing time leads to further melting and hence increases the degree of macromolecular degradation. On the other hand, in extrusion experiments it was found that melting occurred in a very short transition section as soon as the first restrictive screw element was encountered (Colonna *et al.*, 1983), probably due to the high local shear. This suggests that the effect described above may not be highly important during extrusion processes.

3.4 Selectivity of breakdown

Baud *et al.* (1999) found that only the larger starch molecules were broken down during extrusion. If we assume that the force on a molecule can be interpreted roughly as the product of stress and frontal area of the molecule, we can understand this finding. As soon as the molecule is broken down, its frontal area is smaller and the force hence will be smaller. For each value of a stress, a certain critical molecular weight can be defined, below which the molecules will not be broken down because the force is too low. Hence, mechanical degradation is expected to be highly selective, as shown in figure 4.

4. Effects of extrusion on macromolecular degradation

With the findings described above it is possible to understand some of the most important effects of extruder parameters such as screw speed on molecular weight reduction found during extrusion trials described in literature. Table 2 gives an overview of the effects of all parameters described in this section as found in earlier studies.

4.1. Effect of screw speed and temperature

The effect of screw speed on starch breakdown in a single screw extruder, which was highly dependent on temperature, as found by Davidson *et al.* (1984a), can be understood from the two mechanisms described above. At the low moisture contents that they used (table 2),

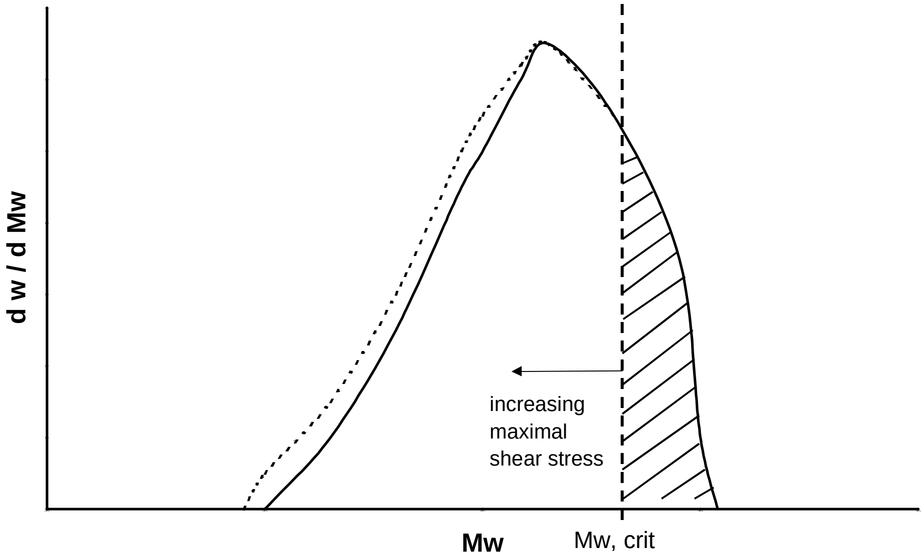

Figure 4: Example of molecular weight distribution of starch and selective breakdown. Large molecules (shaded area) will be broken down until they reach a certain critical molecular weight. The frontal area is then too low to cause any further degradation. The amount of material with lower molecular weight is necessarily increased, with the fragments of the large molecules. Increasing the shear stress will decrease the critical molecular weight.

stresses are high as long as the temperature is reasonably low. Hence, increasing the screw speed increases the maximal stress and more degradation takes place. The effect is less pronounced at 149°C probably because thermal effects already become more important. At 177°C the viscosity is most likely too low for significant mechanical degradation so that thermal breakdown becomes the dominant mechanism. Then, increasing the screw speed decreases the residence time so that less thermal breakdown takes place. The latter effect is more pronounced at higher moisture content as water is probably involved in the reaction. Govindasamy *et al.* (1996) found that screw speed increased the degree of degradation of sago starch in a twin screw extruder if the water content was high. As no viscosity data were given, only speculation on their findings is possible. Starch breakdown was in this study highly correlated to the degree of gelatinization, suggesting that this transition was a prerequisite for depolymerization, as earlier described in the section on time-dependent and time-independent breakdown.

4.2. Effect of re-extruding

Willett *et al.* (1997) conducted an interesting study on extruding waxy corn starch twice. The first extrusion run caused the molecular weight distribution to shift completely and *Mw* could be related well to mechanical energy input; re-extruding the material from the first run resulted only in a very small fraction of material changing from one molecular weight fraction towards the other. These results are again consistent with mechanical and (limited) thermal breakdown respectively. In the first pass, the high maximal stresses in the first extruder run caused the large molecules to breakdown completely. In the second pass, no additional mechanical breakdown could be obtained, probably due to reduced melt viscosity. Furthermore, higher stresses are required to break down lower molecular weight material thermomechanically (Van den Einde *et al.*, 2004a). Hence, the degradation during the second run was mainly or completely thermal, resulting in breakdown of only small fractions.

4.3. Effect of SME

The specific mechanical energy (*SME*) is an often-used parameter to quantify the amount of shear that is put on material during extrusion (table 2). It is defined as (Bruemmer, 1999):

$$SME = \frac{M_d \cdot \omega}{Q_m} \qquad \text{(J/kg)} \qquad [1]$$

where M_d denotes the torque (N·m), ω denotes the angular velocity (s^{-1}) and Q_m denotes the mass flow (kg/s). For a continuously operated system, *SME* is closely related to (but not identical to) the maximal stresses during the operation, as these largely determine the torque on the engine. For that reason, it is clear that a higher SME during extrusion generally leads to more breakdown of the starch as found in many studies (table 2).

4.4. Effect of amylose content

Using starch having a higher amylose content seems to have two, partially counter-acting, influences. Firstly, the higher the amylose content of corn starch, the lower is the temperature above which thermal breakdown takes place (Bruemmer, 1999). Secondly, in certain studies it was suggested that amylose itself is only susceptible to a small extent or even not at all susceptible to shear-induced breakdown so that the relative decrease in molecular weight will be less (Baud *et al.*, 1999; Chinnaswamy and Hanna, 1990; Della Valle *et al.*, 1996). Baud *et al.* (1999) suggested that molecules having a molecular weight less than $5 \cdot 10^6$ g/mole were

Table 2: Effects of temperature, screw speed, moisture content, amylose content and specific mechanical energy (*SME*) on the macromolecular degradation during extrusion as measured by chromatographic methods and intrinsic viscosity. Abbreviations: *T* = temperature, *N* = screw speed, *MC* = moisture content, TSE = twin screw extruder, co = co-rotating. DE = dextrose equivalent measurement; GPC = gel permeation chromatography; LPSEC = low pressure size exclusion chromatography; GFC = gel filtration chromatography; other analysis abbreviations: see text; + = an increase of the independent variable results in an increase of the degree of breakdown, - implies the opposite dependency.

Author	Type of starch	Extruder type	Measuring method	*T* range (°C)	*T* effect	*N* range (rpm)	*N* effect	*MC* range (%)	*MC* effect	% amylose range	% amylose effect	*SME* range (10^5 J/kg)	*SME* effect
Baud *et al.* (1997)	corn1)	TSE, co	HPSEC MALLS	100-180	unclear			20-33	unclear	0-70	-	3.6-21	+
Bindzus *et al.* (2002b)	wheat, corn, rice	TSE, co	GPC	90-150	2)	190-390	2)	16-24	2)			2.9-13	+
Bruemmer (1999)	corn	TSE, co	LPSEC	100-180 180-200	03) +4)						5)	3.2-9.4	+
Bruemmer (1999)	waxy corn	TSE, co	LPSEC									2.2-21	+
Bruemmer (1999)	high amylose corn	TSE, co	LPSEC	100-160 >160	0 +4)						5)	3.6-14	unclear
Cai *et al.* (1995)	wheat	TSE, co	HPSEC	100-120 140-160	+ -6) +7)	200-300	+	25-30	-				
Chinnaswamy and Hanna (1990)	corn1)	SSE	GPC	110-150 150-200	+ -			10-30	-	0-70	8)		
Davidson *et al.* (1984a)	wheat	SSE	GPC; intrinsic viscosity	121-177	9)	50-100	+10) -10)	20-25	-				

Govindasamy *et al.* (1996)	sago	TSE, co	HPSEC; DE	81-149	+	315-484	-6) +7)	34-47	-				
Guha and Ali (2002)	rice	TSE, co	GPC	80-100	+11) -12)					5.0-28.6	13)		
Orford *et al.* (1993)	waxy corn	TSE, co	SEC; intrinsic viscosity	130-180	0	150-200	+	20-25	0			3.6-7.9	+
Della Valle *et al.* (1996)	corn1)	TSE, co	LPSEC; intrinsic viscosity	102-190 14)	2)	80-240 14)	2)	20.5-36 14)	2)	0-70	-	15)	+
Willett *et al.* (1997)	waxy corn	TSE, co	GPC; MALLS									0-17	+
Wen *et al.* (1990)	corn16)	TSE, co	GFC	100-200	-	100-300	+	20-30	-				
Yamada *et al.* (1990)	potato	TSE	GPC	110-230	+								

---

1) With various amylose contents (0-70%).

2) Variable was varied, but not any conclusion was drawn from it, as the authors defined treatments in terms of SME.

3) Product temperature increased somewhat the polydispersity, but not the average molecular weight.

4) Product temperature also strongly increased polydispersity in this temperature range.

5) Amylose fraction of the starch was not broken down.

6) At the lower moisture content(s).

7) At the higher moisture content(s).

8) No direct conclusion was drawn; amylose fraction degraded less than amylopectin fraction.

9) Depending on moisture content and screw speed positive or negative

10) Determined by GPC: effect of screw speed was always positive; determined by intrinsic viscosity: effect of screw speed positive or negative, depending on moisture content and screw speed (see text).

11) If amylose was present in the rice starch.

12) If no amylose was present in the rice starch (waxy rice).

13) Amylose content determined temperature of maximal degradation (see 11) and 12)).

14) Range was different for different amylose contents.

15) Defined as "less severe" or "more severe" conditions (SME value for less severe or more severe treatment depending on amylose content of the starch).

16) Corn meal was used; the authors suggested that the extent of starch fragmentation might be greater using corn meal than using pure corn amylopectin.

almost unsusceptible to degradation during extrusion in a twin screw extruder at screw speeds up to 240 rpm. Understanding the overall effect of amylose content remains difficult. Therefore, more research is needed in order to understand completely the effect of amylose on the degradation of amylopectin and whether or not it is degraded itself.

4.5. Degradation along the extruder screw

During extrusion, degradation progresses along the screw (Colonna *et al.*, 1983; Cai *et al.*, 1995). This is not contrary to the instantaneous breakdown by shear described earlier in this paper because of two reasons. Firstly, thermal effects probably take place all along the screw. Secondly, the shear and elongation rates in the extruder are different at various locations in the extruder. The degradation pattern therefore becomes complex after the first crystallites have molten as on one hand viscosity and stress decrease due to the breakdown of the macromolecules, but on the other hand the amount of material susceptible to mechanical degradation increases due to further melting. Furthermore, the breakdown will be inhomogeneous, because the shear rate, and thus the stress, strongly varies locally in the extruder. We can therefore expect that the degradation continues in time along the length of the extruder, although the local degradation process itself is time-independent.

5. Analytical issues

As mentioned earlier, molecular breakdown of starch has strong effects on the properties of the final product. However, to quantify molecular breakdown itself and its relation to product properties, it is important to have direct analytical methods available.

Which method is most useful to measure the starch molecular weight (distribution) and thus starch degradation depends on the type of breakdown that needs to be characterized. While certain methods can be used to measure endodegradation, other ones are useful for determining exodegradation. An overview of the methods is given below.

Intrinsic viscosity. The advantage of using intrinsic viscosity is the good reproducibility compared to chromatography (Millard *et al.*, 1997). Furthermore, intrinsic viscosity is a property that is closely related to parameters important for product properties. The method is sensitive towards endodegradation. It has been suggested (Colonna *et al.*, 1984; Zhiqiang *et al.*, 1999; Fujio *et al.*, 1995) that the intrinsic viscosity is directly related to the viscosity averaged molecular weight Mv according to the Mark-Houwink relation:

$$[\eta] = K \cdot Mv^{\alpha} \qquad \text{(ml/g)} \qquad [2]$$

The parameters K and α depend on starch type and amylose content. Recently, Millard *et al.* (1997) showed that intrinsic viscosity of waxy corn starch in DMSO could even be correlated well to the weight-average molecular weight Mw found in chromatographic measurements according to a Mark-Houwink type equation.

Chromatography and laser light scattering. Chromatographic methods can be applied to obtain information on the molecular weight distribution. Using High Performance Size Exclusion Chromatography (HPSEC) measurements, it is possible to describe changes in the molecular weight distribution by changes in the weight fractions of several molecular size ranges defined in terms of retention time (Cai *et al.*, 1995). HPSEC is often combined with laser light scattering detection (HPSEC MALLS, where MALLS denotes Multi Angle Laser Light Scattering), which allows direct determination of the molecular weight of the passing fraction. Still, the determined molecular mass should not be interpreted as highly accurate absolute values but only as a good indication (Van Soest and Kortleve, 1999) due to the fact that recovery is certainly not 100%. Endodegradation can be measured using HPSEC MALLS. Measurement of exodegradation is also possible, provided that the fragments that arise are large compared to the molecules of the solvent used. HPSEC MALLS systems were used successfully in various studies to determine starch molecular weight distribution as a function of applied processing (Baud *et al.*, 1999; Willett *et al.*, 1997; Van Soest *et al.*, 1996; Van Soest and Kortleve, 1999), although both extremely large and very small molecular weight fractions might not be detected.

Field flow fractionation. Various sorts of field flow fractionation (FFF) coupled with SEC have already been applied for the analysis of amylopectin. Practically, FFF uses one added flux perpendicular to the main elution direction. The main usual fluxes are temperature gradient, gravitation (sedimentation) or cross flow (Roger *et al.*, 2001). The eluted fractions can be detected by MALLS. Sedimentation FFF allows separation even for molar masses larger than 10^9 Da (Hanselmann *et al.*, 1996). Cross flow FFF was shown to be promising for the fractionation of starch polysaccharides (Roger *et al.*, 2001), although the elution behavior of the largest molecules still requires more investigation (Van Bruijnsvoort *et al.*, 2001).

Water solubility index (WSI). Some authors used the WSI as a measure for starch degradation or suggested that changes in WSI were due to the breakdown of starch (Vergnes *et al.*, 1987; Orford *et al.*, 1993; Martinez-Bustos *et al.*, 1998; Govindasamy *et al.*, 1996; Davidson *et al.*, 1984a; Choudhury and Gautam, 1998). The advantage of using WSI as a degradation measure is that it is correlated to the presence of low molecular weight compounds and hence to the degree of exodegradation. However, the use of this measure has also a major disadvantage. WSI is strongly positively correlated to the degree of gelatinization (Cai and Diosady, 1993). Hence, it is best to extract the degradation effect from this analysis by measuring the degree of gelatinization separately. WSI is directly suitable to measure to the degree of exodegradation if all products compared are fully gelatinized.

Dextrose Equivalent (DE). DE values can be measured to get an impression of the formation of very small molecular weight compounds (Govindasamy *et al.*, 1996). DE measurements on extruded starch are not often carried out, because mechanical degradation is not expected to result in formation of small molecular weight products. Therefore, DE is useful as an additional measurement only. On the other hand, DE measurements can be highly important when extrusion trials in the presence of enzymes are carried out (see, for example, Linko *et al.*, 1983).

Considering the measurement methods described in this chapter, it is clear that no single measurement exists that provides a full picture of starch degradation. Therefore, combining different methods is currently the best way to obtain a complete view of the molecular breakdown of starch.

6. Control of shear-induced breakdown in extruders

As explained earlier, control of molecular weight reduction during extrusion is important to ensure specific product characteristics. Combining trial and error type experiments with estimations on the degradation can be useful in this respect. The maximal stress, which was shown to determine mechanical breakdown, can be calculated using estimated shear and elongation rates at different places in the extruder and the estimated viscosity of the material. This chapter deals with both issues. Thermal effects are not taken into account, as these have not been quantified well yet.

6.1. Estimating shear and elongation rates in the extruder

The shear rate at different locations in the extruder can be obtained from calculations or measurements. Estimating the shear rate in transport, single lead and reverse elements can be done using the equations derived by Martelli (1983) and Yacu (1985). The calculation of shear rate in paddle sections is more complex. In the last decade, advances have been made in numerical calculation of the flow patterns in these elements, for both regular paddles and three-tip kneading blocks (Bravo *et al.*, 2000; Bruce *et al.*, 1997; Ishikawa *et al.*, 2000; Yoshinaga *et al.*, 2000). However, only a few studies focussed on the average shear rate in these elements or on the shear rate distribution at different locations in the element. Van der Wal *et al.* (1996) estimated the mean shear and elongation rates in a paddle as a function of throughput and screw speed by solving the equations for isothermal laminar flow of a Newtonian incompressible fluid without body forces. Mohamed *et al.* (1990) proposed an elegant but laborious experimental method to estimate the mean shear rate during extrusion. Their method requires off-line measurement of rheological properties of both a Newtonian and a non-Newtonian liquid combined with extruder experiments.

Velocity profile measurements also enable calculation of the shear rate. Table 3 gives an overview on the technologies used so far to measure velocity profiles in extruders. All these measurements were done on model extruders with a model fluid as flow material, as described in the table.

Table 3: Methods for measuring velocity and flow profiles in extruders, including type of extruder, model material and limitations. SSE = single screw extruder, TSE = twin screw extruder, co = co-rotating.

Author	Method	Extruder type	Model material	Limitations
McCarthy *et al.* (1992); Agemura *et al.* (1995)	MRI (Magnetic Resonance Imaging)	SSE	CMC solution	extruder constructed from non-magnetic materials
Bakalis and Karwe (1997); Karwe and Sernas (1996)	LDA (Laser Doppler Anemometry)	TSE, co	corn syrup	only for optically transparent materials
Carneiro *et al.* (1999)	video camera	TSE, co	silicone oil	acrylic barrel; only for optically transparent materials

Only limited knowledge is available on the rates of exchange between the high and low shear zones of the extruder. Calculation of the pathways that the starch molecules follow through the extruder would be useful in this respect. However, so far only for a single-screw extruder such a type of calculation was done (Reed and Baird, 1992), which was unfortunately not used for interpretation in terms of pathways through high- and low-shear spots.

6.2. Estimating melt viscosity and shear and elongation stress

In food extrusion rheology, the key issue is obtaining the required data. The essential difficulty in measuring melt rheology is that the rheological properties are affected by kinetic phenomena (Ghoshdastidar *et al.*, 2000). Modeling the rheology of starch (based) melts has already been attempted for a long time. The first interesting viscosity model for cooking dough was created by Remsen and Clark (1978). It described viscosity, based on power-law behavior, as a function of shear rate, temperature and time-temperature history and included viscosity changes caused by temperature-induced reactions.

MacKey *et al.* (1989) suggested correcting the melt viscosity with a term describing the shear history of the material or more precisely the product of shear rate and time. Although the large number of parameters made the model somewhat difficult to use in practical situations, it has contributed to the awareness that shear history is important in understanding melt rheology.

The use of slit dies allows measurement of the viscosity of the end product on-line and collection of information on the extensional viscosity (Bhattacharya *et al.*, 1994). Such a die was used in many studies (Bhattacharya *et al.*, 1994; Chang *et al.*, 1999; Lai and Kokini, 1990; McMaster *et al.*, 1987; Parker *et al.*, 1990; Seethamraju and Bhattacharya, 1994; Della Valle *et al.*, 1995; Wang *et al.*, 1990) and was shown to be useful in on-line control of the extrusion process as product properties and end product melt viscosity were often well-correlated (Bindzus *et al.*, 2002a). A difficulty in using slit die data for estimating the peak stress is that the viscosity of the end product is in most cases (much) lower than the peak viscosity during the extrusion process, as molecular degradation and granule disruption along the extruder reduce the viscosity during treatment.

A solution to this problem can be off-line measurement of the rheological properties of the material in a rheometer. Vergnes and Villemaire (1987) used a self-built capillary rheometer with a Couette pre-shearing zone to derive expressions for the rheology of molten corn starch as a function of temperature T, moisture content MC and energy input history W, i.e. how much mechanical energy the material had received in the pre-shearing zone prior to the measurement. The equation derived was:

$$\eta = K_0 \exp\left[\frac{E_a}{R}\left(\frac{1}{T}-\frac{1}{T_0}\right)-\beta\left(MC-MC_0\right)-\delta\left(W-W_0\right)\right]\cdot\gamma^{m(T,MC)-1} \text{ (Pa·s)} \qquad [3]$$

where:

$$m(T,MC)=\beta_1 T+\beta_2 MC+\beta_3 T\cdot MC \qquad \text{(-)} \qquad [4]$$

Values of β, β_1, β_2, β_3, δ, K_0 and E/R were determined in their work. The model was recently extended to mixtures of wheat starch and glycerol and water (Martin *et al.*, 2003). Such a model may be useful in calculating the peak viscosity if the mechanical energy input before reaching this viscosity can be estimated.

In extruders, forces are not only put onto the material due to shear flow, but also due to elongation flow. Data on extensional viscosity of starch (based) melts are scarce. However, the extensional viscosity can be calculated from the shear viscosity η using the Trouton ratio Tr (Jones *et al.*, 1987):

$$\eta_e(\varepsilon)=\eta\left(\sqrt{3}\varepsilon\right)\cdot Tr \qquad [5]$$

The Trouton ratio was measured for extruded corn meal (Bhattacharya *et al.*, 1994) resulting in Tr = 20-50. Thus, the extensional viscosity of the material is much higher than the shear viscosity. Average elongation rates in a twin screw extruder were shown to be approximately one tenth of the shear rates, depending on screw speed and throughput (Van der Wal *et al.*, 1996). Substituting the values found by Bhattacharya and by Van der Wal into equation [5] reveals that the resulting extensional stress can be high compared to the shear stress, making it important to take it into account. Hence, it is important that elongation stress is taken into account.

7. Process design for selective polymer breakdown

In modern process design, the general trend is towards selective, energy efficient and small processes (Meeuwse *et al.*, 1999). Clearly, considering the molecular breakdown of starch and probably also other high molecular weight polymers, the current extrusion process does not match all of these criteria. The main disadvantage of the extruder, as shown above, is the inhomogeneous shear and elongation rate, leading to non-selective breakdown. Furthermore, this inhomogeneity also makes it difficult to avoid high stress spots in case that breakdown is undesired.

As earlier mentioned, selective starch breakdown may be possible (figure 4), as long as no thermal breakdown takes place. This would require a completely new range of equipment. Instead of various flow types within one process, more defined flow would be necessary. A process principle would consist of the following steps: 1. the starch is transformed into a melt using limited shear and relatively low temperature (in order to prevent random thermal degradation); 2. the starch melt receives a homogeneous high shear or elongation stress for a short time. The maximum value of the stress attained determines the degree of breakdown. A possible option for such a process would be a slowly rotating chamber to induce quick melting in a well-defined shear field at relatively low temperature combined with a capillary to provide a short-term precise shear or elongation stress. This type of processes would also allow shear stress to be a new design parameter, which is in turn controllable by optimizing the shear and elongation rate.

8. Conclusion

Recent advances in fundamental understanding and control of changes of starch and product properties include development of equipment in which the real process parameters such as temperature, time and shear force can be separated and optimized as well as the development of analytical methods. Investigations with separated process parameters can create a wider window for product-oriented process design and for new products. There are, however, gaps in the knowledge on the following subjects. Firstly, more investigations are required to further qualify and quantify the relations between molecular degradation and product properties. These investigations are not trivial, as “well-defined starch” does not exist. Controlled selective (thermo)mechanical degradation, as described in this paper, might help creating better-defined starch in future. Secondly, if the relations described above are to be applied to existing processes, e.g. extrusion, more knowledge is required on flow fields and particle trajectories in the process equipment used. Investigations on these two subjects could lead to improved process concepts as well as improved product quality and would therefore be important to be carried out in the near future.

Symbols list

E_a	activation energy (J/mole)
K	constant in Mark-Houwink equation (ml g^{-1} $Da^{-\alpha}$)
K_0	consistency factor at $T = T_0$ and $MC = MC_0$ (Pa·s^m)
m	pseudoplastic index (-)
MC	moisture content (%)
MC_0	reference moisture content (%)
M_d	torque (N·m)
Mv	viscosity averaged molecular weight (Da)
Mw	weight averaged molecular weight (Da)
Q_m	mass flow rate (kg/s)
R	gas constant (= 8.31 J/mole, K)
T	temperature (K)
T_0	reference temperature (K)
Tr	Trouton ratio (-)
W	mechanical energy input (J/m^3)
W_0	reference mechanical energy input (J/m^3)

Greek symbols

α	exponent in Mark-Houwink equation (-)
β	factor describing dependence of viscosity on moisture content MC ($\%^{-1}$)
β_1	factor describing dependence of pseudoplastic index m on temperature T (K^{-1})
β_2	factor describing dependence of pseudoplastic index m on moisture content MC ($\%^{-1}$)
β_3	factor describing dependence of pseudoplastic index m on the product of temperature and moisture content $T{\cdot}MC$ ($K^{-1}\%^{-1}$)
δ	factor describing dependence of viscosity on mechanical energy input (m^3/J)
ε	elongation rate (s^{-1})
η	viscosity (Pa·s)
η_e	extensional viscosity (Pa·s)
$[\eta]$	intrinsic viscosity (ml/g)

ω angular velocity (s^{-1})

References

Agemura, C.K., Kauten, R.J., & McCarthy, K.L. (1995). Flow fields in straight and tapered screw extruders using Magnetic Resonance Imaging. *Journal of Food Engineering*, 25, 55-72.

Arisawa, K., & Porter, S. (1970). The degradation of polystyrene during extrusion. *Journal of Applied Polymer Science*, 14, 879-896.

Bakalis, S., & Karwe, M.V. (1997). Velocity field in a twin-screw extruder. *International Journal of Food Science and Technology*, 32, 241-253.

Barron, C., Buleon, A., Colonna, P., & Valle, G. Della (2000). Structural modifications of low hydrated pea starch subjected to high thermomechanical processing. *Carbohydrate Polymers*, 43, 171-181.

Barron, C., Bouchet, B., Valle, G. Della, Gallant, D.J., & Planchot, V. (2001). Microscopical study of the destructuring of waxy maize and smooth pea starches by shear and heat at low hydration. *Journal of Cereal Science*, 33, 289-300.

Barron, C., Valle, G. Della, Colonna, P., & Vergnes, B. (2002). Energy balance of low hydrated starches transition under shear. *Journal of Food Science*, 67, 1426-1437.

Baud, B., Colonna, P., Valle, G. Della, & Roger, P. (1999). Macromolecular degradation of extruded starches measured by HPSEC-MALLS. *Biopolymer Science: Food and Non Food Applications / Les Colloques de l'INRA*, 91, 217-221.

Beyer, M.K. (2000). The mechanical strength of a covalent bond calculated by density function theory. *Journal of Chemical Physics*, 112, 7307-7312.

Bhattacharya, M., Padmanabhan, M., & Seethamraju, K. (1994). Uniaxial extensional viscosity during extrusion cooking from entrance pressure drop method. *Journal of Food Science*, 59, 221-226.

Bindzus, W., Fayard, G., Lengerich, B. van, & Meuser, F. (2002a). Application of an in-line viscometer to determine the shear stress of plasticised wheat starch. *Starch / Staerke*, 54, 243-251.

Bindzus, W., Fayard, G., Lengerich, B. van, & Meuser, F. (2002b). Description of extrudate characteristics in relation to the shear stress of plasticised starches determined in-line. *Starch / Staerke*, 54, 252-259.

Bravo, V.L., Hrymak, A.N., & Wright, J.D. (2000). Numerical simulation of pressure and velocity profiles in kneading elements of a co-rotating twin screw extruder. *Polymer Engineering and Science*, 40, 525-541.

Bruce, D., Wilson, M., & Generalis, S. (1997). Flow field analysis of both the trilobal element and mixing disc zones within a closely intermeshing, co-rotating twin-screw extruder. *International Polymer Processing*, 12, 323-330.

Bruemmer, T. (1999). Charakterisierung molekularer Strukturparameter kochextrudierter Maisstaerken und Ermittlung von Struktur-Eigenschaftsbeziehungen. [PhD dissertation]. Berlin: Technischen Universitaet Berlin.

Bruemmer, T., Meuser, F., Lengerich, B. van, & Niemann, C. (2002). Expansion and functional properties of corn starch extrudates related to their molecular degradation, product temperature and water content. *Starch / Staerke*, 54, 9-15.

Bruijnsvoort, M. van, Wahlund, K.G., Nilsson, G., & Kok, W.T. (2001). Retention behaviour of amylopectins in asymmetrical flow field-flow fractionation studied by multi-angle light scattering detection. *Journal of Chromatography A*, 925, 171-182.

Bueche, F. (1960). Mechanical degradation of high polymers. *Journal of Applied Polymer Science*, 4, 101-106.

Cai, W., & Diosady, L.L. (1993). Modelling of expansion and water solubility index of wheat starch during extrusion cooking. *Acta Alimentaria*, 22, 181-192.

Cai, W., Diosady, L.L., & Rubin, L.J. (1995). Degradation of wheat starch in a twin-screw extruder. *Journal of Food Engineering*, 26, 289-300.

Carneiro, O.S., Caldeira, G., & Covas, J.A. (1999). Flow patterns in twin-screw extruders. *Journal of Materials Processing Technology*, 92-93, 309-315.

Chinnaswamy, R., & Bhattacharya, K.R. (1986). Characteristics of gel-chromatographic fractions of starch in relation to rice and expanded rice-product quality. *Starch / Staerke*, 38, 51-57.

Chinnaswamy, R., & Hanna, M.A. (1990). Macromolecular and functional properties of native and extrusion cooked starch. *Cereal Chemistry*, 67, 490-499.

Chang, Y.K., Martinez-Bustos, F., Park, T.S., & Kokini, J.L. (1999). The influence of specific mechanical energy on corn meal viscosity measured by an on-line system during twin-screw extrusion. *Brazilian Journal of Chemical Engineering*, 16, 285-295.

Choudhury, G.S., & Gautam, A. (1998). Comparative study of mixing elements during twin-screw extrusion of rice flour. *Food Research International*, 31, 7-17.

Colonna, P., Melcion, J.P., Vergnes, B., & Mercier, C. (1983). Flow, mixing and residence time distribution of maize starch within a twin-screw extruder with a longitudinally split barrel. *Journal of Cereal Science*, 1, 115-125.

Colonna, P., Doublier, J.L., Melcion, J.P., Mondredon, F. de, & Mercier, C. (1984). Extrusion cooking and drum drying of wheat starch. I. Physical and macromolecular modifications. *Cereal Chemistry*, 61(6), 538-543.

Davidson, V.J., Paton, D., Diosady, L.L., & Larocque, G. (1984a). Degradation of wheat starch in a single-screw extruder: characteristics of extruded starch polymers. *Journal of Food Science*, 49, 453-458.

Davidson, V.J., Paton, D., Diosady, L.L., & Rubin, L.J. (1984b). A model for mechanical degradation of wheat starch in a single-screw extruder. *Journal of Food Science*, 49, 1154-1157.

Diosady, L.L., Paton, D., Rosen, N., Rubin, L.J., & Athanassoulias, C. (1985). Degradation of wheat starch in a single-screw extruder: mechano-kinetic breakdown of cooked starch. *Journal of Food Science*, 50, 1697-1699, 1706.

Einde, R.M. van den, Bolsius, A., Soest, J.J.G. van, Janssen, L.P.B.M., Goot, A.J. van der, & Boom, R.M. (2004a). The effect of thermomechanical treatment on starch breakdown and the consequences for process design. *Carbohydrate Polymers*, 55(1), 57-63. (Chapter 2 of this thesis).

Einde, R.M. van den, Linden, E. van der, Goot, A.J. van der, & Boom, R.M. (2004b). A mechanistic model on the relation between molecular structure of amylopectin and macromolecular degradation during heating-shearing processes. Accepted for publication in *Polymer Degradation and Stability*. (Chapter 3 of this thesis).

Fujio, Y., Igura, N., & Hayakawa, I. (1995). Depolymerization of molten-moisturized-starch molecules by shearing force under high temperature. *Starch / Staerke*, 47, 143-145.

Ghoshdastidar, P.S., Ghai, G., & Chhabra, R.P. (2000). Computer simulation of three-dimensional transport during moistened defatted soy flour processing in the metering section of a single-screw extruder. *Proceedings of the Institution of Mechanical Engineers*, 214, 335-349.

Govindasamy, S., Campanella, O.H., & Oates, C.G. (1996). High moisture twin-screw extrusion of sago starch: 1. Influence on granule morphology and structure. *Carbohydrate Polymers*, 30, 275-286.

Grandbois, M., Beyer, M.K., Rief, M., Clausen-Schaumann, H., & Gaub, H.E. (1999). How strong is a covalent bond? *Science*, 283, 1727-1730.

Guha, M., & Ali, S.Z. (2002). Molecular degradation of starch during extrusion cooking of rice. *International Journal of Food Properties*, 5, 509-521

Hanselmann, R., Burchard, W., Ehrat, M., & Widmer, H.M. (1996). Structural properties of fractionated starch polymers and their dependence on the dissolution process. *Macromolecules*, 29, 3277-3282.

Igura, N., Hayakawa, I., & Fujio, Y. (1997). Effect of longer heating time on depolymerization of low moisturized starches. *Starch / Staerke*, 49, 2-5.

Igura, N., Katoh, T., Hayakawa, I., & Fujio, Y. (2001). Degradation profiles of potato starch melts through a capillary type viscometer. *Starch / Staerke*, 53, 623-628.

Ishikawa, T., Kihara, S.I., & Funatsu, K. (2000). 3-D Numerical simulations of nonisothermal flow in co-rotating twin screw extruders. *Polymer Engineering and Science*, 40, 357-364.

Jones, D.M., Walters, K., & Williams, P.R. (1987). On the extensional viscosity of mobile polymer solutions. *Rheologica Acta*, 26, 20-30.

Karwe, M.V., & Sernas, V. (1996). Application of Laser Doppler Anemometry to measure veolocity distribution inside the screw channel of a twin-screw extruder. *Journal of Food Process Engineering*, 19, 135-152.

Lai, L.S., & Kokini, J.L. (1990). The effects of extrusion operating conditions on the on-line apparent viscosity of 98% Amylopectin (Amioca) and 70% Amylose (Hylon 7) corn starches using extrusion. *Journal of Rheology*, 34, 1245-1266.

Linko, P., Linko, Y.Y., & Olkku, J. (1983). Extrusion cooking and bioconversions. *Journal of Food Engineering*, 1, 243-257.

Mackey, K.L., Ofoli, R.Y., Morgan, R.G., & Steffe, J.F. (1989). Rheological modeling of potato flour during extrusion cooking. *Journal of Food Process Engineering*, 12, 1-11.

Martelli, F.G. (1983). Twin-screw extrusion. New York: Van Nostrand Reinhold Company.

Martin, O., Averous, L., & Valle, G. Della. (2003). In-line determination of plasticized wheat starch viscoelastic behavior: impact of processing. *Carbohydrate Polymers*, 53,169-182.

Martinez-Bustos, F., Chang, Y.K., Bannwart, A.C., Rodriguez, M.E., Guedes, P.A., & Gaiotti E.R. (1998). Effects of calcium hydroxide and processing conditions on corn meal extrudates. *Cereal Chemistry*, 75, 796-801.

McCarthy, K.L., Kauten, R.J., & Agemura, C.K. (1992). Application of NMR imaging to the study of velocity profiles during extrusion processing. *Trends in Food Science and Technology*, 3, 215-219.

McMaster, T.J., Senouci, A., & Smith, A.C. (1987). Measurement of rheological and ultrasonic properties of food and synthetic polymer melts. *Rheologica Acta*, 26, 308-315.

Meeuwse, F.M., Grievink, J., Verheijen, P.J.T., & Stappen, M.L.M. van der. (1999). Conceptual design of processes for structured products. 5th international conference on foundations of computer-aided process design (FOCAPD 1999), Colorado.

Mercier, C., & Feillet P. (1975). Modification of carbohydrate components by extrusion-cooking of cereal products. *Cereal Chemistry*, 52, 283-297.

Millard, M.M., Dintzis, F.R., Willett, J.L., & Klavons, J.A. (1997). Light-scattering molecular weights and intrinsic viscosities of processed waxy maize starches in 90% dimethyl sulfoxide and H_2O. *Cereal Chemistry*, 74, 687-691.

Mohamed, I.O., Ofoli, R.Y., & Morgan, R.G. (1990). Modeling the average shear rate in a co-rotating twin screw extruder. *Journal of Food Process Engineering*, 12, 227-246.

Mua, J.P., & Jackson, D.S. (1997). Relationships between functional attributes and molecular structures of amylose and amylopectin fractions from corn starch. *Journal of Agricultural and Food Chemistry*, 45, 3848-3854.

Orford, P.D., Parker, R., & Ring, S.G. (1993). The functional properties of extrusion-cooked waxy-maize starch. *Journal of Cereal Science*, 18, 277-286.

Parker, R., Ollett, A.L., & Smith, A.C. (1990). Starch melt rheology: measurement, modelling and applications to extrusion processing. In P. Zeuthen. Processing and quality of foods (p. 1.290-1.295). London: Elsevier.

Reed, C.M., & Baird, D.G. (1992). Numerical modeling of cooking extrusion of food doughs. In J.L. Kokini, C.T. Ho, & M.V. Karwe. Food extrusion science and technology (p. 307-321). New York: Marcel Dekker, Inc.

Remsen, C.H., & Clark, J.P. (1978). A viscosity model for a cooking dough. *Journal of Food Process Engineering*, 2, 39-64.

Roger, P., Baud, B., & Colonna, P. (2001). Characterization of starch polysaccharides by flow field-flow fractionation-multi-angle laser light scattering-differential refractometer index. *Journal of Chromatography A*, 917, 179-185.

Seethamraju, K., & Bhattacharya, M. (1994). Effect of ingredients on the rheological properties of extruded corn meal. *Journal of Rheology*, 38, 1029-1044.

Soest, J.J.G. van, Benes, K., Wit, D. de, & Vliegenthart, J.F.G. (1996). The influence of starch molecular mass on the properties of extruded thermoplastic starch. *Polymer*, 37, 3543-3552.

Soest, J.J.G. van, & Kortleve, P.M. (1999). The influence of maltodextrins on the structure and properties of compression-molded starch plastic sheets. *Journal of Applied Polymer Science*, 74, 2207-2219.

Steeneken, P.A.M., & Woortman, A.J.J. (2001). Identification of thermal transitions in low-moisture starch systems by preparative DSC. Lecture given at the Starch Workshop, Wageningen.

Tegge, G. (1984). Staerke und Staerkederivate. Hamburg: Behr's Verlag.

Theander, O., & Westerlund, E. (1987). Studies on chemical modifcations in heat-processed starch and wheat flour. *Starch / Staerke*, 39, 88-93.

Tomasik, P., & Wiejak, S. (1989). The thermal decomposition of carbohydrates. Part II. The decomposition of starch. *Advances in Carbohydrate Chemistry and Biochemistry*, 47, 279-343.

Valle, G. Della, Boche, Y., Colonna, P., & Vergnes, B. (1995). The extrusion behaviour of potato starch. *Carbohydrate Polymers*, 28, 255-264.

Valle, G. Della, Colonna, P., Patria, A., & Vergnes B. (1996). Influence of amylose content on the viscous behaviour of low hydrated molten starches. *Journal of Rheology*, 40, 347-362.

Vergnes, B., Villemaire, J.P., Colonna, P., & Tayeb, J. (1987). Interrelationships between thermomechanical treatment and macromolecular degradation of maize starch in a novel rheometer with preshearing. *Journal of Cereal Science*, 5, 189-202.

Vergnes, B., & Villemaire, J.P. (1987). Rheological behaviour of low moisture molten maize starch. *Rheologica Acta*, 26, 570-576.

Wal, D.J. van der, Goffart, D., Klomp, E.M., Hoogstraten, H.W., & Janssen, L.B.P.M. (1996). Three-dimensional flow modeling of a self-wiping corotating twin-screw extruder. Part II: the kneading section. *Polymer Engineering and Science*, 36, 912-924.

Wang, S.M., Bouvier, J.M., & Gelus, M. (1990). Rheological behaviour of wheat flour dough in twin-screw extrusion cooking. *International Journal of Food Science and Technology*, 25, 129-139.

Wen, L.F., Rodis, P., & Wasserman, B.P. (1990). Starch fragmentation and protein insolubilization during twin-screw extrusion of corn meal. *Cereal Chemistry*, 67, 268-275.

Willett, J.L., Millard, M.M., & Jasberg, B.K. (1997). Extrusion of waxy maize starch: melt rheology and molecular weight degradation of amylopectin. *Polymer*, 38, 5983-5989.

Yacu, W.A. (1985). Modelling a twin screw co-rotating extruder. *Journal of Food Engineering*, 8, 1-21.

Yamada, T., Suzuki, K., Hisamatsu, M., & Komiya, T. (1990). GPC profile change of potato starch with extrusion processing. *Starch / Staerke*, 42, 217-223.

Yoshinaga, M., Katsuki, S., Miyazaki, M., Liu, L., Kihara, S.I., & Funatsu, K. (2000). Mixing mechanism of three-tip kneading block in twin screw extruders. *Polymer Engineering and Science*, 40, 168-178.

Zheng, X., & Wang, S.S. (1994). Shear induced starch conversion during extrusion. *Journal of Food Science*, 59(5), 1137-1143.

Zhiqiang, L., Xiao-su, Y., & Hangzhou, F.Y. (1999). Effect of bound water on thermal behaviours of native starch, amylose and amylopectin. *Starch / Staerke*, 51, 406-410.

Summary

Introduction and aims

Starch is a major ingredient in various food products. During production of starch-based foods, often a combination of high temperature and (shearing) forces is applied. An important example is the extrusion process. In this process, a mixture of starch, a limited amount of water and often other component (proteins) is kneaded and mixed by a rotating screw in a heated barrel and then extruded through a die towards the desired shape.

The molecular weight of starch determines the overall product properties to a large extent. It is known that thermomechanical treatment leads to a reduction of the molecular weight of the starch. However, the exact cause and control of this effect are still matters of uncertainty. The aims of the investigations described in this thesis were:

1. to gain insight into and to model the effect of the different process parameters involved in thermomechanical treatment (time, temperature, shear or elongation stress, energy input, moisture content) on the degree of macromolecular degradation of starch;
2. to apply these results to existing processes (extrusion) in order to be able to describe the molecular weight reduction during these processes and to asses the scope for development of processes regarding controlled selective starch breakdown.

New equipment able to apply a well-defined thermomechanical treatment at high temperatures was developed, consisting of a non-rotating cone and a rotating plate. Whereas in conventional equipment the different process parameters involved in product transformations (time, shear rate, temperature, forces) are strongly coupled, the new shear cell (figure 1) allowed studying the effects of these parameters separately. Using this equipment, mixtures of starch and water in different ratios were subjected to a thermomechanical treatment with various temperatures, times and shear rates.

Starch breakdown by heating and shearing

Chapter 2 of this thesis gives the results of an experimental study on starch breakdown by heating and shearing. Waxy corn starch mixed with 30% water was subjected to a variety of heat and shear treatments at temperatures 85-110°C in order to find the key parameter determining the degree of macromolecular degradation. At the temperatures and moisture

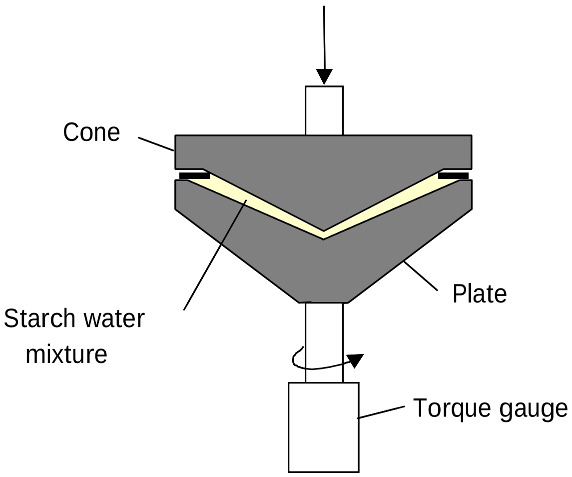

Figure 1: Schematic representation of the shear cell (Van der Goot *et al.*, 2003).

content investigated, thermal effects on waxy corn starch were negligible and all degradation was induced by mechanical effects. A first order model based on the maximum shear stress during the treatment gave a clearly improved prediction compared to existing first order models in literature that include time dependence. It was therefore concluded that molecular weight reduction of starch at the temperatures investigated is a time-independent process, during which the starch molecules are broken down virtually instantaneously by high shear forces within the time scales investigated. This finding was in a second study confirmed for corn starch (chapter 4). In this study, also thermal effects were investigated, both by heating only and by thermomechanical treatment. Various moisture contents (30-43%) and temperatures (85-140°C) were used. Thermal treatment resulted during the first 5 minutes in starch breakdown, after which longer heating had no significant effect. Thermomechanical breakdown could be split into two parts:

1. a mechanical part depending on maximal shear stress;
2. an independent thermal breakdown part.

The thermal breakdown part was dependent on time more or less the same way as during a purely thermal treatment without shear: during a relatively short time it resulted in starch breakdown, after which longer heating had no significant effect. Increasing moisture content had three effects on starch molecular weight reduction: it decreased the stresses, but it also decreased the stresses *required* for mechanical breakdown and increased thermal breakdown. These effects are partially counteracting. Therefore, it is difficult to predict the effect of moisture content on starch breakdown, but the findings described in the thesis may provide a first guideline for estimating the effects of changing moisture content on starch molecular weight reduction.

In chapter 3 of this thesis, a model allowing molecular scale explanation of the starch breakdown phenomena occurring during heating shearing treatment is explained and compared to the engineering scale experiments. This model was based on the assumption that the maximum shear stress on the polymer equals the effective surface stress on that polymer, which is related to the strength of the glucosidic bonds. The molecules were approximated as spheres, with a radius that exhibits fractal scaling with molecular weight. The molecular weight reduction as a function of applied maximum shear stress deduced from the model agreed satisfactorily with the ones experimentally determined. The results show a successful example of a coupling between engineering scale experiments and micro-scale models.

Application to extrusion processes and consequences for process design

Chapters 5 and 6 of this thesis focus on the process that is currently used to modify starch-water mixtures: extrusion cooking. The extruder (figure 2) consists of one or two screws (in the extruder used in this thesis: two), which transport and mix the material, surrounded by a cylindrical barrel. Various types of screw elements can be used. At the end of the extruder the product is pushed through a die, resulting in the desired shape.

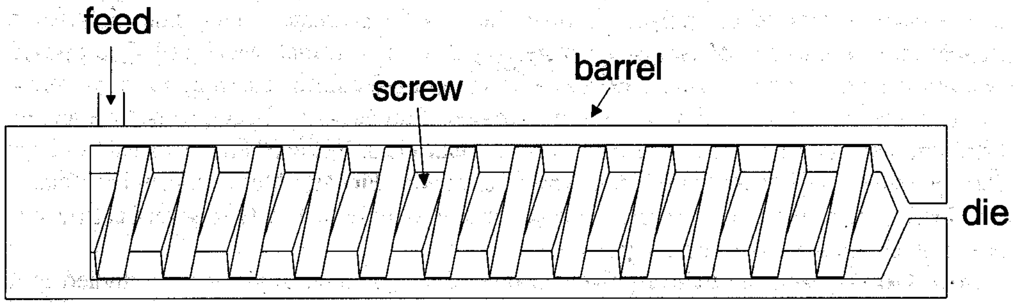

Figure 2: Schematic representation of an extruder.

Mixing effects of different screw elements were measured using a local Residence Time Distribution (RTD) determination system in a twin screw extruder completely filled with a dilute solution of pre-gelatinized waxy corn starch as a model fluid (chapter 6). Elements in a completely filled twin screw extruder were found to induce mixing downstream, but also upstream. These local mixing effects are important as they influence the time-temperature history, which is important for thermal breakdown as described above and also for other effects. The mixing effect of transport and single lead element was dependent on the available downstream volume. This means that the positioning of elements in the extruder influences the local mixing effect.

Chapter 5 focuses on molecular breakdown of starch in a twin screw extruder. Molecular breakdown of regular corn starch after extrusion at moisture contents 23-45%, screw speeds 90-180 rpm and temperatures 97-126°C was predicted using the results on starch breakdown described above (chapter 4). The maximum shear stresses in the extruder were estimated using simulations from literature on the flow in paddle sections, which are known to provide the highest stresses. In the extruder, two types of flow can induce significant breakdown: shear flow (as measured in the equipment described above) and elongation flow. Elongation stresses were calculated using the estimated Trouton ratio *Tr* of the starch. A reasonably good prediction of the degree of degradation was obtained, suggesting that the approach of describing a complex process, such as an extruder, using results obtained in a well-defined geometry was successful. Interestingly, our model was able to describe the molecular weight reduction in a complete extruder quite well by concentrating on a single paddle. This result suggests that extruders are in fact oversized when considering molecular weight reduction.

Finally, a literature review (chapter 7) shows that many results of extrusion trials described in literature can be well understood using the findings of this thesis. This chapter also provides guidelines for process design regarding controlled, selective starch breakdown. Better homogeneous shear fields are a key factor in the design of such processes. Furthermore, residence time can be short; longer shear sections are not effective.

Recommendations

With respect to the goals of this thesis, it can be concluded that a good insight has been obtained in the effects of the various process parameters on starch degradation. The thesis shows that uncoupling of process parameters can be a successful route to a better understanding of the effects of complex processes on molecular scale phenomena. In this work, the effects of shear and temperature were investigated specifically. Gaps still exist in understanding the effects of elongation flow. Therefore, the development of a device able to apply well-defined elongation flow and temperature treatments to material is recommended.

Recent advances in analysis technology will increase the rate of success expected from uncoupling of process parameters even further.

Reference

Van der Goot, A.J., Van den Einde, R.M., Peighambardoust, S.H. (2003). Poster: The effect of plain shear on biopolymers.

Samenvatting

Inleiding

Dit proefschrift beschrijft de effecten van afschuifkrachten en hoge temperatuur op het molecuulgewicht van zetmeel. Zetmeel wordt gewonnen uit onder andere verschillende granen (maïs, tarwe, rijst) en knollen (aardappel) en wordt gebruikt als ingrediënt in veel levensmiddelen. Om van het zetmeel een levensmiddel te maken, wordt het vaak eerst gemengd met een geringe hoeveelheid water (en evt. andere ingrediënten) waarna dit mengsel verder verwerkt wordt. Deze verwerking vindt vaak plaats bij hoge temperaturen en tevens kunnen grote mechanische krachten op het zetmeel komen te staan. Een proces waarbij dit beide gebeurt wordt een thermomechanische behandeling genoemd. Zetmeel bestaat uit moleculen die, vergeleken met veel andere stoffen, groot zijn. Onder invloed van de krachten en / of de hoge temperatuur kunnen de zetmeelmoleculen afbreken tot kleinere fragmenten, waardoor het molecuulgewicht lager wordt. Omdat de afbraak van het zetmeel de eigenschappen van het uiteindelijke levensmiddel beïnvloedt, is het van belang te begrijpen hoe en bij welke procesomstandigheden deze plaatsvindt. De doelen van dit proefschrift waren dan ook:

1. Het beschrijven hoe de verschillende procesparameters gedurende een thermomechanische behandeling van mengsels van zetmeel en water het molecuulgewicht van het zetmeel beïnvloeden.
2. Het toepassen van de resultaten hiervan op bestaande processen met als doel de veranderingen in molecuulgewicht gedurende deze processen te kunnen beschrijven en om ideeën te ontwikkelen voor nieuwe processen waarin zetmeel gecontroleerd en selectief wordt afgebroken.

De krachten die op het mengsel van zetmeel en water staan tijdens het proces worden bepaald door de gebruikte temperatuur, de hoeveelheid water in het mengsel en de snelheden in de gebruikte procesapparatuur. De afbraak van zetmeel wordt dus door een groot aantal procesfactoren beïnvloed. Nu is het in de apparaten die momenteel gebruikt worden bij de verwerking van mengsels van zetmeel en water (extruders, zie verderop in deze samenvatting) moeilijk of zelfs onmogelijk om de genoemde procesfactoren onafhankelijk van elkaar te variëren. Daarom is een nieuw apparaat ontwikkeld, waarin dit wel mogelijk is (figuur 1).

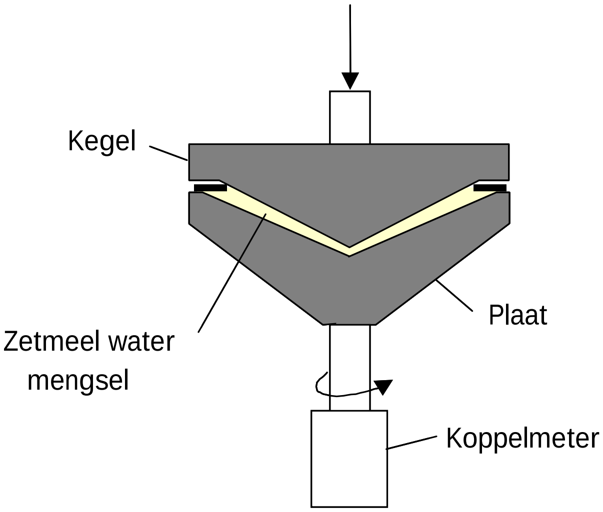

Figuur 1: Schematische voorstelling van het nieuw ontwikkelde apparaat, de “shear cell”. (Van der Goot *et al.*, 2003).

Afbraak van zetmeel onder invloed van krachten en temperatuur

Drie hoofdstukken in dit proefschrift gaan over de afbraak van zetmeel: hoofdstuk 2 en 3 behandelen mechanische afbraak van zetmeel (= als gevolg van krachten); hoofdstuk 4 behandelt zowel thermische afbraak (= als gevolg van hoge temperatuur) als thermomechanische afbraak (= waarbij temperatuur en kracht tegelijkertijd afbraak veroorzaken).

Hoofdstuk 2 laat zien dat de mate van mechanische afbraak van zetmeel afhangt van de spanning die maximaal op het zetmeel water mengsel heeft gestaan gedurende het proces. Deze ontdekking staat haaks op een aantal eerdere studies, waarin werd beschreven dat de afbraak van zetmeel afhing van het product van spanning en tijd. In deze eerdere studies werd dus gesuggereerd dat een lange tijd een lage spanning op het zetmeel hetzelfde effect zou hebben als een korte tijd een hoge spanning. De resultaten van hoofdstuk 2 laten zien dat de afbraak van zetmeel kan worden gerealiseerd in een korte tijd en dat langere procesduur wat dit effect betreft niet nodig is. In hoofdstuk 3 van het proefschrift wordt een model gepresenteerd waarmee voorspeld kan worden hoe hoog de maximumspanning tijdens een behandeling moet zijn om zetmeel tot een bepaald gewenst molecuulgewicht mechanisch af te breken.

In hoofdstuk 4 is gekeken naar zowel thermische als thermomechanische afbraak. Bij een thermische behandeling leidde een hogere temperatuur tot meer afbraak. Bovendien leidde meer water in het mengsel ook tot meer afbraak. Interessant genoeg was het niet altijd zo dat langere behandeling tot meer afbraak leidde: verhitten leidde initieel tot afbraak van het zetmeel, maar langere tijd zorgde niet voor meer afbraak. Thermomechanische afbraak van zetmeel bleek goed beschreven te kunnen worden door de behandeling in twee delen te splitsen:

1. een mechanische behandeling
2. en een thermische behandeling onafhankelijk daarvan.

De afbraak als gevolg van de mechanische behandeling kon weer worden beschreven als afhankelijk van de maximaal optredende spanning (zoals in hoofdstuk 2). De afbraak door de thermische behandeling volgde weer hetzelfde patroon als hierboven beschreven, namelijk de eerste paar minuten leidden tot afbraak, maar een langere tijd had geen effect meer.

Het effect van de hoeveelheid water op de thermomechanische afbraak was interessant. Gebruik van een hoger watergehalte had drie verschillende effecten op de zetmeelafbraak: het verlaagde de krachten die optraden, het leidde tot meer thermische afbraak en de krachten die nodig waren om zetmeel mechanisch af te breken werden er lager door. Deze effecten zijn gedeeltelijk tegengesteld. Daarom is het moeilijk om het effect van watergehalte op zetmeelafbraak te voorspellen, maar de resultaten beschreven in dit proefschrift kunnen een globaal idee geven.

Toepassing op bestaande processen en consequenties voor procesontwerp

Hoofdstukken 5 en 6 van dit proefschrift beschrijven het proces dat op dit moment veel wordt gebruikt bij de productie van levensmiddelen gebaseerd op zetmeel: extrusie. Een extruder is een apparaat dat veel wordt toegepast in de levensmiddelenindustrie, maar ook in de kunststoffenindustrie. De extruder (figuur 1) bestaat uit een cilindrisch schroefhuis waarin zich één of twee (in de in dit proefschrift gebruikte extruder: twee) ronddraaiende schroeven bevinden, die het materiaal transporteren en mengen. Om de schroefas kunnen verschillende typen elementen bevestigd worden, die ieder hun eigen werking hebben. Een voorbeeld zijn kneedelementen. Aan het einde van de extruder bevindt zich een spuitkop waarmee het product in de juiste vorm wordt gebracht.

Hoofdstuk 5 beschrijft afbraak van zetmeel gedurende extrusie wanneer thermische afbraak (voor een groot gedeelte) mag worden verwaarloosd. In hoofdstuk 6 is gekeken naar de menging in de extruder. Deze bepaalt hoe lang het zetmeel in de extruder op een bepaalde

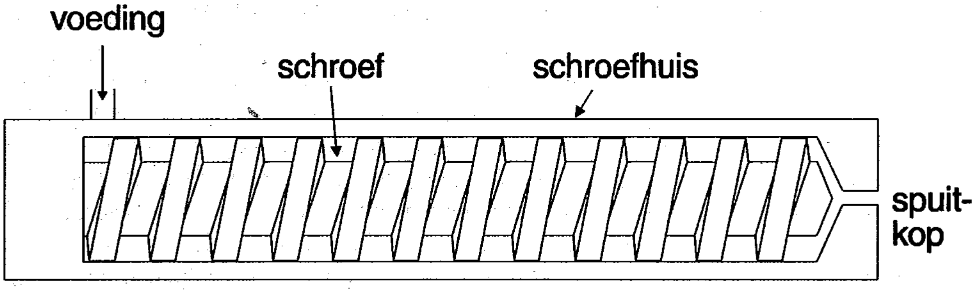

Figuur 1: Schematische voorstelling van een extruder.

temperatuur is geweest en is dus van groot belang wanneer ook thermische afbraak een rol speelt.

In hoofdstuk 5 wordt een model beschreven waarmee voor allerlei extrusiecondities (verschillende temperaturen, draaisnelheden, watergehalten) kan worden voorspeld in welke mate het zetmeel afbreekt. Het model geeft goede voorspellingen terwijl het gebaseerd is op het voorspellen van de afbraak in één kneedelement. Dit suggereert dat extruders groter zijn gebouwd dan vanuit het oogpunt van afbraak van zetmeel nodig is.

In hoofdstuk 6 is de menging bepaald die locaal veroorzaakt wordt door de verschillende typen schroefelementen. Schroefelementen zorgen voor locale menging stroomafwaarts, maar ook stroomopwaarts. Deze locale menging is belangrijk, omdat deze de tijd-temperatuur geschiedenis van het materiaal beïnvloedt, dat wil zeggen gedurende welke tijd het materiaal in de extruder een bepaalde temperatuur heeft gehad. Deze tijd kan diverse producteigenschappen beïnvloeden, waaronder ook het molecuulgewicht van zetmeel zoals hierboven beschreven.

Hoofdstuk 7 beschrijft dat veel resultaten van eerdere onderzoeken goed verklaard kunnen worden met de resultaten uit dit proefschrift. Dit hoofdstuk beschrijft daarnaast een proces voor gecontroleerde afbraak van zetmeel tot een gewenst molecuulgewicht. Hierbij kan de behandelingstijd kort zijn, omdat – zoals hierboven beschreven – lange tijden niet tot meer afbraak zullen leiden.

Tot slot

In dit proefschrift is het inzicht beschreven dat is verworven in de processen die een rol spelen tijdens bijvoorbeeld extrusie van mengsels van zetmeel en water. Dit inzicht is niet verkregen door de bestaande procesapparatuur (extruders) toe te passen, maar door het materiaal met een beter gedefinieerd apparaat te bestuderen. De resultaten helpen het begrip van bestaande processen verder, zeker ook vergeleken met studies waarbij wel die extruders zijn gebruikt. Daarom lijkt deze strategie ook bij verder onderzoek naar het effect van procesfactoren op de eigenschappen van het eindproduct een goede te kunnen zijn.

Referentie

Van der Goot, A.J., Van den Einde, R.M., Peighambardoust, S.H. (2003). Poster: The effect of plain shear on biopolymers.

List of publications

Einde, R.M. van den, Veen, M.E. van der, Bosman, H., Goot, A.J. van der, & Boom, R.M. Modeling macromolecular degradation of corn starch in a twin screw extruder. Submitted for publication.

Einde, R.M. van den, Akkermans, C., Goot, A.J. van der, & Boom, R.M. Molecular breakdown of corn starch by thermal and mechanical effects. Submitted for publication.

Einde, R.M. van den, Kroon, P., Goot, A.J. van der, & Boom, R.M. Local mixing effects of screw elements during extrusion. Submitted for publication.

Einde, R.M. van den, Linden, E. van der, Goot, A.J. van der, & Boom, R.M. A mechanistic model on the relation between molecular structure of starch and macromolecular degradation during heating-shearing processes. Accepted for publication in *Polymer Degradation and Stability*.

Einde, R.M. van den, Bolsius, A., Soest, J.J.G. van, Janssen, L.P.B.M., Goot, A.J. van der, & Boom, R.M. (2004). The effect of thermomechanical treatment on starch breakdown and the consequences for process design. *Carbohydrate Polymers*, 55(1), 57-63.

Goot, A.J. van der, Einde, R.M. van den, & Boom, R.M. (2003). A fresh look into shear-based biopolymer processing. *NPT Procestechnologie*, 10(6), 28-30.

Einde, R.M. van den, Goot, A.J. van der, & Boom, R.M. (2003). Understanding molecular weight reduction of starch during heating-shearing processes (review). *Journal of Food Science*, 68(8), 2396-2404.

Einde, R.M. van den, Peters, J., Goot, A.J. van der, & Boom, R.M. (2002). In-line measurement of local residence time distribution in a twin screw extruder. In: Proceedings of ANTEC 2002 San Francisco, vol. 1 Processing (p. 28-30). Brookfield: Society of Plastics Engineers, Inc.

Goot, A.J. van der, Abrahamse, A.J., Einde, R. M. van den, Padt, A. van der, & Boom, R.M. (2000). [Development of structures.] Ontwerpen van structuren. *VMT Voedingsmiddelentechnologie*, 33(7), 19, 21-22.

Einde, R.M. van den, Zuilichem, D.J. van, Wolters, I., & Stolp, W. (1999). [Combination of microwave treatment and boiling water for fresh potato slices.] Combinatie microgolven en kokend water spaart aardappelschijfjes. *VMT Voedingsmiddelentechnologie*, 32(25), 10-11, 13-14.

Nawoord

Tijdens dit promotieonderzoek kreeg ik van mensen die niet in het onderzoek werken vaak de volgende vraag: “Jij werkt vier jaar lang aan één onderwerp? Is dat niet ontzettend saai?” Als ik nu, aan het eind van dit onderzoek, terugkijk kan ik alleen maar concluderen dat de vier jaar ontzettend snel om waren en tevens dat het werk als AIO veel afwisselender is dan veel mensen denken: het varieert van proeven doen en apparatuur bouwen tot cursussen volgen en congressen bezoeken en van studenten begeleiden tot rapporten en artikelen schrijven.

Het doen van een promotieonderzoek is gelukkig al lang geen soloactie meer en ik wil hier op deze plaats dan ook een aantal mensen bedanken, zonder wiens hulp dit proefschrift niet tot stand was gekomen.

Allereerst bedank ik Atze Jan voor de fantastische begeleiding die hij me de afgelopen vier jaar heeft gegeven. Atze, je hield me op het goede spoor als ik weer eens te veel zijsprongen wilde maken, je hebt ontzettend goed in de gaten gehouden dat alles op tijd afkwam, me behoed voor mijn eigen perfectionisme en niet te vergeten me er doorheen gesleept op een aantal momenten (met name na ca. 2,5 jaar) waarop ik het onderzoek bijna niet meer zag zitten. Daarnaast heb je me begeleid op een aantal reizen, onder andere naar Groningen, Detmold, en niet te vergeten op de verre reis naar San Francisco, sterker nog: daar heb je de lezing van me overgenomen, omdat ik als gevolg van jet lag (of iets anders) zo ziek was dat ik die niet meer kon houden…

Remko, de maandelijkse ontmoetingen met jou brachten veel goede ideeën in het onderzoek, maar minstens zo belangrijk was jouw positieve kijk op het werk. Vaak als ik niet zo tevreden was over de voortgang en me daar niet zo blij over voelde, had ik er na zo’n ontmoeting met jou weer helemaal zin in, doordat jij zo duidelijk aangaf wat voor een leuke dingen er allemaal met mijn metingen te doen zouden kunnen zijn.

Een groot gedeelte van het werk beschreven in dit proefschrift is uitgevoerd op nieuw gebouwde apparatuur, onder andere de ‘shear cell’. Dit apparaat was er nooit gekomen zonder het werk van Mees, Jan, Evert, Hans en André van de Mechanische Werkplaats. Bedankt voor al het werk dat jullie hebben uitgevoerd, de vele ideeën die jullie hadden en voor jullie snelle beschikbaarheid als wij weer eens een experiment hadden bedacht waar het apparaat niet tegen bleek te kunnen… Eveneens bedankt voor alle ideeën voor en hulp bij de experimenten met de perspex extruder; zonder dat was hoofdstuk 6 van dit proefschrift er niet geweest. Reinoud en Hans van de afdeling Elektronica, bedankt voor jullie bijdrage op elektrotechnisch gebied. Bij het vertalen van een vaag idee naar iets waarmee we naar de werkplaats konden heeft Pieter een belangrijke rol gespeeld. Pieter, bedankt hiervoor en voor het uitvoeren van een aantal labexperimenten voor mij (ik weet dat dit laatste niet je favoriete werk was…). Ook Laurens Bosgra en prof. Janssen van de Rijksuniversiteit Groningen hebben een belangrijke rol gespeeld in het ontwerp van de apparatuur en bij de optimalisatie van de meetopstellingen. Saskia, bedankt voor het uitvoeren van een aantal labexperimenten voor me en voor de hulp bij de laatste shear cell experimenten. Ik wens je veel succes bij de vervolgonderzoeken en bij je taak als labhoofd (die je van mij hebt overgenomen).

Een deel van dit proefschrift is tot stand gekomen in samenwerking met de sectie Levensmiddelennatuurkunde. Bij deze dank ik Erik van der Linden voor het tot stand helpen komen van hoofdstuk 3 van dit proefschrift, en Harry Baptist en Katja Grolle voor hun begeleiding bij het opzetten van de Ubbelohde experimenten zoals gebruikt in hoofdstukken 2 t/m 5.

Tijdens mijn onderzoek heb ik negen studenten mogen begeleiden bij hun afstudeervak. In volgorde van aankomst: Daniël, Marcel, Joris, Neleke, Arjen, Coen, Anne, Hans en Cynthia. Allemaal bedankt voor het vele werk dat jullie hebben uitgevoerd en voor de ideeën waarmee jullie kwamen. Zonder jullie was dit boekje waarschijnlijk toch een stuk minder dik geweest! Ik heb het begeleiden als ontzettend leuk en leerzaam ervaren en bovendien dwong het me om op tijd keuzes in het onderzoek te maken. Verder bedank ik op deze plaats Jeroen van Soest van Agrotechnology & Food Innovations (voormalig ATO) voor het medebegeleiden van een groot aantal van de hier genoemde studenten, voor het feit dat we gebruik konden maken van de nodige bij ATO aanwezige apparatuur en voor het delen van zijn zetmeelkennis met mij.

Veel van het werk van een AIO gebeurt ook achter het bureau. Mark, Anneke, Ed en Sandra, bedankt voor de gezellige sfeer op kamer 615 en de gezellige kameretentjes en –uitstapjes (inclusief een onvergetelijk bezoek aan de Volkswagen dealer)! Ed, bedankt voor de hulp die je me gaf als ik ‘voor het eerst’ een cursusformulier in moest vullen, een Matlab upgrade moest kopen enz. Het contrast tussen onze bureaus was groot, maar ik ben blij dat je in je proefschrift schreef dat je mijn “rommel in positieve zin zou gaan missen”. Anneke, om maar even bij de woorden uit jouw nawoord aan te sluiten, ik ben erg blij dat jij membraan emulsificatie als onderwerp hebt gekozen, zodat ik aan zetmeel kon werken. Mark, jij bent oprecht geïnteresseerd in je collega’s en dat werkt erg prettig. Het feit dat jij zo gemakkelijk aan het lachen te krijgen bent terwijl je wel heel serieus werkt maakt jou een fijne kamergenoot. Daarnaast heeft het feit dat jij in het midden van jouw onderzoek ook de overstap naar zetmeel hebt gemaakt geleid tot veel nuttige discussies. Bovendien heb jij er samen met Hadi en je studenten voor gezorgd dat de shear cell pas echt goed ging werken. Bedankt voor alle humor (‘de verwarming staat al hoog genoeg, er hoeft niet gestookt te worden’), je hulp als ik me niet zo happy voelde en alle gezelligheid! Ik ben blij dat je één van mijn paranimfen wilt zijn. Sandra, als mijn directe buurvrouw op de kamer vanaf mijn derde jaar was je vaak mijn aanspreekpunt (of liever gezegd: begon ik vaak gewoon tegen jou te kletsen zonder dat daarom gevraagd was…). Ik ben blij dat je eveneens mijn paranimf wilt zijn.

Aan de verdere collega’s van de vakgroep: bedankt voor alle gezelligheid bij de borrels, labuitjes, diners, filmavonden, koffiepauzes, lunches en niet te vergeten bij de AIO reizen naar Polen en Zuid-Afrika. Ik heb me goed thuisgevoeld bij Proceskunde en ik zal de sfeer zeker missen. Hadi, thank you for the useful discussions about the shear cell and for your help in optimizing it. Maria, thank you for the nice dinners and chats, I hope you are well in France now. Isabel, thank you for the nice trips to Haarlem, Amsterdam and The Hague. I wish you all the best now that you are living here in Wageningen. Eira, bedankt voor de goede gesprekken (vooral) tijdens de koffiepauzes en voor de drie geweldige feesten die je hebt georganiseerd. Martijn, ik heb de samenwerking met jou tijdens mijn eerste ‘grote’ onderwijsopdracht als erg prettig ervaren.

De rol van vrienden (m/v) tijdens een promotieonderzoek moet niet onderschat worden. Diana, Marieke, Anoeska, Maarten, Caroline, André, Martine, Angelique, Martijn, Bart, Floortje, Floris, Rieneke, Eric, Sigelinde en Monique, allemaal hebben jullie op één of meerdere manieren geholpen om me hier aan de eindstreep te krijgen, door me op te peppen als ik het niet zag zitten, door gezelligheid en ontspanning te bieden, door mee te denken of gewoon door er op het goede moment voor me te zijn.

Buiten het werk ben ik met veel plezier actief geweest als organist en als DJ. Van het Verrijzeniskoor van Wageningen en de Cantores en de leden van het Dameskoor van Doorwerth wil ik iedereen bedanken die op zijn of haar manier hieraan heeft bijgedragen. Ook het bestuur van de Borney’s, in het bijzonder Jan, wil ik bedanken voor het mij de gelegenheid geven me als DJ te bewijzen, iets wat ik al heel lang graag wilde doen. We hebben er met z’n allen vaak een leuk feestje van gemaakt!

Tot slot wilde ik graag mijn familie bedanken, in het bijzonder de onderstaande personen. Maurice, bedankt voor alle gezelligheid en steun. Anneke en Cees, bedankt dat jullie geregeld meeleefden de afgelopen 4 jaar. En niet te vergeten pa en ma: heel erg bedankt voor het mij de gelegenheid geven om te gaan studeren en om dit promotieonderzoek te gaan doen en voor alle steun op de momenten dat ik het moeilijk had.

René van den Einde, december 2003

Curriculum vitae

René Martin van den Einde werd op 21 september 1976 geboren te Voorburg. In 1994 behaalde hij het VWO diploma met lof aan het Sint Oelbert Gymnasium te Oosterhout. In datzelfde jaar startte hij met de studie Levensmiddelentechnologie aan de Landbouwuniversiteit Wageningen (heden Wageningen Universiteit). Twee afstudeervakken werden afgelegd bij de Sectie Proceskunde. Hij liep stage bij RHM Technology in High Wycombe, UK en bij Honig in Nijmegen. Na voor zowel het propedeutisch examen in 1995 als het doctoraalexamen in 1999 met lof te zijn geslaagd, startte hij in september 1999 als AIO bij de sectie Proceskunde van Wageningen Universiteit. Van dit AIO onderzoek zijn de resultaten in dit proefschrift beschreven.

De omslag van dit proefschrift is een voorbeeld van de op internet veel te vinden ‘fractal kunst’, gebaseerd op de uitkomsten van fractale berekening. Ook in dit proefschrift is gebruik gemaakt van een fractale berekening, in hoofdstuk 3. Verder doet dit plaatje enigszins denken aan extruderschroeven, die in dit proefschrift (met name in hoofdstuk 5 en 6) een rol spelen.